

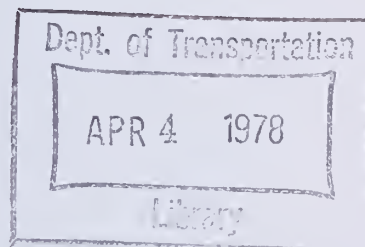
10

Report No. FHWA-RD-75-52

TE
662
.A3
no.
FHWA-
RD-
75-52

EVALUATION OF FLOOD RISK FACTORS IN THE DESIGN OF HIGHWAY STREAM CROSSINGS

Vol. II Analysis of Bridge Backwater Experiments



April 1977
Final Report

Document is available to the public through
the National Technical Information Service,
Springfield, Virginia 22161

Prepared for
FEDERAL HIGHWAY ADMINISTRATION
Offices of Research & Development
Washington, D. C. 20590


Foreword

This report describes large scale laboratory tests of bridge backwater studies and will be of interest to bridge and hydraulics engineers interested in the effects of bridges on water surface profiles.

This report is Volume II of a five volume series presenting the results of the Water Resources Engineers, Inc., research on "Evaluation of Flood Risk Factors in the Design of Highway Stream Crossings." This is the last of the five volumes to be distributed; the other four volumes were distributed as they were completed over a 2-year period beginning in 1975. The research was conducted for the Federal Highway Administration, Office of Research, Washington, D.C., under Contract DOT-FH-11-7669.

This document is disseminated under the sponsorship of the Department of Transportation in the interest of information exchange. The United States Government assumes no liability for its contents or use thereof.

Sufficient copies of the report are being distributed by FHWA Bulletin to provide a minimum of two copies to each FHWA Regional office, one copy to each FHWA Division office, and two copies to each State highway agency. Direct distribution is being made to the Division offices.

for 
for Charles F. Scheffey
Director, Office of Research
Federal Highway Administration

1. Report No. FHWA-RD-75-52	2. Government Accession No.	3. Recipient's Catalog No.	
4. Title and Subtitle EVALUATION OF FLOOD RISK FACTORS IN THE DESIGN OF HIGHWAY STREAM CROSSINGS. Vol. II. Analysis of Bridge Backwater Experiments		5. Report Date April 1977	6. Performing Organization Code
7. Author(s) A. J. Knepp R. P. Subinski M. T. Tseng	<div style="border: 1px solid black; padding: 5px; text-align: center;"> Dept. of Transportation APR 4 1978 Library </div>		8. Performing Organization Report No. WRE 20810
9. Performing Organization Name and Address Water Resources Engineers, Inc. 8001 Forbes Place Springfield, Virginia 22151			10. Work Unit No.
12. Sponsoring Agency Name and Address Offices of Research and Development Federal Highway Administration U. S. Department of Transportation Washington, D.C. 20590			11. Contract or Grant No. DOT-FH-11-7669
15. Supplementary Notes FHWA Contract Administrator: Gilbert Trainer FHWA Implementation Manager: Dan O'Connor FHWA Contract Manager: J. Sterling Jones FHWA Project Manager: Roy E. Trent		13. Type of Report and Period Covered Final Report	14. Sponsoring Agency Code
<p>16. Abstract</p> <p>This report presents the results of a series of experiments carried out using a large scale physical model of backwater caused by highway stream crossings of wide, heavily-vegetated flood plains. Variables studied included wingwall and spillthrough abutments, spur dikes, prototype bridge openings between 100 and 1100 ft and prototype flows between 8,000 and 36,000 cfs. An important aspect of these experiments was the use of large scale roughness elements protruding the free surface to provide the necessary ranges of roughness to simulate prototype conditions. Five combinations of roughness densities in patterns were tested in the course of experimentation. Primary emphasis was on crossings normal to flow; however, eccentric and skewed crossings were also tested.</p> <p>Results of the study included an analysis of the sensitivity of water surface elevation to the principal variables, quantification of both the location and height of the maximum backwater, and data for possible future study and modification of existing backwater methods.</p> <p>The other volumes of this study are:</p> <ul style="list-style-type: none"> I Experimental Determination of Channel Resistance for Large Scale Roughness 75-51 III Finite Element Model for Bridge Backwater Computation FHWA-RD-75-53 IV Economic Risk Analysis for Design of Bridge Waterways FHWA-RD-75-54 V Data Report for Spur Dike Experiments FHWA-RD-75-55 			
17. Key Words Backwater computation, analysis of variance, sensitivity analyses, highway stream crossing design	18. Distribution Statement No Restrictions. This document is available to the public through the National Technical Information Service, Springfield, Virginia 22151		
19. Security Classif. (of this report) Unclassified	20. Security Classif. (of this page) Unclassified	21. No. of Pages 182	22. Price

TABLE OF CONTENTS

	<u>Page No.</u>
NOTICE	ii
TABLE OF CONTENTS	iii
ACKNOWLEDGEMENTS	v
LIST OF FIGURES	vi
LIST OF TABLES	x
I. INTRODUCTION	1
STUDY OBJECTIVES	1
BACKGROUND	2
II. LITERATURE REVIEW	7
III. HYDRAULIC MODEL DESIGN	22
GENERAL DESCRIPTION	22
DYNAMIC SIMILITUDE	23
GOVERNING FLOW EQUATIONS IN BRIDGE WATERWAYS	26
REQUIREMENTS OF MODEL SCALES	30
CHANNEL RESISTANCE	36
IV. EXPERIMENTAL EQUIPMENT	42
FLUME DESCRIPTION	42
ROUGHNESS ELEMENTS	44
DESCRIPTION OF CROSSING CONFIGURATIONS	51
V. EXPERIMENTAL PROCEDURE	58
GENERAL DESCRIPTION	58
HYDRAULIC FLUME TESTS	63
DATA COLLECTION	64
QUALITY CONTROL	80
OPERATIONAL PROBLEMS	80
VI. PRESENTATION AND ANALYSIS OF DATA	83

TABLE OF CONTENTS
(Cont'd)

	<u>Page No.</u>
INTRODUCTION	83
DIMENSIONAL ANALYSIS	84
DEFINITION OF VARIABLES	84
ANALYSIS	85
TWO-DIMENSIONAL ANALYSIS OF WATER SURFACE ELEVATIONS	89
ANALYSIS OF VARIANCE	90
ANALYSIS OF DATA FOR ROUGHNESS PATTERN C	95
ANALYSIS OF TOTAL BACKWATER COEFFICIENT, K^*	103
ANALYSIS OF MAXIMUM BACKWATER LOCATION (l^*/b)	133
ANALYSIS OF MAXIMUM BACKWATER HEIGHT (h^*/y_0)	153
VII. CONCLUSIONS	164
VIII. RECOMMENDATIONS	166
DATA COLLECTION	166
DATA ANALYSIS AND INTERPRETATION	168
LIST OF REFERENCES	170
APPENDIX	A-1

ACKNOWLEDGEMENTS

Numerous personnel from both the Federal Highway Administration and Water Resources Engineers, Inc., have made valuable contributions to the completion of this project. While it is impossible to individually acknowledge the contributions of each individual, certain do deserve special recognition. Among these are the staff of the Environmental Control Group, Office of Research and Development, Federal Highway Administration, particularly J. Sterling Jones and Roy E. Trent.

Within WRE, overall project direction has been the responsibility, initially, of G. Kenneth Young and in the last three years of the study effort Robert P. Shubinski. Ming Te Tseng designed the experiment and directed the data collection activities. The data analysis described in this volume was performed and documented by Anthony J. Knepp; Mr. Knepp and Dr. Shubinski assume all responsibility for the conclusions and recommendations of this volume.

Of the many others at WRE who worked on the project a particular note of thanks is extended to Stanley W. Zison, Richard A. Schmalz, Larry S. Costello, John L. Matticks and Bert Black. For the final format of the document a grateful acknowledgement is extended to Phyllis Weiner, who drafted Chapter II, "Literature Survey," and provided technical editing; Luanne Wohler, who was responsible for the technical drafting; and to Kathy Settle and Joan Lagasse, who typed the manuscript.

LIST OF FIGURES

<u>Figure No.</u>		<u>Page No.</u>
II-1	Definition Sketch of Backwater Reach	9
II-2	Backwater Ratio for Channels Having Vertical-Faced Constrictions with Square-Edged Abutments	11
II-3	Energy Losses for Schneider Method	13
II-4	Backwater Analysis	17
III-1	Types of Roughness Elements	38
IV-1	Basic Flume Characteristics	43
IV-2	Definition of Roughness Pattern	46
IV-3	Manning's "n" for Roughness Patterns as a Function of Flow	48
IV-4	Wingwall Abutment Design	53
IV-5	Spillthrough Embankment	55
IV-6	Spur Dike Design	56
V-1	Crossing Configurations	58
V-2	Flow Lines for Typical Normal Crossing	59
V-3	Abutment Shapes	61
V-4	Velocity Measurement Locations for Centered Crossing Configuration	74
V-5	Skewed Model Velocity Sampling Configuration	76
V-6	Eccentric Model Velocity Sampling Configuration	76
V-7	Point Gages	77
V-8	Beam Apparatus Used for Locating Maximum Backwater	82
VI-1	Analysis of Variables Affecting Water Surface Elevation	97
VI-2	Analysis of Variables Affecting Water Surface Elevation-Excluding Spur Dikes	101
VI-3	Maximum Backwater Coefficient (K^* vs M)	109

LIST OF FIGURES
(Cont'd)

<u>Figure No.</u>		<u>Page No.</u>
VI-4	Maximum Backwater Coefficient (K^* vs M) for Spillthrough Roughness Pattern A	110
VI-5	Maximum Backwater Coefficient (K^* vs M) for Spillthrough Roughness Pattern B	111
VI-6	Maximum Backwater Coefficient (K^* vs M) for Spillthrough Roughness Pattern C	112
VI-7	Maximum Backwater Coefficient (K^* vs M) for Spillthrough Roughness Pattern D	113
VI-8	Maximum Backwater Coefficient (K^* vs M) for Spur Dike Roughness Pattern A	114
VI-9	Maximum Backwater Coefficient (K^* vs M) for Spur Dike Roughness Pattern B	115
VI-10	Maximum Backwater Coefficient (K^* vs M) for Spur Dike Roughness Pattern C	116
VI-11	Maximum Backwater Coefficient (K^* vs M) for Spur Dike Roughness Pattern D	117
VI-12	Maximum Backwater Coefficient (K^* vs M) for Wingwall Roughness Pattern A	118
VI-13	Maximum Backwater Coefficient (K^* vs M) for Wingwall Roughness Pattern B	119
VI-14	Maximum Backwater Coefficient (K^* vs M) for Wingwall Roughness Pattern C	120
VI-15	Maximum Backwater Coefficient (K^* vs M) for Wingwall Roughness Pattern D	121
VI-16	Maximum Backwater Coefficient (K^* vs M) for Wingwall Roughness Pattern P	122
VI-17	Experimental Eccentricity Definition	125
VI-18	Maximum Backwater Coefficient (K^* vs M) for Skew $\gamma = 15^\circ$	129
VI-19	Maximum Backwater Coefficient (K^* vs M) for Skew $\gamma = 15^\circ$ (centered)	130

LIST OF FIGURES
(Cont'd)

<u>Figure No.</u>		<u>Page No.</u>
VI-20	Maximum Backwater Coefficient (K^* vs M) for Skew γ 45°	131
VI-21	Maximum Backwater Location (ℓ^*/b vs M) for Wingwall Roughness Pattern P	137
VI-22	Maximum Backwater Location (ℓ^*/b vs M) for Wingwall Roughness Patterns A and B	138
VI-23	Maximum Backwater Location (ℓ^*/b vs M) for Wingwall Roughness Patterns C and D	139
VI-24	Maximum Backwater Location (ℓ^*/b vs M) for Spillthrough Roughness Patterns A and B	140
VI-25	Maximum Backwater Location (ℓ^*/b vs M) for Spillthrough Roughness Patterns C and D	141
VI-26	Maximum Backwater Location (ℓ^*/b vs M) for Spur Dike Roughness Patterns A and B	142
VI-27	Maximum Backwater Location (ℓ^*/b vs M) for Spur Dike Roughness Patterns C and D	143
VI-28	Plot of Residuals vs ℓ^*/b	148
VI-29	Maximum Backwater Height (h^*/y_0 vs M) for Spillthrough Roughness Patterns A and B	156
VI-30	Maximum Backwater (h^*/y_0 vs M) for Spillthrough Roughness Patterns C and D	157
VI-31	Maximum Backwater Height (h^*/y_0 vs M) for Wingwall Roughness Patterns A and B	158
VI-32	Maximum Backwater Height (h^*/y_0 vs M) for Wingwall Roughness Patterns C and D	159
VI-33	Maximum Backwater Height (h^*/y_0 vs M) for Wingwall Roughness Pattern P	160

LIST OF FIGURES
(Cont'd)

<u>Figure No.</u>		<u>Page No.</u>
VI-34	Maximum Backwater Height (h^*/y_0 vs M) for Spur Dike Roughness Patterns A and B	161
VI-35	Maximum Backwater Height (h^*/y_0 vs M) for Spur Dike Roughness Patterns C and D	162

LIST OF TABLES

Table No.		Page No.
III-1	Values of α , β , α_1 and β_1	40
IV-1	Roughness Combinations	47
V-1	Summary Table of Experimental Runs	63
V-2	Experimental Investigation Chart Centered Opening Runs	65
V-3	Experimental Investigation Chart Eccentric Runs	68
V-4	Experimental Investigation Chart Skew Runs	69
V-5	Experimental Investigation Uniform Flows	70
V-6	Spillthrough Runs Not Analyzed (All Roughness Pattern B)	71
V-7	Raw Data Collected for Each Run	72
V-8	Numbers of Moveable Gages	78
V-9	Stationary Gage Locations	78
VI-1	Analysis of Variance	93
VI-2	ANOVA of K^* With and Without Spur Dikes	106
VI-3	Testing of K^* With and Without Spur Dikes at 95 Percent Confidence Level	107
VI-4	ANOVA of K^* for 15° and 45° Skew Crossings	127
VI-5	Testing of K^* for Skew Crossing at 95 Percent Confidence Level	128
VI-6	ANOVA of ℓ/b With and Without Spur Dikes	134
VI-7	Testing of ℓ^*/b With and Without Spur Dikes	135
VI-8	Correlation Coefficients for Independent Variables	145
VI-9	Log-Linear Regressions for ℓ^*/b	147
VI-10	Beta Weights	150

LIST OF TABLES
(Cont'd)

<u>Table No.</u>		<u>Page No.</u>
VI-11	ANOVA of h^*/y_0 for Roughness Pattern C With and Without Spur Dike Data	154
VI-12	Testing of h^*/y_0 for Roughness Pattern C at 95 Percent Confidence Level	155

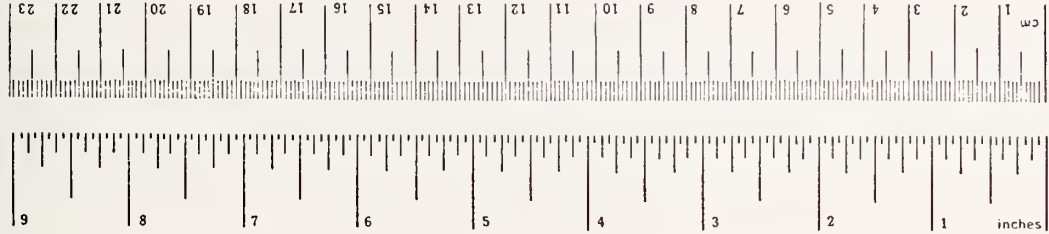
METRIC CONVERSION FACTORS

Approximate Conversions to Metric Measures

Symbol	When You Know	Multiply by	To Find	Symbol
LENGTH				
in	inches	2.5	centimeters	cm
ft	feet	30	centimeters	cm
yd	yards	0.9	meters	m
mi	miles	1.6	kilometers	km
AREA				
in ²	square inches	6.5	square centimeters	cm ²
ft ²	square feet	0.09	square meters	m ²
yd ²	square yards	0.8	square meters	m ²
mi ²	square miles	2.6	square kilometers	km ²
	acres	0.4	hectares	ha
MASS (weight)				
oz	ounces	28	grams	g
lb	pounds	0.45	kilograms	kg
	short tons (2000 lb)	0.9	tonnes	t
VOLUME				
tsp	teaspoons	5	milliliters	ml
Tbsp	tablespoons	15	milliliters	ml
fl oz	fluid ounces	30	milliliters	ml
c	cups	0.24	liters	l
pt	pints	0.47	liters	l
qt	quarts	0.95	liters	l
gal	gallons	3.8	liters	l
ft ³	cubic feet	0.03	cubic meters	m ³
yd ³	cubic yards	0.76	cubic meters	m ³
TEMPERATURE (exact)				
°F	Fahrenheit temperature	5/9 (after subtracting 32)	Celsius temperature	°C

Approximate Conversions from Metric Measures

Symbol	When You Know	Multiply by	To Find	Symbol
LENGTH				
mm	millimeters	0.04	inches	in
cm	centimeters	0.4	inches	in
m	meters	3.3	feet	ft
m	meters	1.1	yards	yd
km	kilometers	0.6	miles	mi
AREA				
cm ²	square centimeters	0.16	square inches	in ²
m ²	square meters	1.2	square yards	yd ²
km ²	square kilometers	0.4	square miles	mi ²
ha	hectares (10,000 m ²)	2.5	acres	ac
MASS (weight)				
g	grams	0.035	ounces	oz
kg	kilograms	2.2	pounds	lb
t	tonnes (1000 kg)	1.1	short tons	st
VOLUME				
ml	milliliters	0.03	fluid ounces	fl oz
l	liters	2.1	pints	pt
l	liters	1.06	quarts	qt
l	liters	0.26	gallons	gal
m ³	cubic meters	35	cubic feet	ft ³
m ³	cubic meters	1.3	cubic yards	yd ³
TEMPERATURE (exact)				
°C	Celsius temperature	9/5 (then add 32)	Fahrenheit temperature	°F



*1 in = 2.54 (exactly). For other exact conversions and more detailed tables, see NBS Misc. Publ. 286, Units of Weights and Measures, NIST Special Publication 330-119/286.

I. INTRODUCTION

This report is the second in a series of five volumes comprising the final report for the study entitled *Evaluation of Flood Risk Factors in the Design of Highway Stream Crossings*, authorized by the Federal Highway Administration (FHWA) under Contract No. DOT-FH-11-7669. The overall objective of the study is to develop an engineering systems analysis method to enhance the decision-making process in the design of highway stream crossings. This method applies economic risk techniques as well as standard hydraulic and hydrologic factors in the design of bridge waterways.

The present volume describes the analysis of the relationship between combinations of bridge openings, abutment shapes, flows and roughness densities and the resultant backwater. The analysis is based on data taken during a two-year period of operation of a large hydraulic flume. The relationships which were defined in the analysis can be extended into the computerized Finite Element Model simulation of the flood flow and backwater as described in Volume III.

STUDY OBJECTIVES

The principal purposes of this phase of the study were:

1. To collect raw data for the analysis and quantification of the effects of abutment shapes, channel roughness, and crossing skew and eccentricity on the magnitude and location of maximum backwater under varied flow conditions.
2. To provide additional information needed to update and possibly modify the FHWA backwater analysis method.

3. To evaluate two-dimensional aspects of backwater and the effects of main channel and overbank flows.

BACKGROUND

Highway design engineers have long understood the problems associated with constricting flow in natural waterways. The introduction of embankments and piers onto the flood plain and in the main channel alters the hydraulic behavior of the waterway and can appreciably affect the flood stage of the river during a major flooding event miles upstream. The result of a higher stage may be property and personal damages over what would have occurred had the waterway not been obstructed.

Awareness of the problem has led state highway departments to include an estimation of the hydraulic efficiency of the highway crossing structure along with the design specifications and cost of the structure. Usually the 50-year, 100-year, or maximum flood of record is used as the design flood for the hydraulic analysis. The importance and/or cost of the structure predicates the exact choice of the design storm. Once this choice is made, the stage and velocity reached in the waterway are determined for both the unobstructed flow and the flow with the crossing in place. This additional stage height attributable to the constriction of the flow is known as backwater.

Numerous methods exist for the estimation of backwater; some of them are described in detail in the literature review. Currently, three distinct methods are extensively used: the Federal Highway Administration Method (FHWA), the Geological Survey Method (USGS), and the Corps of Engineers Method (HEC-2). The FHWA method [1]* is derived from the work of Liu, Bradley and Plate [2] at Colorado State University in 1957. The

*Bracketed numbers refer to references placed at the end of the text material.

expression derived from the work for the computation of backwater is:

$$h_1^* = K^* \alpha_2 \frac{V_{n2}^2}{2g} + \alpha_1 \left[\left(\frac{A_{n2}}{A_4} \right)^2 - \left(\frac{A_{n2}}{A_1} \right)^2 \right] \frac{V_{n2}^2}{2g}$$

where

- h_1^* = total backwater (ft),
- K^* = total backwater coefficient,
- α_1 & α_2 = kinetic energy coefficient,
- A_{n2} = gross water area in constriction measured below normal stage (sq ft),
- V_{n2} = average velocity in constriction at normal depth or Q/A_{n2} (fps),
- A_4 = water area at section 4 where normal stage is reestablished (sq ft), and
- A_1 = total water area at section 1, (where the backwater is greatest), including that produced by the backwater (sq ft).

The total backwater coefficient (K^*) is empirically determined and accounts for the effect of piers, angle of skew, abutment shape and eccentricity. These effects are assumed to be additive and are functionally related to the dimensionless parameter M , where M is the ratio of the flow that can pass unimpeded through the bridge opening to the total flow. This method is restricted since it provides only a one-dimensional analysis along the centerline and it does not allow for natural river meandering, variable channel conveyance capacities, and cross flow from the channel to the overbank and vice versa.

The USGS method experimentally derived in 1965 by Kindsvater and Carter [3] is based on energy and continuity relationships developed between the upstream reaches and the location of the vena contracta. Energy loss is calculated by use of a conveyance method and a division of upstream areas into portions where energy is being dissipated due to both friction and contraction.

A recent report written by Schneider et al. [4] presents a modified method which updates the old USGS method and reportedly improves its accuracy to a considerable extent. Schneider employs a more accurate estimate of streamline length between sections using potential flow theory. He also proposes a slightly modified estimation of energy losses in the flow expansion reach. However, this method also is based on a single-dimension formulation of energy relationships and thus is limited as to the type of problem which can be solved and the accuracy of the solution.

The third widely applied backwater method is that developed by the Corps of Engineers in 1973 and called HEC-2 [5]. This computerized steady state model computes the water surface profile for river channels of any cross section for either subcritical or supercritical flow conditions. The effects of various hydraulic structures such as bridges, culverts, weirs, embankments and dams are considered in the computation. The computational procedure applies Bernoulli's Theorem for the total energy at each cross section and Manning's formula for the friction head loss between cross sections. Total head loss is calculated using an iterative process and includes transition loss, losses through bridges, and through culvert structures.

A fourth method, used as part of the present study, uses the finite element techniques for the solution of the equations describing flow and bulk transport of incompressible fluids. A computer model solving these equations, i.e., continuity and momentum relationships, was used in simulating backwater profiles in a two-dimensional plane at a bridge site located in Tallahalla, Mississippi, with good results. Among the advantages offered by this approach are: (1) a two-dimensional analysis; (2) irregular cross sections and channel bends can be specified; (3) energy losses are divided into frictional and eddy losses allowing the effects to be estimated separately; (4) roughness can be specified in the detail to which it is known; (5) boundary effects can be determined; and (6) multiple runs are possible with only slight additional effort. The principal disadvantages are: (1) the technique

presently does not handle transitional flow across the constriction; (2) the model must be calibrated with the field data to ascertain correct values of the eddy coefficients; (3) the model reliability is sensitive to user's ability to establish a grid for the finite elements; and (4) the model requires substantial computer capability.

This report presents the analysis of information collected from the operation over a two-year period of a 22.7 x 184 ft flume used in studying the effects on backwater of various bridge openings, abutment shapes, flows and roughness densities. The study was restricted to subcritical flow conditions. The range of bridge openings varied from three to eleven feet while abutment shapes included 45° wingwall, spillthrough and elliptical spur dikes. Though most model openings were centered in the flume and perpendicular to the flow, both eccentric and skew crossings were also investigated.

The interactive effects of flood plain and main channel flow areas on backwater were simulated through the use of artificial large scale roughness elements placed in the flume to represent the differing effect on flow of both the heavily vegetated overbank and the main channel areas. The actual degree of roughness produced in the flume was even higher than observed because the distortion of the scale model requires additional roughness to satisfy the law of dynamic similitude between the model and the prototype. Conceptually, the energy loss due to the viscosity of the fluid and the turbulence generated by the roughness elements was treated as energy loss attributable to frictional forces alone.

The choice of the density and location of the roughness elements is the subject of Volume I of this study entitled *Experimental Determination of Channel Resistance for Large Scale Roughness*, Report No. FHWA-RD-75-51, available from the National Technical Information Service.

Chapter II of this report is a literature review of current one-dimensional backwater methods. Chapter III presents an analysis of the hydraulic model design which forms the theoretical basis for the experimental configurations. The experimental equipment is described in Chapter IV and the important procedural methods, both in the collection and the reduction of raw data, are described in Chapter V. Operational and analysis problems encountered either in the collection or the analysis of data are included in this section. Chapter VI describes the dimensional analysis, which to a large extent directs the data analysis presented in the same chapter. Conclusions and recommendations follow in Chapters VII and VIII, respectively.

Listings of the processed and sorted data, including condensed output summaries, is available in a separately bound appendix available through the Federal Highway Administration Office of Research (HRS-42), Washington, D.C. 20590. Condensed output summaries for each flume run are contained in an appendix attached to this report.

II. LITERATURE REVIEW

In the last half of the 1800's and during the early part of this century the effects of stream constriction and pier design on backwater were first defined by D'Aubuisson, Eytelwein, Nagler, Hutton, Rehbock, Lane, Yarnell and many others. The earlier investigators used mathematical analysis while Nagler and his contemporaries developed hydraulic models and gathered data from real-world observations. Nagler focused primarily on the backwater effects of piers, comparing various shapes, sizes and orientations to flow [6]. Rehbock, in Germany, also used hydraulic models to determine the backwater effects of piers, using three classifications of flow. He found that the maximum backwater caused by pier obstruction depends on the channel-bridge waterway contraction ratio, the Froude number of the unobstructed flow and the pier geometry [7].

In the 1930's D.L. Yarnell [8] experimentally verified existing backwater formulas for pier effects and in the process came to a number of important conclusions:

1. The height of the backwater due to bridge piers varies directly as the depth of unobstructed channel,
2. For the lower velocities, a lense-shaped nose and tail offer minimum resistance,
3. The optimum ratio of pier length to width probably varies with the velocity and is generally between 4 and 7,
4. Placing the piers at an angle with the current has an insignificant effect on the amount of backwater if the angle is less than 10° ,
5. Placing the piers at an angle of 20° or more with the current materially increases the amount of backwater, the increase depending upon the quantity of flow, the depth, and the channel contractions.

E.W. Lane [9] was the first to study the effects of channel constriction on open-channel flow, laying the groundwork for backwater formulas by developing an empirical discharge coefficient from the discharges and difference of surface elevation upstream and downstream from the constriction.

A working but generally inapplicable method for computing the maximum backwater height due to channel constriction was developed in the early 1950's by H.J. Tracy and R.W. Carter [10]. This method was based on the laboratory work of Kindsvater, Tracy and Carter [3] to estimate discharge through a channel constriction (see Figure II-1). The relationship established, based on one-dimensional energy and continuity relationship, is given below:

$$Q = C b h_3 \sqrt{2g [\Delta h + \alpha_1 V_1^2/2g - E_{f(1-3)}]} \quad (1)$$

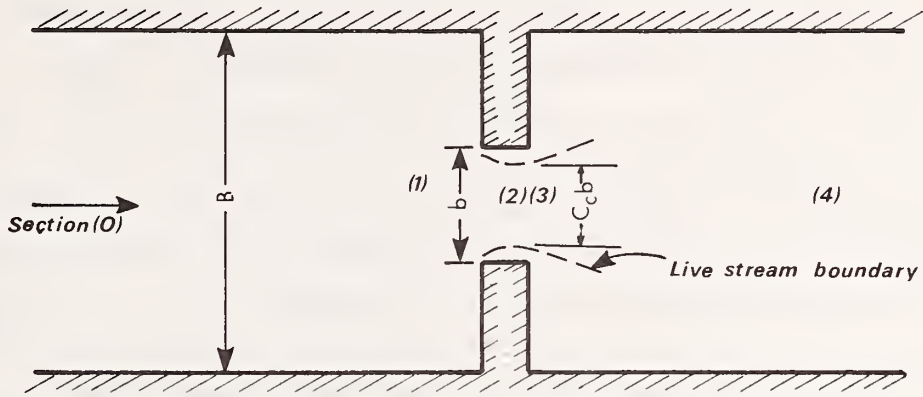
where:

- Q = discharge through the opening (cfs),
- C = Kindsvater discharge coefficient,
- b = width of the opening (ft),
- h_3 = water surface elevation at Section 3 (ft)
(Sections 1, 2, 3 and 4 are shown in Figure II-1),
- Δh = difference in surface elevations at Section 1 and 3 (ft),
- α_1 = energy correction factor to account for unequal velocity distribution at Section 1,
- $V_1^2/2g$ = velocity head (ft), and
- $E_{f(1-3)}$ = head loss due to friction between Sections 1 and 3.

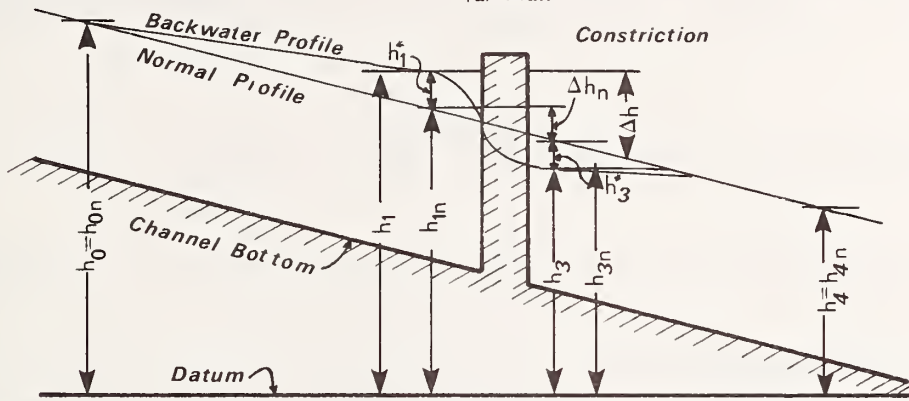
The relationship is a convenient one for computing discharge from field measurements at an existing bridge. It is not, however, in terms of the maximum backwater h_1^* , which is of interest to highway designers.

Parameters shown in the figure but not included in Equation 1 are:

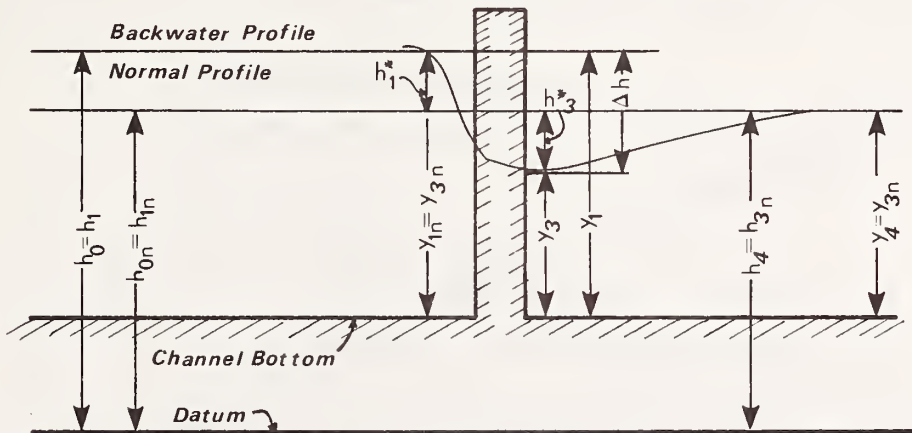
- B = flood plain width,
- C_e = contraction coefficient, and
- h_1^* = maximum backwater above normal elevation at Section 1.



(a) Plan



(b) Elevation



(c) Elevation adapted to assumption of zero friction loss

FIGURE II-1. DEFINITION SKETCH OF BACKWATER REACH
(Source: Reference 10)

Five cross sections are shown in Figure II-1b. Section 0 refers to the area upstream of the constriction unaffected by backwater effects emanating from the constriction, section 1 defines the cross section at the location of the maximum backwater, section 2 is located in the center of the constriction, section 3 is defined by the location of the vena contracta which is the point at which the live stream boundaries are closest, and finally, section 4 is the cross section where normal flow depth returns. Through dimensional analysis it was shown that the Kindsvater discharge coefficient, C , is a function of approach channel shape and roughness, Froude number ($F = \frac{Q}{bh_3\sqrt{gh_3}}$), the geometry of the constriction and the contraction ratio (m).

The contraction ratio, m , is defined as

$$m = 1 - \frac{K_b}{K_B}$$

where

K = conveyance

K_b = conveyance of section of length b

K_B = conveyance of section of length B .

Conveyance is defined from Manning's equation as:

$$K = \frac{1.49}{n} AR^{2/3}$$

where

n = Manning's roughness factor

A = cross-sectional area

R = hydraulic radius.

Note that if channel slopes are constant

$$m = 1 - \frac{q_b}{q_B}$$

where

q_b = flow carried in width b , and
 q_B = flow carried in width B .

Tracy and Carter [10] constructed a family of curves showing the relationship between C and the dimensionless parameters which exhibited a functional response. These curves are not included here.

Tracy and Carter later found that $\frac{h_1^*}{\Delta h}$ was primarily a function of the percentage of contraction. The quantity Δh was defined as

$$\Delta h = \frac{Q^2}{2gb^2h_3^2C^2} - \alpha_1 \frac{V_1^2}{2g} + E_{f(1-3)} \quad (2)$$

The backwater h_1^* was then found by multiplying Δh by the backwater ratio

$\frac{h_1^*}{\Delta h}$, selected from measured laboratory data summarized in Figure II-2.

These calculations assume a standard condition, i.e., vertical constrictions with square-edged abutments in a rectangular (and horizontal) flume for three variations of channel roughness.

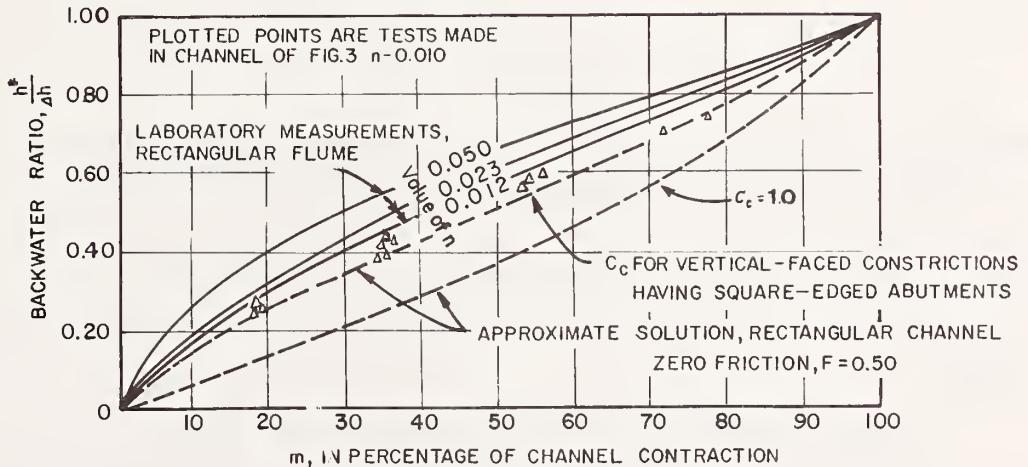


FIGURE II-2. BACKWATER RATIO FOR CHANNELS HAVING VERTICAL-FACED CONSTRICTIONS WITH SQUARE-EDGED ABUTMENTS. Source: Reference 10.

The application of this method is limited for several reasons:

1. Since Δh is an independent variable, the estimation of h_1^* through $\frac{h_1^*}{\Delta h}$ is a trial and error process not practicable for the direct use of h_1^* in bridge design calculations.
2. The small scale of the hydraulic model limits the application of relationships between the contraction ratio, channel roughness and constriction geometry.
3. The hydraulic model used in the experiments was designed with a level-bottom channel, in which for a given discharge the velocity, depth and energy gradient of unobstructed flow vary from section to section; that is, the flow is nonuniform and there is no standard flow condition.
4. The scope of the methodology was limited to steady tranquil flows through single-opening constrictions and does not include effects of scour around bridge piers and abutments or boundary friction due to heavy vegetal growth along the stream banks.

The method proposed by Tracy and Carter [10] has most recently been updated and modified by field data collected by the USGS in conjunction with the FHWA and the State Highway Departments of Mississippi, Alabama and Louisiana. In their report, not yet published, Schneider et al. [4] propose refinements to both the contraction reach and expansion reach energy loss formulations as given in Equation 1, which is repeated here for convenience of referral:

$$Q = C b h_3 \sqrt{2g[\Delta h + \alpha_1 V_1^2/2g - E_{f(1-3)}]}$$

The method of solution for Equation 1 for backwater is an iterative approach using a "step-backwater" technique. Normal water surface elevation is first calculated followed by constricted flow calculations. The distinction between the Carter method and the Schneider method is that modifications for head loss computation proposed by Schneider are incorporated into the solution algorithm.

The energy loss term due to friction, $E_{f(1-3)}$, represents the head loss occurring in moving from cross section 1 to cross section 3 as shown in Figure II-3. The "L" values shown on the horizontal axis represent distances

between cross sections. Thus L_d is the center line distance from cross section "d" to cross section 2. Expanding $E_{f(1-3)}$ according to Figure II-3:

$$E_{f(1-3)} = \frac{L_w Q^2}{K_1 K_q} + \frac{L_d Q^2}{K_d K_3} + \frac{L Q^2}{K_3^2} \quad (3)$$

- where
- L_w = distance from the location of the maximum backwater to the toe of the spur dikes (ft),
 - L_d = length of the spur dike (ft), and
 - L = length of the bridge abutment.
 - K_1 = approach conveyance at section 1 (ft^3/sec),
 - K_q = that portion of the approach conveyance, K_1 , corresponding to the bridge width b (ft^3/sec),
 - K_d = conveyance of the cross section at the toe of the spur dikes (ft^3/sec), and
 - K_3 = conveyance of the cross section at the abutments (ft^3/sec).

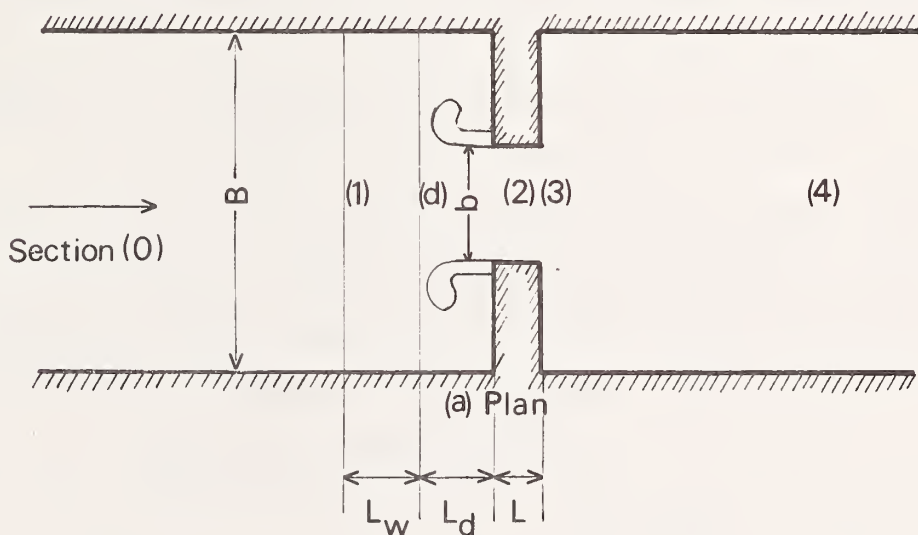


FIGURE II-3. ENERGY LOSSES FOR SCHNEIDER METHOD

Each of the three components of Equation 3 represents the energy loss due to friction over the stated length. The components of Equation 3 represent the geometric mean of the energy slopes at the end cross sections of each reach times the distance between the sections. Schneider assumed the uniform flow equation for some cross section i having conveyance K_i as:

$$Q = K_i S_f^{1/2}$$

which implies

$$S_f^{1/2} = Q/K_i$$

The geometric mean friction slope can then be represented by:

$$S_{f(i-j)} = \frac{Q^2}{K_i K_j}$$

where subscripts i and j refer to upstream and downstream conveyances, respectively.

Schneider et al [4] propose two modifications to Equation 3 which represent changes in approach and expansion reach energy losses. First, in the modification for the contraction reach, L_w , Schneider assumes that for large contraction ratios the average streamline length L_w is actually much greater than the straight line distance L_w . For the determination of the average streamline length, L_w , he studied an idealized constriction using potential flow theory. Average streamline length as a function of the length of the approach reach divided by the width of the opening and the contraction ratio were determined. Tabular values are not presented in this report, but can be found in reference 4.

Second, Schneider calculates head losses in the flow expansion reach as:

$$h_{L(3-4)} = h_{f(3-4)} + h_e \quad (4)$$

where

$$h_{f(3-4)} = \frac{bQ^2}{K_c K_{4n}} \quad (5)$$

and

$$h_e = \frac{Q^2}{2gA_4^2} \left[\left(2\beta_4 - a_4 \right) + 2\beta_3 \frac{A_4}{A_3} + \alpha_3 \left(\frac{A_4}{A_3} \right)^2 \right] \quad (6)$$

Equation 5 represents the frictional head loss between sections 3 and 4. Note that normal depth is assumed to occur one bridge length downstream from section 3. K_{4n} is the conveyance at normal depth for section 4 and K_c is the smaller of the conveyances K_q or K_3 . Equation 6 represents flow expansion losses for an idealized expansion in open channel flow according to Henderson [11]. Here beta and alpha are momentum and energy coefficients while A is cross sectional area. Subscripts refer to cross section locations.

Analyzing the data collected for 31 floods, Schneider reports that the unmodified Geological Survey and FHWA methods underpredict backwater by 45 and 47 percent, respectively. Using the proposed modification the mean error for computing backwater was six percent.

A simple formula for computing backwater was proposed by C.F. Izzard in 1954 [12] in his discussion of the Kindsvater and Carter paper [3]. This provided the basis for the beginnings of the method which became known generally as the FHWA method. It is

$$h_1 - h_n = h_b = K_b \frac{V_{n2}^2}{2g}$$

where $V_{n2} = \frac{Q}{bh_n}$ is a hypothetical velocity and K_b is an empirical backwater coefficient. The data compiled by Tracy and Carter were used by Izzard [13] to develop a simple correlation of the maximum backwater/contraction ratio and Froude number. The correlation was useable for rough estimates but did not

consider important variables such as channel slope and roughness, skew and eccentricity of the crossing and piers.

Liu, Bradley and Plate [2] at the Colorado State University used Izzard's concept for a series of more sophisticated hydraulic model experiments. They defined the backwater expression by applying the principle of conservation of energy between the point of maximum backwater upstream from the contraction and the point downstream at which the flow has reached normal stage. This method assumes that the channel in the vicinity of the bridge is essentially straight, the cross sectional area of the stream is reasonably uniform and the gradient of the bottom is constant between cross sections 1 and 4 (Figure II-4). The analysis applies only to steady tranquil flow.

The theoretical development by Liu et al [2] is essentially an application of one-dimensional energy relationships between cross sections 1 and 4, respectively. The analysis, condensed from reference 14, follows. Equating the two sections:

$$S_0 L_{(1-4)} + y_1 + \frac{\alpha_1 V_1^2}{2g} = y_4 + \frac{\alpha_4 V_4^2}{2g} + h_T$$

where

- S_0 = channel slope (ft/ft),
- $L_{(1-4)}$ = distance between sections 1 and 4,
- y_1 = depth of water at section 1,
- $\frac{\alpha_1 V_1^2}{2g}$ = average velocity head at section 1,
- y_4 = normal depth of water at section 4, and
- h_T = total energy loss between sections 1 and 4.

Since the frictional loss term in feet/foot of channel is contained in the total energy loss term h_T , these quantities can be eliminated from both sides of the equation and h_T replaced by h_b . Rearranging thus yields:

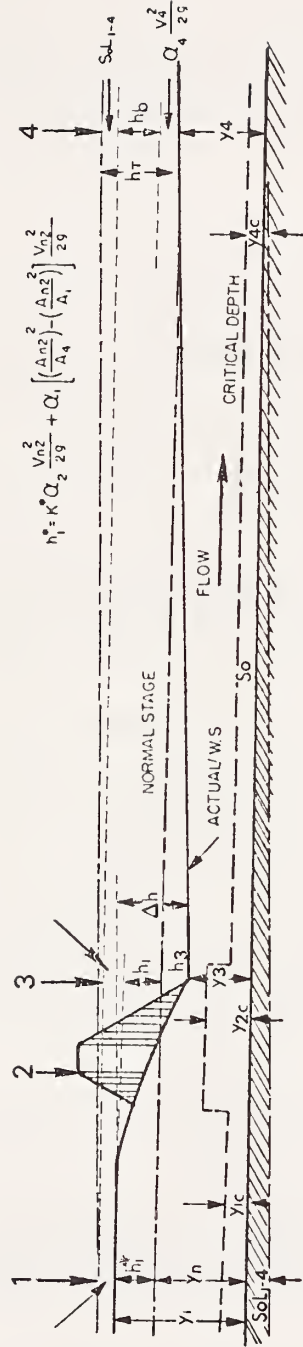


FIGURE II-4.
RACKWATER ANALYSIS

$$y_1 - y_4 = \frac{\alpha_4 V_4^2}{2g} - \frac{\alpha_1 V_1^2}{2g} + h_b$$

The additional loss h_b can be expressed as a product of velocity head in the constriction at normal flow and an energy loss coefficient, K^* .

$$h_b = K^* \frac{\alpha_2 V_{n2}^2}{2g}$$

Replacing h_b with the above expression and $y_1 - y_4$ with h_1^* yields:

$$h_1^* = K^* \frac{\alpha_2 V_{n2}^2}{2g} + \left[\frac{\alpha_4 V_4^2}{2g} - \frac{\alpha_1 V_1^2}{2g} \right]$$

The analysis assumes that the cross sectional areas at 1 and 4 are essentially the same and from continuity-- $A_1 V_1 = A_4 V_4 = A_{n2} V_{n2}$ --allows:

$$V_4 = \frac{A_{n2} V_{n2}}{A_4}, \text{ and}$$

$$V_1 = \frac{A_{n2} V_{n2}}{A_1}$$

Replacing V_1 and V_4 with the above and factoring V_{n2} leaves:

$$h_1^* = K^* \alpha_2 \frac{V_{n2}^2}{2g} + \alpha_1 \left[\frac{A_{n2}^2}{A_4^2} - \frac{A_{n2}^2}{A_1^2} \right] \frac{V_{n2}^2}{2g} \quad (7)$$

Through the aid of dimensional analysis a backwater coefficient K^* was determined experimentally and was found to be a function primarily of

1. Stream constriction as measured by the opening ratio M , where $M = \frac{b}{B}$,

2. Type and shape of bridge abutment--wingwall, spillthrough, etc.,
3. Number, size, shape and orientation of piers in the constriction,
4. Eccentricity or asymmetric position of bridge on the flood plain,
5. Skew (bridge crosses river or flood plain at other than 90 degrees),
and
6. Froude number.

The hydraulic model used for these experiments had a variable flume slope, two flume widths and two types of bed roughness. The experiments conducted with this flume used unobstructed flow data (normal depth and Froude number) taken for each slope, discharge rate and roughness type in order to make a realistic judgment of the effects of the constriction on the flow through the constriction and the resulting backwater. The flume constriction was formed with models of three types of bridge abutments and/or piers. The specific purpose of the study was to determine the maximum height of backwater for a given constriction. Crossing conditions studied were:

1. Simple normal crossing,
2. Abnormal stage-discharge condition,
3. Dual-bridges contraction,
4. Bridge girders partially submerged,
5. Skew crossing,
6. Eccentric crossing, and
7. Piers with and without abutments.

U.S. Geological Survey field surveys in Mississippi conducted to verify the laboratory tests showed that the model application is limited to medium size bridges (i.e., structures up to 220 feet in length with flood plains up to .5 mile in width) since it underpredicts backwater for bridges with a larger channel/opening ratio [14].

The calculations derived from the Colorado State University study and improvements made since are incorporated in the 1970 edition of the Bureau

of Public Roads Design Series, "Hydraulics of Bridge Waterways" [14]. This publication presents the most advanced method in wide use for estimating backwater in a noncritical, uniform flow situation. The manual also presents means for making preliminary estimates of the effects of spur dikes, critical stage-discharge conditions, and Manning roughness coefficients for stream channels and flood plains.

The backwater effects of flood plain flow were the focus of an article by E.M. Laursen [15] which followed the Colorado State University investigation. Laursen noted the two-dimensional aspects of flood flow in a wide valley where the bridge embankment forces overbank flow to move laterally to the bridge opening and, on the downstream side of the constriction, to move laterally back to the flow boundary. Laursen postulated that the downstream diffusion in section 4 is possibly a significant factor in calculating upstream backwater and based his analysis for sections 1 and 4 on momentum principles. He pointed out that previous experiments with hydraulic models actually simulated cross sections 2 and 3 because of the relatively small dimensions involved, leaving unconsidered the flow behavior of cross sections 1 and 4 such as would be characteristic of the prototype.

C.L. Yen has contributed to the description of the characteristics of flood plain flow versus channel flow and in a 1971 paper with D.R. Overton [16] presented a method for subdividing the flood plain cross section in order to evaluate turbulent flow resistance for each subsection. Yen and Overton suggested that since Manning's n -values for both main channel and flood plain are lower than those for wide rectangular channels of the same materials, the n -values reflect not only the roughness but also the effects of channel geometry. While these ideas have not been approached in the current study, they offer an avenue for greater accuracy in flood plain discharge calculations and thus backwater calculations.

A review of the literature demonstrates there are two basic methods in which the estimation of backwater has advanced. The first, and by far the

most rapid, is the physical modeling approach. The second method is an empirical approach in which laboratory analysis techniques are applied to field studies and the results are used to modify the flume-based theories of Kindsvater and Liu. As the effect of flooding on ever-urbanizing areas and the increased cost of construction and maintenance of crossing structures has escalated, so has the interest in more reliable methods of estimating backwater. The present study recognizes this and provides a large data base for the current needs of this study as stated in the purposes for the study and for the needs of both present and future proposed backwater techniques.

III. HYDRAULIC MODEL DESIGN

GENERAL DESCRIPTION

The difficulties involved in measuring flows and velocities during major flood events make the study of hydraulic behavior in the field an expensive if not impossible task. For this reason, hydraulic engineers have historically used physical models of flood plain behavior in order to exercise control over the events taking place and to be able to vary parameters in order to determine important variables and establish functional relationships. If dynamic similitude is maintained between the model and the prototype, results are directly applicable to the field situation. It must be recognized of course that the wide variation in width-depth ratio observed in many streams makes it physically impossible to model the entire stream or even the entire area affected by backwater. However, the physical model can be used to study flow patterns adjacent to the bridge embankments and opening.

This chapter presents the analysis demonstrating dynamic similitude between an average set of prototype conditions and the model. Model distortion, which is practically unavoidable in studying any flood plain situation, is developed and its effect on model roughness quantified. The chapter concludes with a development of the theory applicable to the artificial roughness elements and configurations used in the model studies.

DYNAMIC SIMILITUDE

The water surface elevation in an open-channel flow is governed by the mutual interaction of forces of inertia, gravity and viscosity. Due to the presence of a free surface in open-channel flow, the gravity forces are always important. In some stretches of river where the water surface slope is mild, the viscous effect may become important and both gravity and viscous forces control the flow.

The effect of gravity is characterized by the Froude number:

$$Fr = \frac{V^2}{gR}$$

where

V = average velocity

R = hydraulic radius

g = gravitational constant

and the viscous effect by the Reynolds number:

$$Re = \frac{VR\rho}{\mu} = \frac{VR}{\nu}$$

where

Re = Reynolds number,

μ = dynamic viscosity,

ρ = density, and

ν = kinematic viscosity.

When a scale model is used to study the flow characteristics of its prototype, dynamic similarity requires that the Froude number and Reynolds number be the same in both model and prototype. That is,

$$\frac{V_m R_m}{\nu_m} = \frac{V_p R_p}{\nu_p} \qquad \frac{V_m^2}{g_m R_m} = \frac{V_p^2}{g_p R_p}$$

where the subscripts m and p refer to the model and prototype, respectively. Under ordinary conditions, $g_m = g_p$, hence to satisfy both the above conditions simultaneously it is necessary to have

$$\frac{v_m}{v_p} = \left(\frac{R_m}{R_p} \right)^{3/2}$$

That is, in order to achieve the dynamic similarity a scale model will be such that the kinematic viscosity of the fluid in the model must be less than that in the prototype. Unfortunately, there are few liquids less viscous than water, and none of those is inexpensive and safe to use. If water is used in the model, i.e., $v_m = v_p$, then R_m must equal R_p . Hence, the model is identical to the prototype. In other words, the realization of a dynamically similar small scale model is practically impossible.

In open channel flow the gravity forces and thus the Froude number are considered to be the predominant factors. Consequently, the Froude number of the model and prototype should be held identical. In prototype open channel flow, the Reynolds number is high, thus the viscous forces are usually only secondary. In order to account for the viscous effect a scale model is normally calibrated for its roughness by trial and error process. Such a process involves successive adjustment of model roughness until the appropriate flows and depths in the prototype are reproduced in the model. The model was not calibrated in this study because the study is intended for a spectrum of riverine situations rather than a specific stream crossing site. The roughness field selected in the study represents an average condition over the spectrum.

A further complication frequently ensues in dealing with physical models of river and tidal conditions. Since the laboratory space is usually limited, the model scale in depth is necessarily small. The actual water depth in the

model may be only a fraction of an inch, producing a laminar flow. Since the flow in the prototype is invariably turbulent, the viscous forces in the laminar flow of the model would be of an entirely different type compared with the prototype. As a result, the two systems would be virtually unrelated to one another, and the model results could not be used to represent the prototype conditions.

This difficulty may be overcome by the use of different scales for vertical and horizontal dimensions in the model. The vertical (depth) scale is exaggerated in relation to the horizontal (distance) scale to increase the velocity scale and produce turbulent flow in the model. As described by Henderson [11], the scale distortion does not seriously affect the flow pattern, and in fixed-bed models it gives satisfactory results. Such exaggerated scale models have the advantage of saving laboratory space. For example, if M is the ratio of the vertical scale to the horizontal scale, then there is an M -fold economy for the model space requirements compared to an undistorted model.

The background analysis leading to the experimental setup of this study is presented in the following sections. It has been assumed that the flow is subcritical, the width of flood plain is large in comparison with the main channel, and the channel geometry is nonprismatic. The flow has been assumed to be dominated by gravity and channel resistance except in the immediate vicinity of the bridge.

GOVERNING FLOW EQUATIONS IN BRIDGE WATERWAYS

Consider a gradually-varied flow in an open channel. The total energy at a section x is given as

$$H = y + \frac{\alpha V^2}{2g} \quad (8)$$

where

- y = water surface elevation,
- V = average velocity,
- α = energy coefficient and
- g = gravitational acceleration.

Differentiating Equation 8 with respect to x yields:

$$\frac{dH}{dx} = \frac{dy}{dx} + \frac{\alpha}{2g} \frac{dV^2}{dx} \quad (9)$$

Since $y = h + z$

$$\frac{dy}{dx} = \frac{dh}{dx} + \frac{dz}{dx} = \frac{dh}{dx} - s \quad (10)$$

where

- h = flow depth,
- z = bottom elevation, and
- s = slope of the channel bed.

If the flow rate of the channel is Q, and the cross-sectional area at x is A,

$$V = \frac{Q}{A} \quad (11)$$

The second term in Equation 9 can be expressed as

$$\frac{\alpha}{2g} \frac{dV^2}{dx} = \frac{\alpha Q^2 dA^{-2}}{2g} = - \frac{\alpha Q^2}{gA^3} \frac{dA}{dx} \quad (12)$$

In the nonprismatic channel, A is a function of x and h. In functional form

$$A = \phi(x, h). \text{ Thus,}$$

$$\frac{dA}{dx} = \frac{\partial A}{\partial x} + \frac{\partial A}{\partial h} \frac{dh}{dx} = \frac{\partial A}{\partial x} + B \frac{dh}{dx} \quad (13)$$

where

$$B = \text{width of water surface at depth } h.$$

Substituting Equation 13 into Equation 12, we obtain

$$\frac{\alpha}{2g} \frac{dV^2}{dx} = - \frac{\alpha}{g} \frac{Q^2}{A^3} \left(\frac{\partial A}{\partial x} + B \frac{dh}{dx} \right) \quad (14)$$

By substituting Equations 10 and 14 into Equation 9, we obtain

$$\frac{dH}{dx} = \frac{dh}{dx} - s - \frac{\alpha}{g} \frac{Q^2}{A^3} \left(\frac{\partial A}{\partial x} + B \frac{dh}{dx} \right) \quad (15)$$

Since the total energy, H, decreases when x increases, the rate of change in $\frac{dH}{dx}$ is always negative. Hence the energy slope (gradient) is

$$s_f = - \frac{dH}{dx} \quad (16)$$

At this time the exact determination of the energy gradient of a nonuniform flow is unknown. It is customary to assume that the uniform flow formula and roughness coefficients may be used to evaluate the energy gradient of gradually varied flow (where the energy loss may be regarded as entirely due to surface resistance). At a given section, when the Manning formula is used,

$$s_f = \frac{n^2 V^2}{2.22R^{4/3}} \quad (17)$$

and, when the Chezy formula is used,

$$s_f = \frac{V^2}{C^2 R} \quad (18)$$

where,

n = Manning's roughness coefficient,

C = Chezy roughness coefficient, and

R = hydraulic radius.

Determination of the energy gradient is further complicated if the flow is rapidly varied. In this case the overall flow resistance consists of boundary friction and local energy loss caused by the abrupt change in flow geometry. In the case of bridge waterways the geometric change involves the flow contraction and expansion at the bridge. The local energy loss is usually treated as proportional to the velocity head at a given section. For a particular geometric variation, i (e.g., channel expansion), the energy loss is expressed as:

$$(H_L)_i = K_i \frac{V^2}{2g} \quad (19)$$

where K_i is the loss coefficient. The total energy loss due to N geometric variations existing in the river reach L is:

$$H_L = \left(\sum_{i=1}^N K_i \right) \frac{V^2}{2g} = K \frac{V^2}{2g} \quad (20)$$

The average energy gradient of reach L is:

$$\frac{H_L}{L} = \frac{K}{L} \frac{V^2}{2g} \quad (21)$$

Hence, for rapidly-varied flow, the value of s_f is given by the sum of frictional losses and the loss incurred due to the changes in the stream geometry. Thus

$$-\frac{dH}{dx} = s_f = \frac{n^2 V^2}{2.22R^{4/3}} + \frac{K}{L} \frac{V^2}{2g} \quad (22)$$

or

$$-\frac{dH}{dx} = s_f = \frac{V^2}{C^2 R} + \frac{K}{L} \frac{V^2}{2g} \quad (23)$$

Equation 23 can be rearranged to yield:

$$-\frac{dH}{dx} = \left(\frac{g}{C^2} + \frac{KR}{2L} \right) \frac{V^2}{gR} \quad (24)$$

Substituting Equation 24 into Equation 15, we obtain:

$$\frac{dh}{dx} = s - \left(\frac{g}{C^2} + \frac{KR}{2L} \right) \frac{V^2}{gR} + \frac{\alpha}{g} \frac{Q^2}{A^3} \left(\frac{\partial A}{\partial x} + B \frac{dh}{dx} \right) \quad (25)$$

Applying $A = RP$ and $\frac{Q}{A} = V$, where P is the wetted perimeter, to Equation 25 we have

$$\frac{1}{s} \frac{dh}{dx} = \frac{1 - \frac{\alpha F^2}{s} \left[\left(\frac{g}{C^2} + \frac{KR}{2L} \right) - \frac{\alpha}{P} \frac{\partial A}{\partial x} \right]}{1 - \frac{\alpha B}{P} \alpha F^2} \quad (26)$$

where

$$\alpha F = \frac{V^2}{gR} \quad .$$

Equation 26 is the differential equation for one-dimensional non-uniform flow. The flow could be either gradually varied or rapidly varied. The purpose of deriving Equation 26 is to use the equation for establishing the similarity requirements for the scale model, as will be described in the following section.

REQUIREMENTS OF MODEL SCALES

Equation 26 may be written for the prototype as:

$$\frac{1}{s_p} \frac{dh_p}{dx_p} = \frac{1 - \frac{\gamma F_p^2}{s_p} \left[\left(\frac{g}{C_p^2} + \frac{K_p R_p}{2L_p} \right) - \frac{\alpha}{P_p} \frac{\partial A_p}{\partial x_p} \right]}{1 - \frac{\alpha B_p}{P_p} \gamma F_p^2} \quad (27)$$

The model version of Equation 27 is:

$$\frac{1}{s_m} \frac{dh_m}{dx_m} = \frac{1 - \frac{\gamma F_m^2}{s_m} \left[\left(\frac{g}{C_m^2} + \frac{K_m R_m}{2L_m} \right) - \frac{\alpha}{P_m} \frac{A_m}{x_m} \right]}{1 - \frac{\alpha B_m}{P_m} \gamma F_m^2} \quad (28)$$

Substituting $a_r a_p$ for a_m in Equation 28, we obtain:

$$\frac{1}{s_p} \frac{dh_p}{dx_p} \left(\frac{h_r}{s_r x_r} \right) = \frac{1 - \frac{\gamma F_p^2}{s_p} \left[\frac{g}{C_p^2} \left(\frac{\gamma F_r^2}{s_r C_r^2} \right) + \frac{K_p R_p}{2L_p} \left(\frac{\gamma F_r^2 K_r R_r}{s_r L_r} \right) \right]}{1 - \frac{\alpha B_p}{P_p} \gamma F_p^2 \left(\frac{B_r \gamma F_r^2}{P_r} \right)} \quad (29)$$

$$= \frac{1 - \frac{\gamma F_p^2}{s_p} \left(\frac{\alpha}{P_p} \frac{A_p}{s_p} \frac{\gamma F_r^2 A_r}{s_r P_r x_r} \right)}{1 - \frac{\alpha B_p}{P_p} \gamma F_p^2 \left(\frac{B_r \gamma F_r^2}{P_r} \right)}$$

If the model is expected to be dynamically similar to the prototype with respect to the section properties only, then the prototype and model versions

of Equations 27 and 28 of the dimensionless equation of motion must necessarily be identical. From a comparison of Equations 27 and 29 it follows that these equations can be identical only if each of the expressions in the square brackets of Equation 29 is equal to unity, that is:

$$\left. \begin{aligned}
 \frac{h_r}{s_r x_r} &= 1 \\
 \frac{\pi F_r^2}{s_r C_r^2} &= 1 \\
 \frac{\pi F_r^2 K_r R_r}{s_r L_r} &= 1 \\
 \frac{\pi F_r^2 A_r}{s_r P_r x_r} &= 1 \\
 \frac{B_r \pi F_r^2}{P_r} &= 1
 \end{aligned} \right\} \quad (30)$$

where the subscript r represents the ratio of model to prototype.

If the flow cross section is sufficiently wide, it is possible to express the scale of the wetted perimeter P in terms of the horizontal scale alone. We may arrive at the following set of scales of the geometric properties of the flow cross section:

$$h_r = y_r, \quad A_r = x_r y_r, \quad B_r = x_r, \quad P_r = x_r \quad (31)$$

Substituting Equation 31 in Equation 30 yields:

$$s_r = \frac{y_r}{x_r}$$

$$F_r = 1 \tag{32}$$

$$K_r = 1$$

$$C_r^2 = \frac{x_r}{y_r} \tag{32}$$

Equation 32 gives the conditions of dynamic similarity for nonuniform flow, including gradually varied as well as rapidly varied, in distorted models. According to Equation 32, a vertically exaggerated model must be designed to have:

1. The same Froude number as the prototype,
2. A larger slope than the prototype,
3. A larger roughness than the prototype, and
4. Similar coefficients of local energy loss to that of the prototype.

In the design of a scale model for studying bridge backwater, problems exist with the third condition in Equation 32 since loss coefficients associated with the bridge constriction have not been established yet. Indeed, these coefficients are part of the information sought in the study itself. Fortunately, coefficients of the local energy losses are usually a function of certain dimensionless ratios describing the geometry responsible for the local energy losses. It appears that these ratios are often identical for both model and prototype, in spite of the length distortion. Consequently, the third condition (i.e., $K_r = 1$) in Equation 32 can frequently be regarded as satisfied automatically.

In specifying the roughness requirement, $C_r^2 = \frac{x_r}{y_r}$ in Equation 32, roughness factors may be expressed by Manning's n as well as Chézy's C . The expression for the n ratio in the model and the prototype is derived as follows:

Since

$$C = \frac{R^{1/6}}{n} ,$$
$$C_r^2 = \frac{R_r^{1/3}}{n_r^2} = \frac{x_r}{y_r} . \quad (33)$$

Equation 33 then yields:

$$n_r^2 = R_r^{1/3} \cdot \frac{y_r}{x_r}$$

or

$$n_r = \frac{R_r^{1/6} y_r^{1/2}}{x_r^{1/2}} \quad (34)$$

Application of Equation 31 to Equation 34 yields:

$$n_r = \frac{y_r^{2/3}}{x_r^{1/2}} \quad (35)$$

Equation 35 can also be derived by the direct application of the Manning equation.

For the practical purposes of this study, the design of the scale model is based upon the conditions of:

$$F_r = 1 , \quad s_r = \frac{y_r}{x_r} , \quad C_r = \left[\frac{x_r}{y_r} \right]^{1/2} , \quad \text{or } n_r = \frac{y_r^{2/3}}{x_r^{1/2}} . \quad (36)$$

Field data collected by the U.S. Geological Survey [1] for over one hundred streams in the states of Alabama, Louisiana and Mississippi have yielded the following information:

1. Width of flood plain: 200 to 9800 ft, average 2000 ft,
2. Depth: 3 to 15 ft,
3. Bridge length: 45 to 5900 ft, average 550 ft,
4. Manning n: 0.03 to 0.2,
5. Slope: 0.001 to 0.0018,
6. Discharge: 1400 to 205,000 cfs; average 25,000 cfs.

From these data the following scales and physical model requirements were derived:

$$y_r = \frac{1}{12} \quad \text{thus,} \quad y_m = 0.25 \text{ ft to } 1.25 \text{ ft}$$

$$x_r = \frac{1}{100} \quad x_m = 20 \text{ ft, } b_m = 5.5 \text{ ft}$$

$$\text{Distortion} = 8.33$$

$$s_r = 8.33 \quad s_m = 0.008 \text{ to } 0.015$$

$$C_r = 0.346$$

$$n_r = 1.9 \quad n_m = 0.057 \text{ to } 0.38$$

The actual model was 22.7 ft wide, 184 ft long and sloped at 0.0022 ft/ft. Discharges in the model ranged from 1.0 to 9.6 cfs, Manning's "n" values ranged from 0.05 to 0.36, measured depths from 0.5 to 1.5 ft, and bridge lengths from 1.0 to 11 ft (predominant range was 3 to 8 ft). Experimental results should be limited to those field conditions actually modeled:

1. Flood plain width approximately 2,000 ft.
2. Bridge opening 100 to 1,100 ft.
3. $M = \frac{\text{bridge opening}}{\text{flood plain width}} = 0.07 \text{ to } 0.5.$

It is suggested that the flood plain width can vary from 400 to 16,000 ft if the above ratio is within the specified range.

4. Manning's "n" 0.026 to 0.189.
5. Depth 6 to 18 ft.
6. Slope around 0.0003.
7. Discharge 8,000 to 40,000 cfs. The discharge range is computed from the Froude criterion where:

$$F_r = 1 \quad \text{or} \quad F_m = F_p$$

$$\frac{V^2}{gR}_m = \frac{V^2}{gR}_p$$

$$\frac{Q^2}{A^2R}_m = \frac{Q^2}{A^2R}_p \quad \text{or} \quad Q_p = \frac{Q_m}{A_r \sqrt{R_r}}$$

The model adequately scaled all the parameters for Alabama, Louisiana and Mississippi bridge sites except for slope. While it would have been desirable to run the test at other slopes, such an investigation was beyond the scope of this study.

The applicability of the model results can be viewed from a different perspective by using the scale ratios of Equation 36. Since the slope is the primary limiting factor, it is possible to use the slope ratio as a controlling factor. Assume that a stream has a slope of 0.0014 and a flood plain width of 1,000 ft. Then the critical scale ratios and prototype limitations can be deduced as follows:

$$s_r = \frac{s_m}{s_p} = \frac{0.0022}{s_p} = 1.57$$

$$x_r = \frac{x_m}{x_p} = \frac{22}{x_p} = \frac{22}{1000} = 0.022 \approx \frac{1}{45}$$

$$y_r = s_r x_r = 0.0345 = \frac{1}{29}$$

$$n_r = \frac{y_r^{2/3}}{x_r^{1/2}} = 0.715$$

Bridge opening 67 to 495 ft.

Manning's "n" 0.036 to 0.25.

Depth 14.5 to 43 ft.

Discharge 860 to 3,800 cfs.

CHANNEL RESISTANCE

The resistance of the prototype flood plain channel was simulated for the purposes of this study by an arrangement of artificial roughness elements. The determination of size, shape and location of these roughness elements required for an accurate simulation is described in Volume I of this study, *Experimental Determination of Channel Resistance for Large Scale Roughness*. The process of determining the characteristics of the roughness elements is summarized briefly below.

In the prototype condition of densely forested flood plains, the energy losses of the flow are due to bed roughness, bank roughness and the resistance of bushes, plants and trees in the flood plains. These roughness elements either are submerged or protrude through the free surface during floods. Their distribution is invariably random, making it impracticable to scale size and distribution patterns in the model flume.

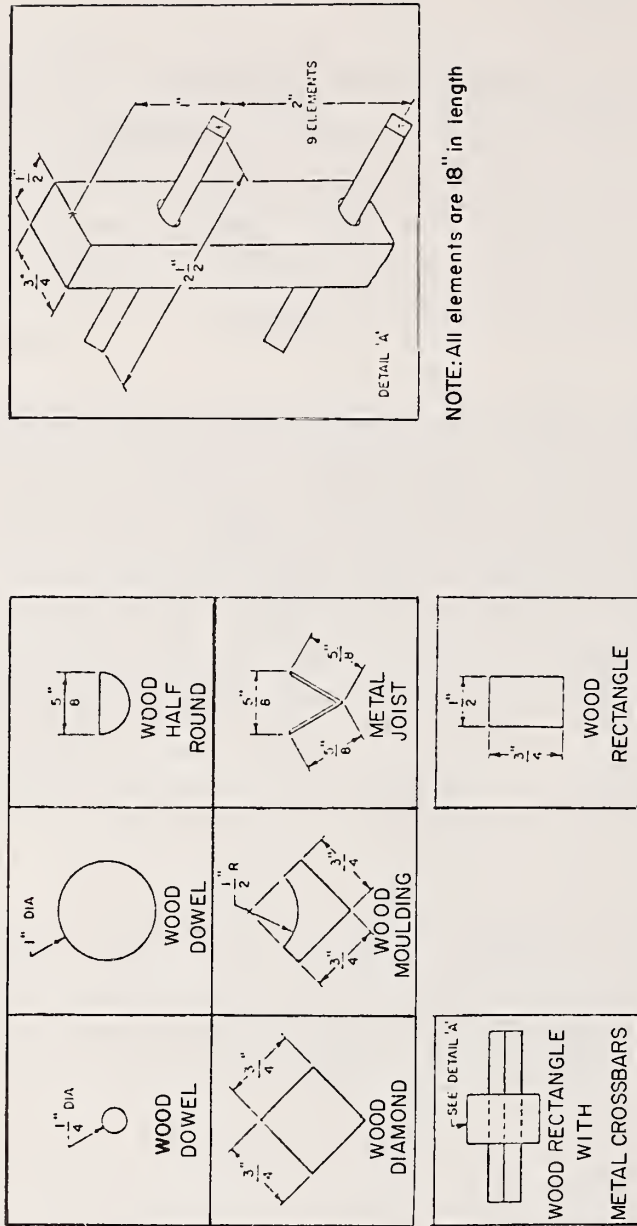
Traditionally, roughness element studies have been conducted with bottom roughness elements that are completely submerged. The bridge backwater problem, on the other hand, is influenced by trees and brush that penetrate the water surface and are spaced randomly. It was not considered feasible to use model trees for the experiment, so attention concentrated on achieving various

levels of channel resistance and relating that resistance to statistical representations of spacing parameters where roughness elements are spaced randomly as well as on a regular pattern.

The hydraulic experiments for this study were conducted in a 22.7-foot wide flume with large scale roughness to simulate the densely vegetated flood plains in the prototype. The roughness fields to be installed in the large flume were determined by performing preliminary testing and screening experiments of a 9-inch wide flume. These small flume experiments isolated the effects of various shapes and densities of roughness patterns.

Altogether there were seven different shapes of roughness element tested in the preliminary study. Three types of element distribution, random, rectangular, and staggered (or diamond), were tested for flow rates ranging from 0.1 to 0.6 cfs. For each roughness element shape and pattern, the elements were attached to the channel bed and were of sufficient length to protrude through the water surface. The density (number of elements per square foot of the channel bed) of the roughness elements was determined for each configuration. All tests were performed for a steady, nonuniform flow condition. Resistance coefficients for each roughness configuration were determined from the test data.

The experiments were performed using eight types (see Figure III-1) of roughness elements. All the elements were approximately 18 inches in length. Their projected widths varied from 0.25 inches to 1.06 inches and their cross-sectional areas varied from approximately 0.05 square inch to 0.8 square inch.



NOTE: All elements are 18" in length

TYPES OF ROUGHNESS ELEMENTS

FIGURE III-1

The small flume study established the relationships between roughness and the Froude and Reynolds numbers, depth to width ratio, element concentration, and element pattern. The functional form is given below.

$$f = \phi_1(F, R, \frac{d}{B}, \sigma, \xi)$$

where f is the function factor.

The study concluded that:

$$f = \phi_2(\sigma) \quad \xi = K$$

Essentially that for a given roughness element pattern, ξ , the channel resistance, f , is a unique function of the roughness concentration, σ . Relationships were developed of the form:

$$f = \alpha \sigma^\beta$$

or

$$n = \alpha_1 \sigma^{\beta_1}$$

to quantify both the friction factor, f , and/or Manning's n as a function of σ . Values of α , β , α_1 , and β_1 are given in Table III-1.

Table III-1. Values of α , β , α_1 and β_1

Roughness Pattern	α	β	α_1	β_1
Random	5.60	0.887	0.208	0.480
Rectangular	3.80	0.870	0.183	0.520
Diamond	5.10	1.045	0.210	0.602
Diamond	11.40	0.955	0.357	0.706
Diamond	7.60	0.941	0.275	0.635
Diamond	10.08	1.333	0.345	0.862
Rectangular	5.90	1.360	0.215	0.824
Diamond	6.03	0.980	0.238	0.603
Diamond	7.40	0.735	0.293	0.497
Diamond	4.80	0.897	0.247	0.598
Diamond	4.40	0.837	0.226	0.565
Diamond	11.50	1.007	0.374	0.673
Diamond	13.30	0.992	0.374	0.589

where

$$f = \alpha \sigma^\beta, \text{ and}$$

$$n = \alpha_1 \sigma^{\beta_1} .$$

As stated previously the objective of this study was to determine the roughness patterns to be placed in a large test flume to produce sufficiently high resistance to characterize the flow field in heavily vegetated flood plains. The selection of such roughness patterns was governed by (1) ease of installing the roughness elements, (2) degree of roughness in the prototype flood plain, and (3) scale of the model.

The bridge backwater experiments conducted in the large flume were not intended to represent the hydraulics of any site-specific case; rather, they

cover a wide range of typical hydraulic characteristics of bridge crossing sites. The kind of roughness field to be installed in the large flume thus must provide sufficient range of variation to characterize the field conditions. As stated previously, roughness coefficients show a range of between 0.03 to 0.2 for the flood plains.

The range of n values (0.057 to 0.38) required for the large test flume was used to find a roughness pattern from the small flume test data which satisfied the selection factors given at the beginning of this section. For a given value of n , that pattern is selected which gives the minimum number of roughness elements required to produce the specified roughness field.

In this manner it was found that the v-shaped metal joists roughness elements in the diamond pattern yield the Manning's n values needed for the model. Moreover, the metal roughness elements were considered the easiest to install in the large flume.

IV. EXPERIMENTAL EQUIPMENT

FLUME DESCRIPTION

All experimental runs were conducted in a constant slope-rectangular flume consisting of a concrete substructure with baffles, weirs, pumps, and tailgate located as shown in Figure IV-1. Dimensions of the flume were 22.7 ft wide, 184 ft long, and a maximum depth of 3.0 ft with a bottom slope of 0.0022. At the upstream end, pumps were installed to provide a variable flow of water from a reservoir situated on the level below the flume. The water was pumped from the reservoir and discharged through the palette diffusers into a stilling pond bounded upstream by the flume wall and downstream by a rock and wire baffle. The baffle was designed for through-flow and was never used as a weir. This arrangement was not adequate to distribute the flow, so additional baffles were added after the initial runs were made.

The stone and wire baffle formed the upstream boundary for a second stilling pond, which in turn was bounded downstream by a wood and metal-plate weir. Downstream from the weir, the water flowed over and through a gravel and wire baffle, and thence into the main test section of the flume.

At the downstream end of the flume, a large wooden plank baffle was used to regulate flow out of the flume. This wooden baffle or tailgate was calibrated to produce uniform flow for each flow and roughness configuration without the bridge model in place. During test runs with the bridge models in place, the downstream baffle was set at proper calibrated openings.

An arbitrary reference station was established at the longitudinal 28 ft 11 in. mark of the flume. This was designated as 90 ft. Relative to this value,

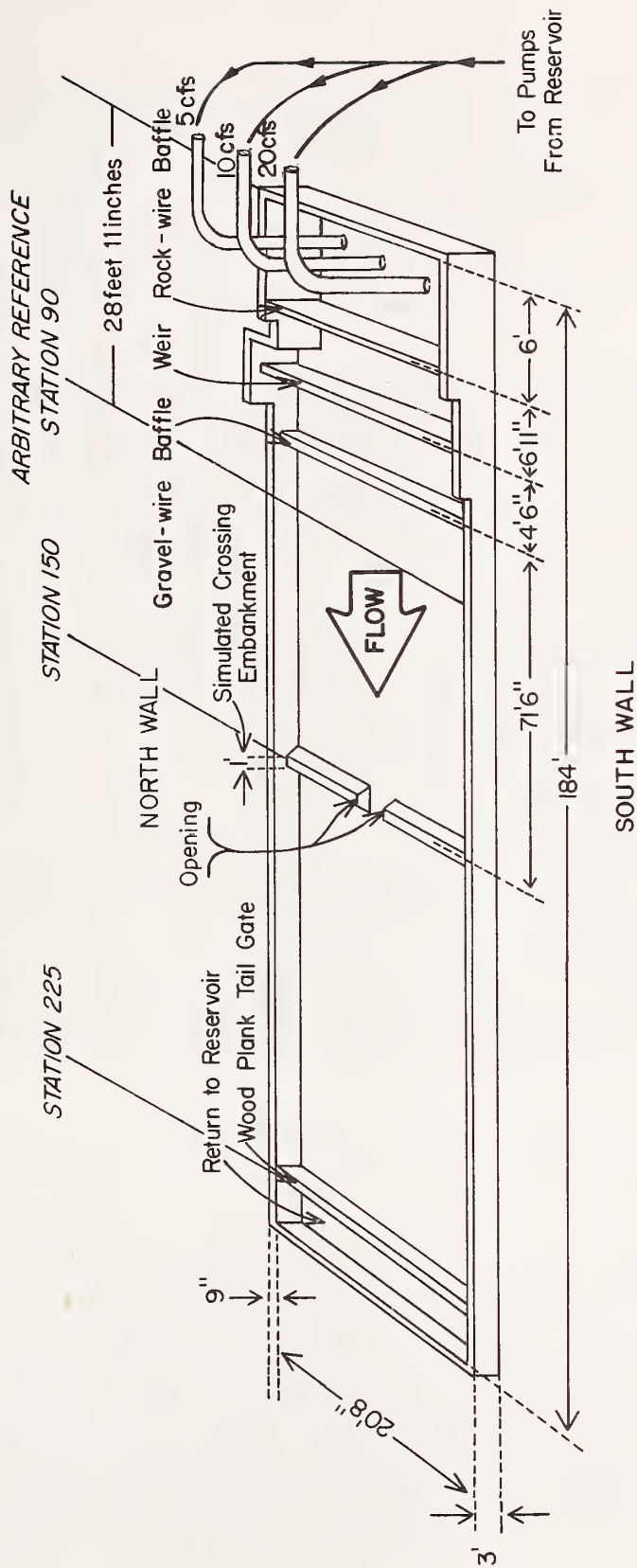


FIGURE IV-1
 BASIC FLUME CHARACTERISTICS

the crossing centerline (centerline of the simulated crossing) was at 150 ft and the tailgate at 225 ft. The model embankments had a top width of 1 ft and a bottom width of 2 ft with sloping embankments extending 6 in. at the bottom from each side. Embankments were constructed in 4-ft modular sections to allow the opening width to be easily varied. The bottom of the flume was lined with 4 ft x 8 ft x 3/4 in. marine plywood to provide a surface for attaching roughness elements. Extending 1 ft into the flume on north and south walls were energy absorbing mats of rubberized horsehair matting. This allowed a data gathering area of 20.7 ft x 125 ft. Both the weir and subsequently a manometer were calibrated with a volumetric tank (not shown in Figure IV-1) located on the level below the flume and connected to the flume by a flow bypass.

A rectangle grid system was defined and marked on the flume. A point just beyond the gravel wire baffle against the energy absorbing matting on the north wall was given the coordinate (90.0, 0.0). The first coordinate of the pair, x, is in the direction of flow and ranged between 90.0 and 215 ft. The center of the crossing structures (embankments) was located at $x = 150.0$ ft. The second, or Y coordinate, ranged between 0.0 and 20.7 ft. The centerline was located at $Y = 10.3$ marker. All data collected is referenced using this coordinate system. In some instances the X coordinate is translated by 90 ft to give a (0.0, 0.0) reference point. This causes the X coordinate to range between 0.0 and 125.0. When this occurs it is either stated in the text or obvious from the context of the material.

ROUGHNESS ELEMENTS

A primary objective of this study is to quantify the relationship between backwater and roughness. Roughness in the large flume was simulated by bolting V-shaped metal joists to the 3/4 in. marine plywood sheets which were anchored to the concrete floor of the flume. Each roughness element was 18 in. high and extended through the free surface. This was purposely done to achieve the conditions noted on heavily vegetated flood plains where often

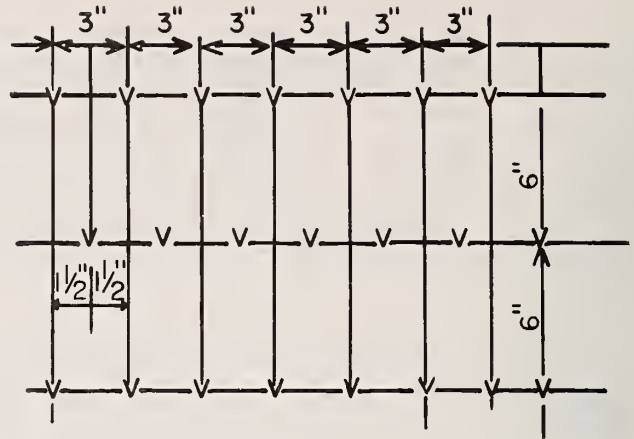
trees are not inundated by the flood waters. No attempt was made to approach geometric similitude in the flood plain with the arrangement of roughness elements. However, since previous flume studies had underpredicted backwater, possibly by not including an accurate representation of roughness, part of the goals of this study was to estimate their effect.

It is important to note that the bridge backwater experiments conducted in the large flume were not intended to represent the hydraulics of any site-specific case. Instead, they cover a wide range of typical hydraulic characteristics of bridge crossing sites. As reported in Chapter III, the prototype range of Manning's n was between 0.03 and 0.2 for flood plains. The exaggeration in vertical scale (distortion) of the model, with the dynamic similitude derivation given in Chapter III, requires roughness in the large flume model to range between 0.06 and 0.4. The development of the shape and location of the elements, briefly summarized in the preceding chapter, is the subject of Volume I of this report, *Experimental Determination of Channel Resistance for Large Scale Roughness*, Report No. FHWA-RD-75-71. Figure IV-2 shows actual roughness patterns that were used in the large flume. The number in percent for the various roughness patterns represents the percentage density compared to the reference pattern shown in Figure IV-2. The various patterns will be identified hereafter in this report simply by these percentages and/or a corresponding letter code.

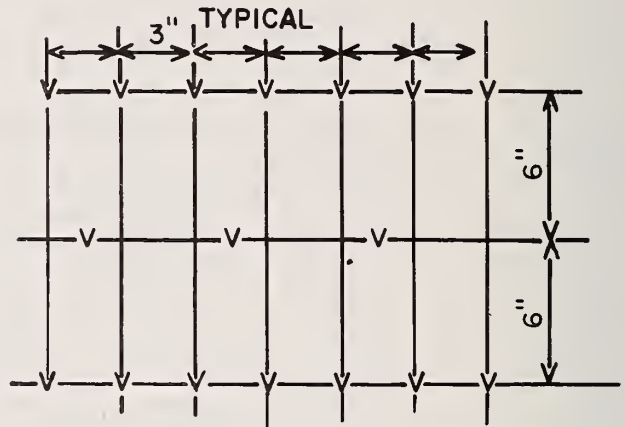
The combination of two separate densities was used to simulate flood plain and main channel conditions for centered crossings only. The main channel was defined as that area extending 1.5 ft on either side of the model centerline (10.3) and extending the length of the flume.

Table IV-1 lists the roughness combinations used in this study. Figure IV-3 shows the measured Manning's n as observed in the flume for each of the roughness combinations as a function of flow. These calculations were made using a flume slope of 0.0022, normal runs, and the overall average normal depth.

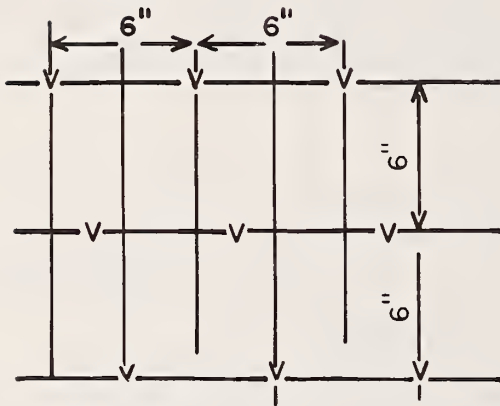
I. 100%



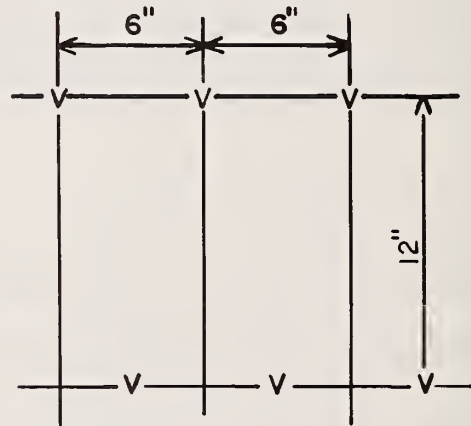
II. 75%



III. 50%



IV. 25%



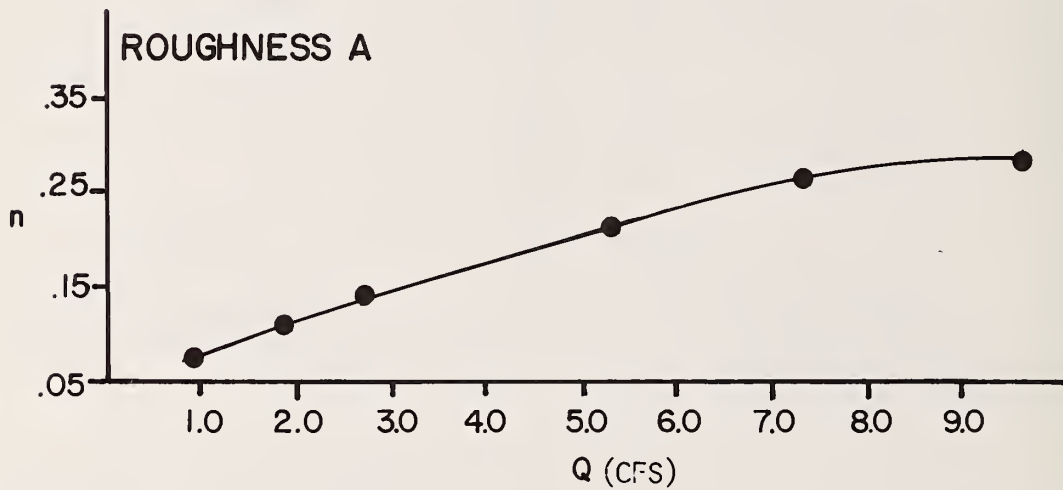
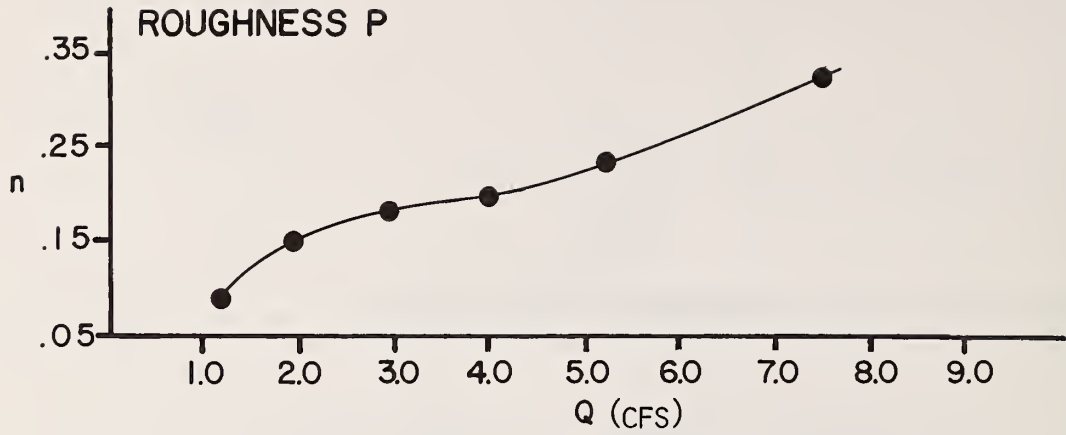
DEFINITION OF ROUGHNESS PATTERN

FIGURE IV-2

TABLE IV-1
ROUGHNESS COMBINATIONS

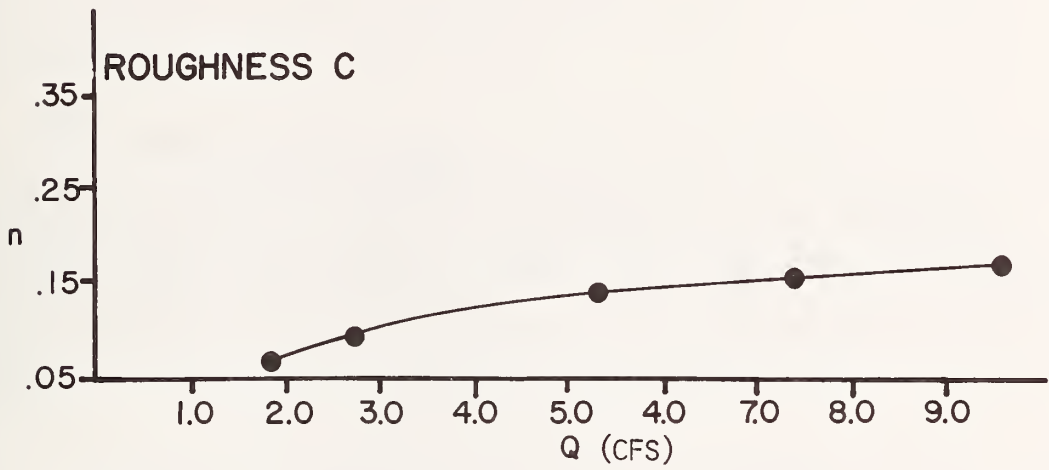
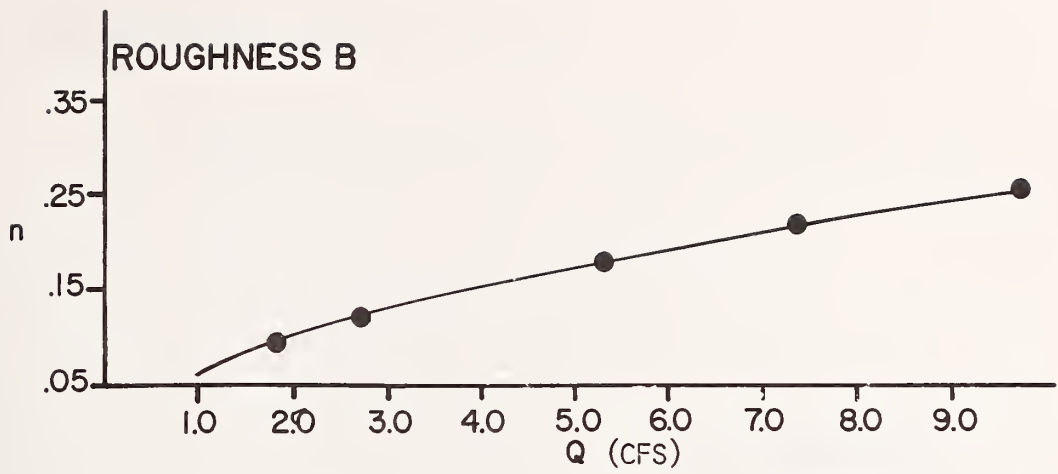
Letter Designation	Roughness Density Expressed as Percent of Density of Reference Pattern*	
	Flood Plain	Main Channel
P	100	100
A	100	50
B	75	75
C	75	25
D	50	50

*See Figure IV-2.



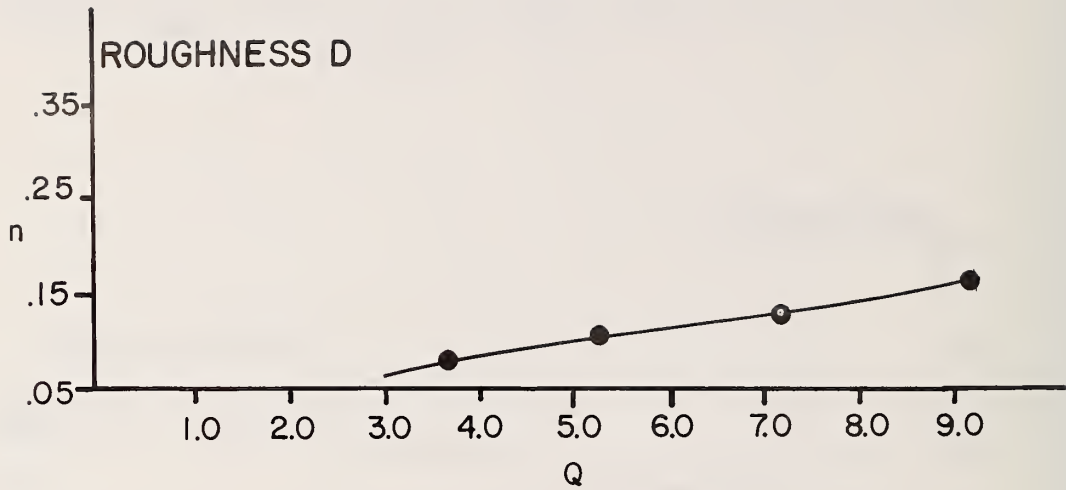
MANNING'S "n" FOR ROUGHNESS PATTERNS AS A FUNCTION OF FLOW

FIGURE IV-3
(cont'd.)



MANNING'S "n" FOR ROUGHNESS PATTERNS AS A FUNCTION OF FLOW

FIGURE IV - 3
(cont'd.)



MANNING'S "n" FOR ROUGHNESS PATTERNS AS A FUNCTION OF FLOW

FIGURE IV-3
(cont'd.)

DESCRIPTION OF CROSSING CONFIGURATIONS

Each crossing configuration consisted of an interior 4 ft x 1 ft x 1-2/3 ft metal frame constructed of steel angles covered with 1/2 in. marine plywood. Wood surfaces, both exterior and interior, were painted with two or more coats of high quality white enamel paint to prevent their deterioration in water. The wooden embankments and abutment shapes were connected to the metal frame by means of 8 in. toggle bolts, which did not penetrate the exterior surface of the marine plywood. Marine plywood extensions were appended to the metal frame on both the upstream and downstream faces to allow easy adjustment of the opening size. The width of each model was 2 ft measured at the toe of the upstream and downstream embankments to 1 ft at the top. All of the models had the same height of 20 in.

The center of each crossing configuration, with the exception of skewed, was located at the 150 ft marker in the flume. The toe of the upstream and downstream embankments were located at 149.0 and 151.0 respectively. This provided approximately 60 ft upstream and 75 ft downstream for measurement. Skewed configurations had their centers at 150.0 and formed an angle at either 15 degrees or 45 degrees with respect to the flow direction.

All joints of the crossing configuration were well caulked. Care was taken to maintain the roughness characteristics of the exterior surface. Caulking was applied around the upstream base of the embankments at the junction of the wooden appendages to the wood covered metal frame, and at the abutment face to the frame. The hollow crossing configuration was filled with water.

Each crossing configuration was inserted into a 1 ft wide by 3/4 in. deep cut in the marine plywood sheets covering the floor of the flume. This cut extended completely across the flume. The roughness elements were mounted

on these 4 ft x 8 ft sheets. After the crossings were put in place, a piece of the plywood was laid across the cut in the opening to keep the floor even. No roughness element was placed on this 2-ft strip across the opening.

WINGWALL

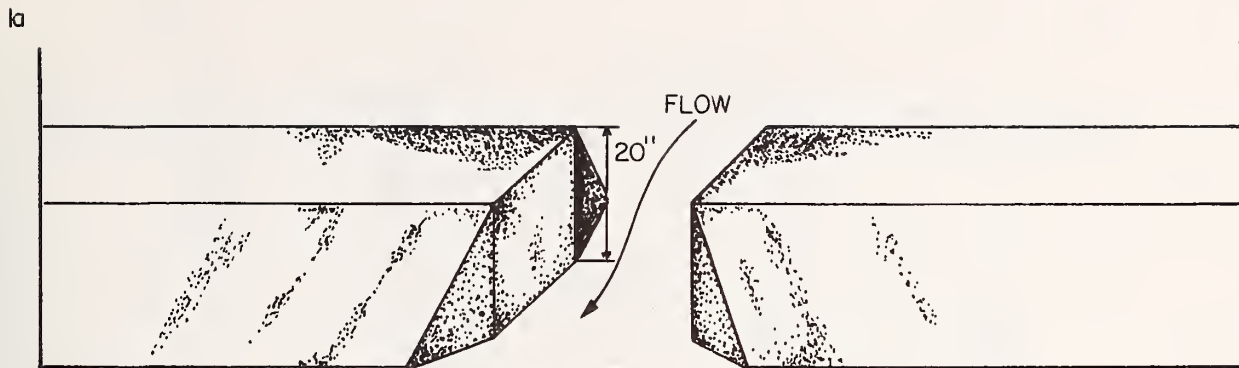
The abutment shape used most extensively in the testing was the 45 degree wingwall shown in Figure IV-4. Figure IV-4 shows the as-constructed dimensions of the embankments. Embankment sides were attached to the upstream and downstream faces of the crossing extending from the edge of the flume to the abutment face.

SPILLTHROUGH

A second abutment face, the spillthrough, was also tested in the flume. The face of the abutment is tapered from the top to bottom and thus makes a trapezoidal opening shape. Each face of the abutment is sloped so that the toe protrudes 6 in. into the constriction, or, for two abutments, 1 ft. Opening size is measured from the toe of the embankment but of course varies with depth. Embankments attached to the upstream and downstream faces of the crossing were the same as for the wingwall. Figure IV-5 provides a sketch of the spillthrough abutment and pertinent dimensions.

SPUR DIKES

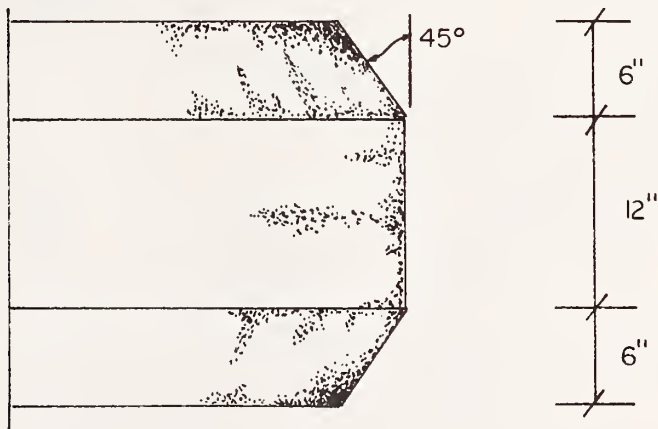
An upstream elliptical spur dike was the third shape tested in the large flume. The elliptic spur dikes consisted of 40 layers of 1/2 in. marine plywood, 18 in. wide at the bottom and 6 in. at the top, for an embankment ratio of 1.6:1 (horizontal/vertical). The elliptic dikes constructed have a major axis of 4.85 ft with a ratio of major axis to minor axis of 2.5:1. Figure IV-6 shows the elliptical spur dike used in all experiments.



WINGWALL SKETCH

lb

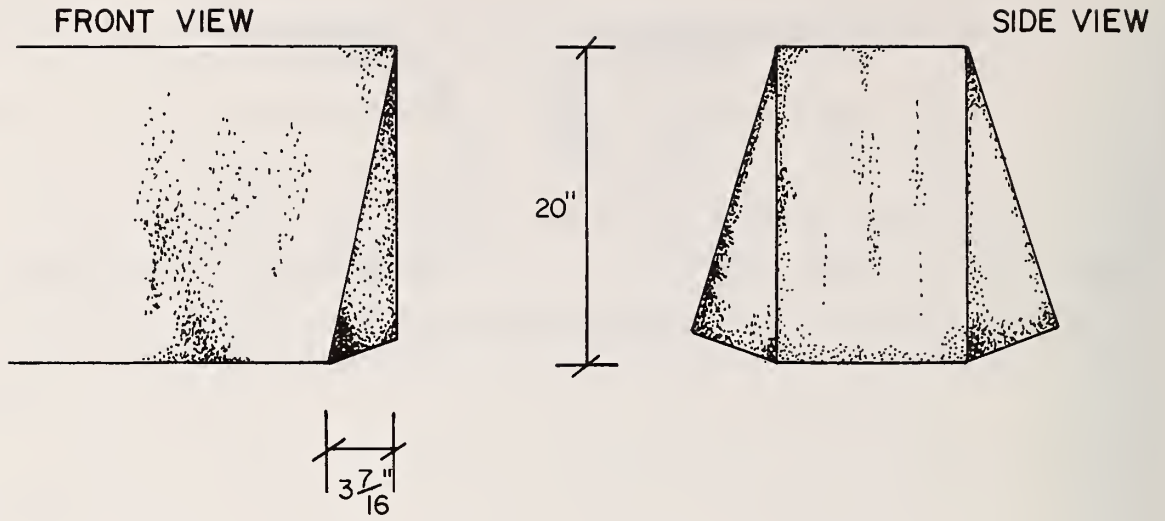
TOP VIEW



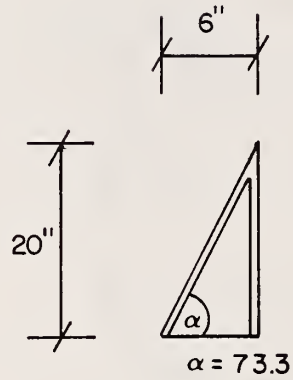
WINGWALL ABUTMENT DESIGN

FIGURE IV-4

lc

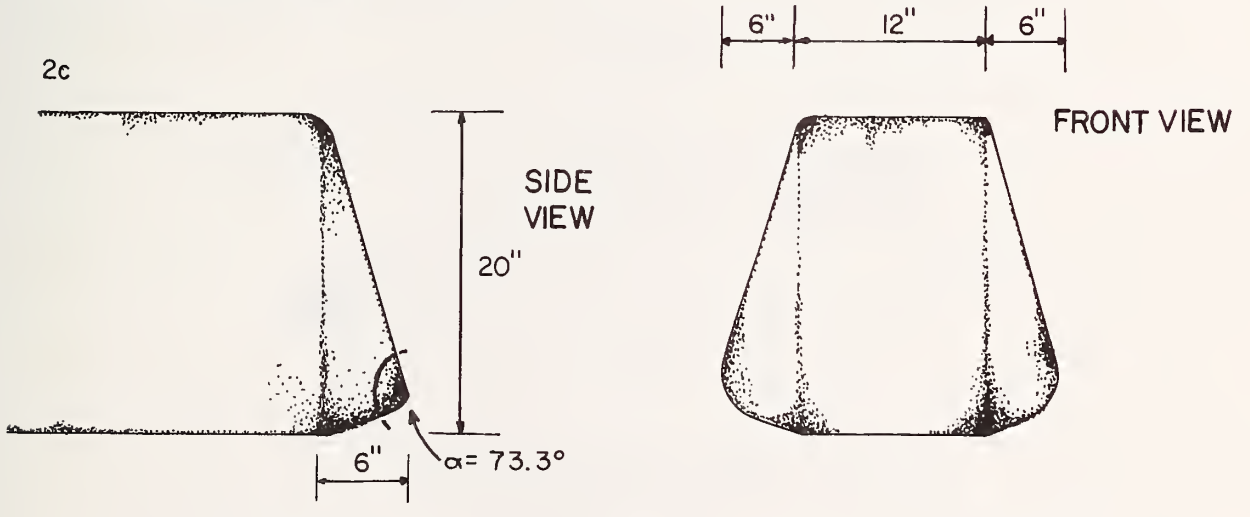
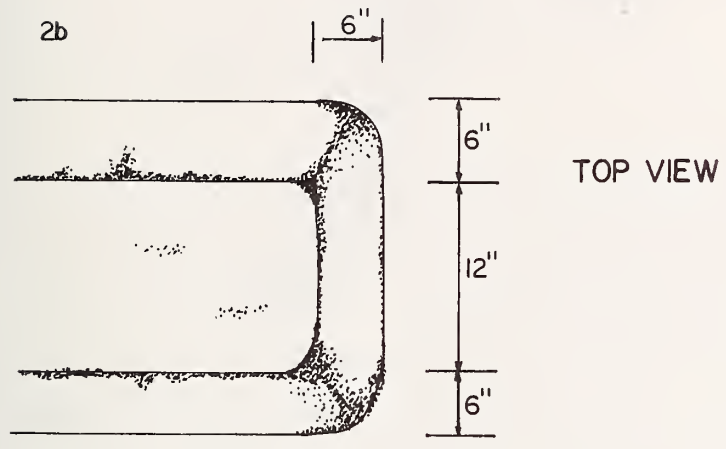
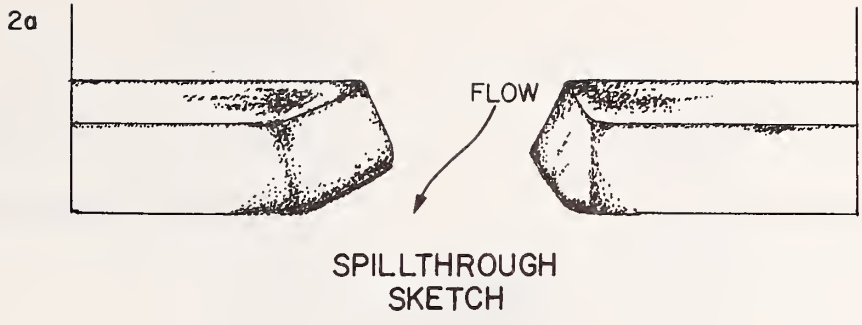


ld



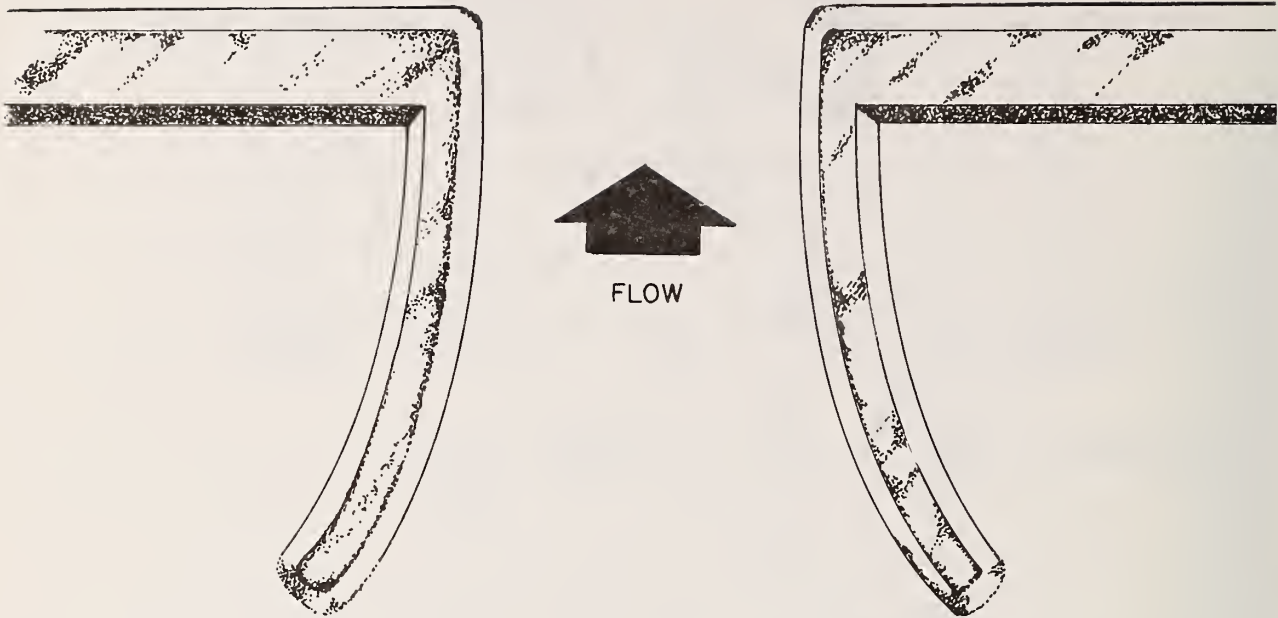
WINGWALL ABUTMENT DESIGN

FIGURE IV-4
(cont'd)

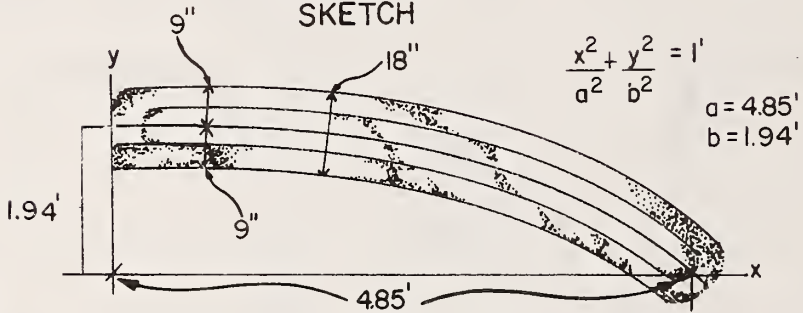


SPILLTHROUGH EMBANKMENT
FIGURE IV-5

UPSTREAM
SPUR DIKE



SPUR DIKE
SKETCH



SPUR DIKE DESIGN
FIGURE IV-6

The equation describing the construction is:

$$\frac{Y^2}{a^2} + \frac{X^2}{b^2} = 1 \quad (37)$$

where

- Y = coordinate in the direction of flow,
- X = coordinate perpendicular to the direction of flow,
- a = major axis,
- b = minor axis, and
- a/b = 2.5.

In a late phase of the study, logarithmic spur dikes were tested. In these tests, the opening was moved to one side of the flume so that the flume served essentially as a symmetrical half of a larger channel which, in effect, doubled the discharge and horizontal dimensions of the model. Detailed velocities and depths were recorded for flow around the spur dikes. These data are summarized in Volume V, *Data Report for Spur Dike Experiments*, but their analysis was beyond the scope of the present contract.

V. EXPERIMENTAL PROCEDURE

GENERAL DESCRIPTION

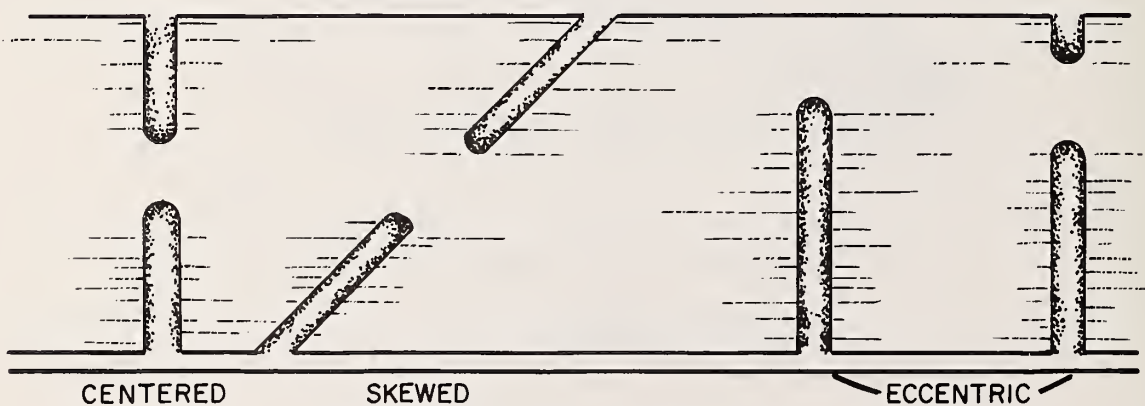
The flume studies analyzed in this report were conducted from June 1972 to July 1973. The site of the flume was the old National Bureau of Standards hydraulics laboratory located at 4200 Connecticut Avenue, N.W., Washington, D.C. The flume, constructed by the Federal Highway Administration, was operated under the supervision of Water Resources Engineers.

During the course of the experiment three types of crossings were studied (Figure V-1). These were centered, skewed, and eccentric crossings.

Eccentricity is defined as:

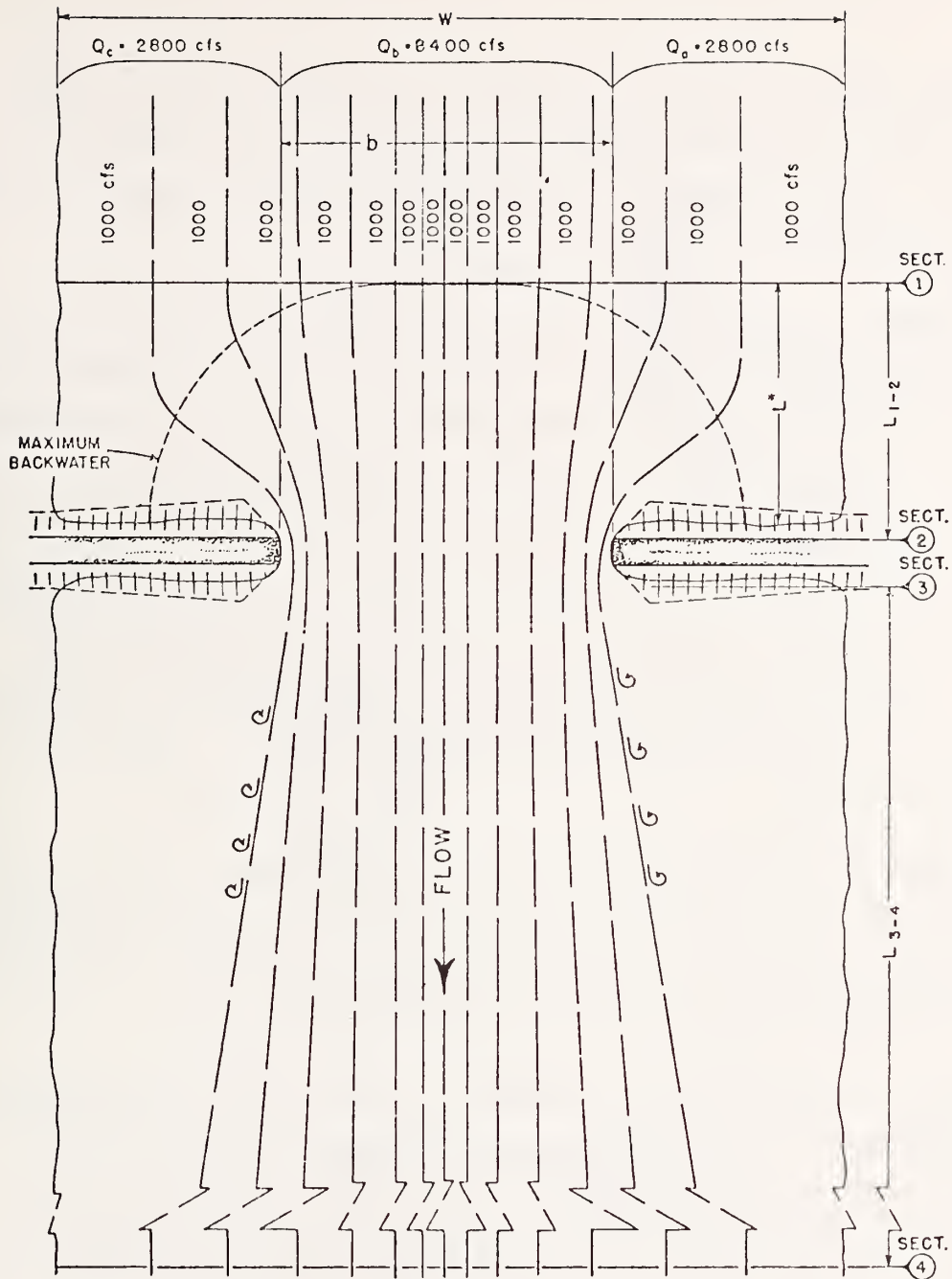
$$1 - \frac{Q_c}{Q_a}, \text{ where } Q_c < Q_a \quad \text{or} \quad 1 - \frac{Q_a}{Q_c}, \text{ where } Q_a < Q_c$$

Flow, or Q , is defined as the flow occurring over the cross section of the flood plain obstructed by the roadway embankments (Figure V-2).



CROSSING CONFIGURATIONS

FIGURE V-1



FLOW LINES FOR TYPICAL CENTERED CROSSING

FIGURE V-2

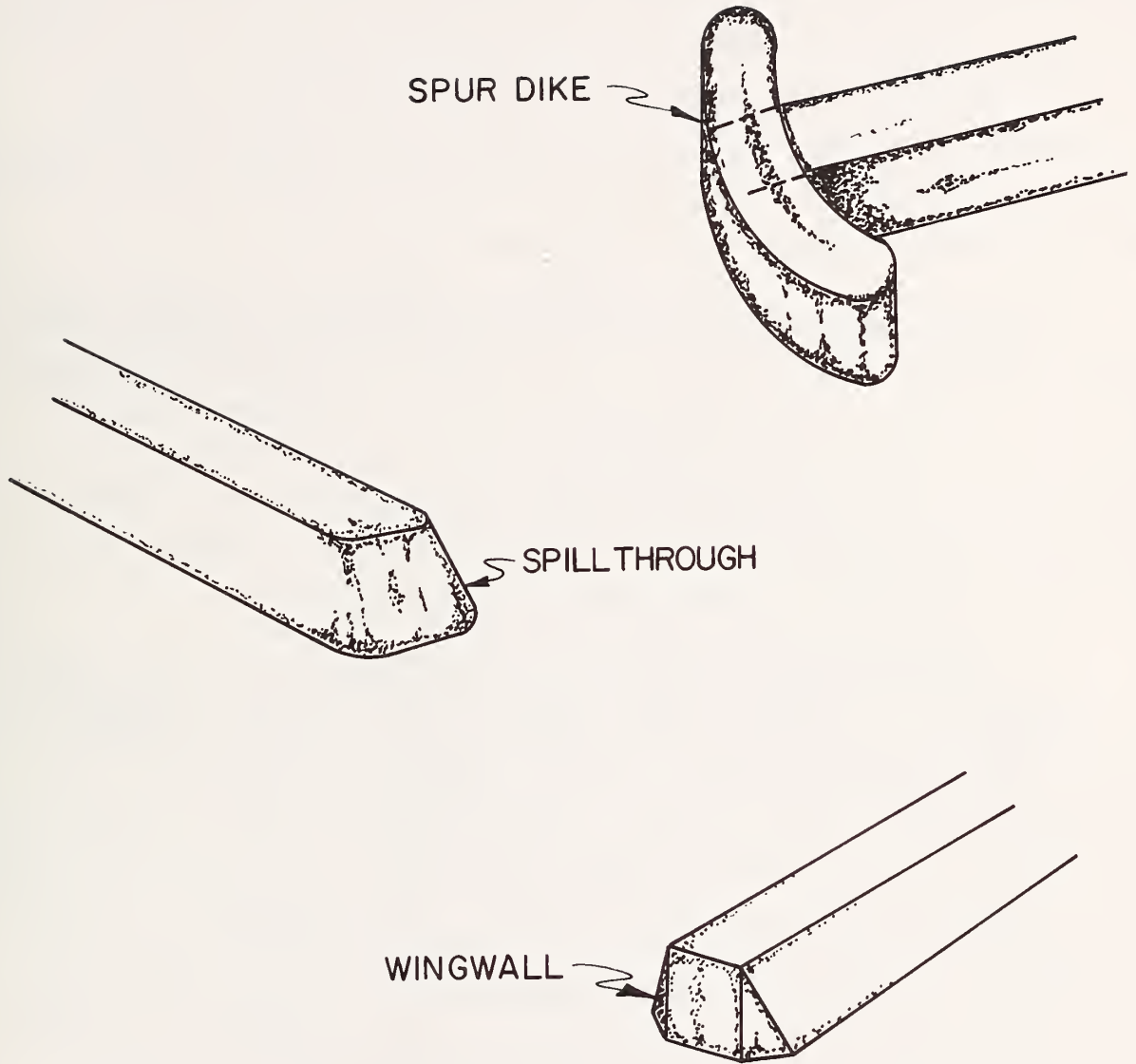
Three abutment shapes were studied in conjunction with the centered crossing. These were 45 degree wingwall, spillthrough, and upstream elliptical spur dikes as shown on Figure V-3. All tests conducted for skewed and eccentric crossings used wingwall abutments.

An important aspect of this experiment, previously described in Chapter III, was the simulation of roughness by the use of artificial roughness elements penetrating the free surface. Roughness elements were installed and checked in both the flood plain area and main channel. Ten separate patterns were used in the flume which gave an effective Manning's n ranging from 0.06 to 0.4. These values are necessarily higher than those observed in nature in order to compensate for model distortion. All eccentric and skewed crossing configurations used the same roughness pattern (type D - 50 percent flood plain and main channel). Centered crossings accounted for all other roughness configurations. A description of the roughness patterns related to the model runs is presented in following sections.

In general, bridge openings for all flume runs were set at 1, 3, 5, 8, or 11 ft, respectively. Few flume runs were made with the 11-ft opening due to the difficulty in locating and measuring the maximum backwater. A 5-ft opening modeled the average prototype opening on a 1:100 scale.

Flows for model runs varied between 1.0 and 9.6 cfs. Typically flows in the neighborhood of 2.0, 5.0, 7.0 and 9.0 cfs were used for any set of roughness configurations, opening size, abutment type, and crossing type. Calculations for dynamic similitude indicated a flow of approximately 6.0 cfs is needed to satisfy average prototype flow conditions of 25,000 cfs.

Operating procedures for every series of runs were standardized and carefully controlled. Flows that were to be used for the entire series of openings and models were tested in the flume with roughness patterns in both



SPUR DIKE, SPILLTHROUGH, AND WINGWALL SHAPES

FIGURE V-3

the flood plain and main channel but without any embankment construction. This permitted the calculation of normal depth for each flow at all points in the flume. All the different flows used in the experiment were measured in a volumetric tank of known cross-sectional area and measurable depth. Simultaneously, all flow entering the flume passed over an annubar connected to a manometer which was then calibrated against the flow measured in the volumetric tank. This allowed the reproduction of flows and eliminated the need for the constant use of the volumetric tank.

After the normal depth of each flow was determined, an abutment shape and model embankments were installed in the flume and the flows to be tested were run. Typically, after flow was set by use of the manometer, a period of one to two hours was required by recording centerline elevations along the entire flume every 15 minutes until the same values were recorded in successive measurements. When this occurred, the entire flume was considered to be at equilibrium and data were collected over the flume for that run.

The determination of water surface elevation required the measurement of the elevations of the floor of the flume for each of the approximately one hundred depth recording stations. The floor elevation plus depth gives the corresponding water surface elevation. Since this fairly simple procedure was complicated by the 3/4 in. marine plywood installed over the reinforced concrete floor, precautions were taken to minimize error in the measurements. First, at the start of daily operations the flume was allowed to become thoroughly saturated before any data were taken. Second, bottom elevation measurements were taken on a weekly basis with a flow representing an average depth in the flume to check for changes in the floor due to warping or other causes. As the experiment progressed, the measurements of bottom elevations were needed less frequently.

Each run required four technicians and a supervising engineer. Actual data collection usually required two hours after the steady state condition was established.

HYDRAULIC MODEL TESTS

During the period in which the hydraulic model was in operation, a total of 285 roughness, flow, abutment, and opening combination runs were tested. Table V-1 summarizes the test matrix for the roughness pattern types and crossing configurations.

TABLE V-1
SUMMARY OF EXPERIMENTAL RUNS

Roughness Type	Crossing Configurations					Total Runs	
	Centered		Spur Dike	Skew	Eccen.		Normal
	Wing-wall	Spill-through		Wing-wall	Wing-wall		
P	12	4	--	--	--	6	22
A	8	12	7	--	--	6	33
B	9	27	12	--	--	6	54
C	12	12	12	--	--	4	40
D	9	12	11	38	12	4	86
Total	50	67	42	38	12	26	285

Both skew and eccentric crossing configurations used wingwall abutment shapes. The elliptical spur dikes were used only on the upstream side of the embankment. Spur dike data collected using logarithmic spur dikes are not included in the table.

Tables V-2 through V-5 present a complete tabulation of all the flume runs accomplished. Table V-2 contains a listing of the centered opening runs subdivided by roughness element pattern. Flow, further subdivided by either abutment shape or spur dike, is condensed to the nearest 0.1 cfs for the purpose of the presentation. Tables V-3 and V-4 give eccentric and skew runs, respectively, while Table V-5 lists the flows used for normal runs.

All the runs with the exception of the fourteen shown in Table V-6 had roughness elements excluded from the opening. These fourteen runs were not used in any analysis presented in Chapter VI and are included here only for completeness.

DATA COLLECTION

Data collected included primarily water surface and bottom readings, and velocity and direction of flow. Additional depth measurements were taken at centerline positions and in the area between the location of maximum backwater and the embankments of the crossing model. Depth measurements were taken both 60 ft upstream and 65 ft downstream from the crossing model section. Velocity measurements were primarily confined to that area between the cross sections defined by the location of the maximum backwater and the reattachment points as recorded on the flume walls. The reattachment points are the two locations where the flow lines first strike the flume walls downstream of the constriction.

Data gathered during each run included those parameters listed in Table V-7. All the data collected have been computerized and will become property of the FHWA. The analysis, as presented in this report, required the development of special in-house software, which is also the property of the FHWA. The following sections describe the procedure for collecting velocity, depth and flow measurements. Analysis of these data and pertinent calculations using raw data are presented in Chapter VI.

TABLE V-2
EXPERIMENTAL INVESTIGATION CHART
CENTERED OPENING RUNS

Opening Size (ft)	Flow Rate (cfs)	Abutment		
		Wingwall	Spillthrough	Spur Dike
ROUGHNESS PATTERN P (100% FP, 100% MC)				
3	5.2	x		
	2.9	x		
	1.9	x		
	0.9	x		
5	7.4	x		
	5.2	x		
	2.9	x		
	1.9	x		
8	7.9	x	x	
	7.4	x	x	
	5.2	x	x	
	2.9	x	x	
ROUGHNESS PATTERN A (100% FP, 50% MC)				
3	7.4			x
	5.4		x	
	2.7		x	x
	1.9		x	x
5	7.4	x	x	x
	5.4	x	x	x
	2.7		x	x
	1.9		x	
8	9.6		x	
	7.4	x	x	
	5.3	x	x	
	2.7	x	x	

NOTE: FP = flood plain 1 ft = 0.3048 meters
 MC = main channel 1 cfs = 0.0283 m³/sec

TABLE V-2 (Cont'd)
 EXPERIMENTAL INVESTIGATION CHART
 CENTERED OPENING RUNS

Opening Size (ft)	Flow Rate (cfs)	Abutment		
		Wingwall	Spillthrough	Spur Dike

ROUGHNESS PATTERN A (Cont'd)

11	9.8	x		
	7.4	x		
	5.6	x		

ROUGHNESS PATTERN B
 (75% FP, 75% MC)

	9.7			x
3	7.4		x	x
	5.3		x	x
	2.7		x	x
	1.9		x	
5	9.7			x
	7.6	x	x	x
	5.4	x	x	x
	2.7	x	x	x
8	9.7			x
	7.4	x	x	x
	5.4	x	x	x
	2.8	x	x	x
11	9.7	x	x	
	7.4	x	x	
	5.3	x	x	

ROUGHNESS PATTERN C
 (75% FP, 25% MC)

	9.7	x	x	x
3	7.4	x	x	x
	5.4	x	x	x
	2.7	x	x	x

NOTE: FP = flood plain 1 ft = 0.3048 meters
 MC = main channel 1 cfs = 0.0283 m³/sec

TABLE V-2 (Cont'd)
 EXPERIMENTAL INVESTIGATION CHART
 CENTERED OPENING RUNS

Opening Size(ft)	Flow Rate (cfs)	Abutment		
		Wingwall	Spillthrough	Spur Dike
ROUGHNESS PATTERN C (Cont'd)				
5	9.7	x	x	x
	7.4	x	x	x
	5.3	x	x	x
	2.7	x	x	x
8	9.7	x	x	x
	7.4	x	x	x
	5.4	x	x	x
	2.7	x	x	x
ROUGHNESS PATTERN D (50% FP, 50% MC)				
1	7.1			x
	5.3			x
	3.9			x
3	9.2	x	x	x
	7.1		x	x
	6.5	x		
	5.3		x	x
5	3.8	x	x	x
	9.3	x	x	x
	7.2	x	x	x
	5.3		x	x
8	3.8	x	x	x
	9.2	x	x	
	7.2	x	x	
	5.3		x	
8	3.9	x	x	

NOTE: FP = flood plain
 MC = main channel

1 ft = 0.3048 meters
 1 cfs = 0.0283 m³/sec

TABLE V-3
 EXPERIMENTAL INVESTIGATION CHART
 ECCENTRIC RUNS
 (Wingwall Abutment)

Opening Size(ft)	Flow Rate (cfs)	Eccentricity
ROUGHNESS PATTERN D (50% FP, 50% MC)		
3	9.7	1.0
	6.9	1.0
	3.6	1.0
	9.7	0.87
	6.9	0.87
	3.6	0.87
8	9.0	1.0
	6.9	1.0
	3.6	1.0
	9.7	0.81
	6.9	0.81
	3.5	0.81

NOTE: FP = flood plain 1 ft = 0.3048 meters
 MC = main channel 1 cfs = 0.2083 m³/sec

TABLE V-4
EXPERIMENTAL INVESTIGATION CHART

SKEW RUNS
(Wingwall Abutment)
ROUGHNESS PATTERN D
(50% FP, 50% MC)

Opening Size(ft)	15° Skew		45° Skew	
	Flow Rate (cfs)	Eccentricity	Flow Rate (cfs)	Eccentricity
3	9.7	.8	9.7	.7
	7.4	.8	7.2	.7
	3.8	.8	3.9	.7
	9.7	.9	9.7	.0
	7.1	.9	7.1	.0
	3.8	.9	3.8	.0
	9.7	.2	9.7	.9
	7.4	.2	7.1	.9
	3.8	.2	3.8	.9
			7.1	.7
8			3.8	.7

NOTE: FP = flood plain
MC = main channel
1 ft = 0.3048 meters
1 cfs = 0.2083 m³/sec

TABLE V-5
 EXPERIMENTAL INVESTIGATION CHART
 UNIFORM FLOWS (cfs)

P 100% FP, 100% MC	Roughness Pattern			
	A 100% FP, 50% MC	B 75% FP, 75% MC	C 75% FP, 25% MC	D 50% FP, 50% MC
7.46	9.60	9.74	9.74	9.14
5.19	7.39	7.34	7.39	7.22
3.91	5.32	5.35	5.31	5.33
2.83	2.75	2.75	2.75	3.77
1.88	1.89	1.89	1.88	
1.02	1.00			

NOTE: FP = flood plain
 MC = main channel
 1 ft = 0.3048 meters
 1 cfs = 0.2083 m³/sec

TABLE V-6
 SPILLTHROUGH RUNS NOT ANALYZED
 (All Roughness Pattern B)

Run No.	Opening (ft)	Flow (cfs)	Comment
ST20B	5	2.8	75% element in opening
ST23B	5	5.3	75% element in opening
ST26B	5	7.4	75% element in opening
ST17B	8	2.8	2 rows of elements in opening
ST14B	8	9.6	2 rows of elements in opening
ST27B	5	7.4	50% element in opening
ST24B	5	5.3	50% element in opening
ST21B	5	2.8	50% element in opening
ST18B	8	7.4	
ST28B	5	7.4	25% element in opening
ST25B	5	5.3	25% element in opening
ST22B	5	2.8	25% element in opening
ST19B	8	7.4	
ST29B	5	7.4	100% element in opening

NOTE: FP = flood plain 1 ft = 0.3048 meters
 MC = main channel 1 cfs = 0.2083 m³/sec

TABLE V-7
RAW DATA COLLECTED FOR EACH RUN

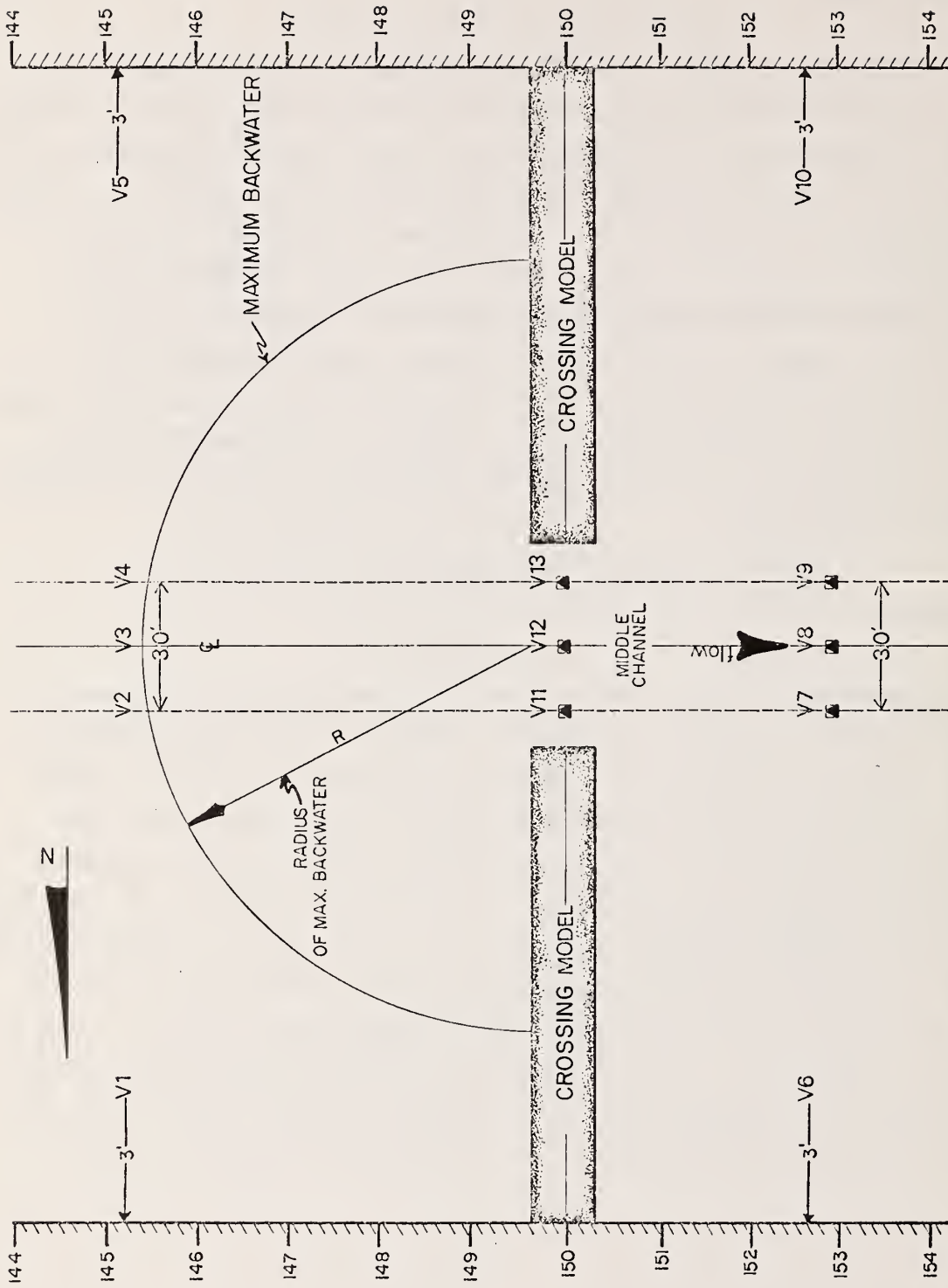
Run number
Flood plain and main channel roughness
Flow
Opening width
Crossing type (angle of skew or degree of eccentricity)
Abutment shape
Vena contracta location
Vena contracta width
Location of maximum backwater
Flow reattachment points
Water surface elevations (approximately 100/run)
Velocity and angle of flow (approximately 15/run)

VELOCITY MEASUREMENTS

As a standard procedure, velocity measurements were taken between the location of the cross section containing the maximum backwater and that containing the reattachment points. Measurements were also taken in the opening at both edges of the vena contracta. Measurements were taken using an Ott small current meter. Each shaft was equipped with a swinging vane to measure the angle of flow. Each meter and shaft were calibrated at the beginning of the experiment by the use of a large towing tank designed for this purpose. Actual measurements were taken by electronically recording the number of "clicks" caused by flow turning the propellor over a 50-sec period. This was done twice for each measurement and the average value recorded. This average value was then used to determine the velocity from the calibration curves for the particular shaft and current meter.

Centered Models

The location of velocity measurements for centered model runs were a function of both the opening size and the location of the maximum backwater. Figure V-4 indicates the location of velocity measurements for all the runs having the crossing configuration centered in the flume. Those points V11, V12, and V13, directly in the opening were usually recorded on both edges of the vena contracta and at the centerline. Point V3 was located on the centerline at the point of maximum backwater. The four points, V1, V2, V4, and V5 flanking the centerline point on both sides were taken to fully characterize the cross section. This cross section corresponds to the beginning of section 1, zone of contraction in Figure II-1. Points numbered V6 through V10 were usually taken at the cross section determined by the reattachment points. This cross section corresponds to section 4, Figure II-1, the end of the flow expansion zone.



VELOCITY MEASUREMENT LOCATIONS FOR CENTERED CROSSING CONFIGURATION

FIGURE V-4

SKEW MODELS

Five to seven velocity measurements were recorded for each skew run depending on opening size. A typical configuration is shown in Figure V-5. Velocity measurements were recorded on centerline and directly behind each edge of the embankment.

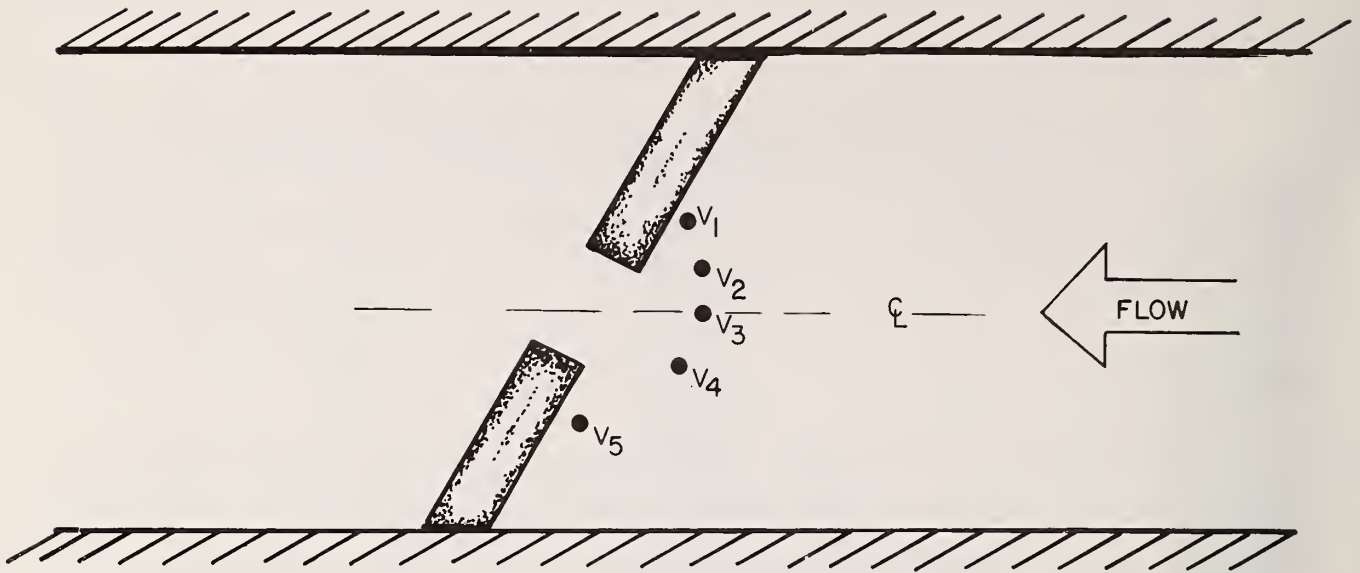
Eccentric Model

Velocities were recorded for the eccentric model runs across the flume at the maximum backwater, in the opening at the vena contracta, and across the flume at the reattachment location. A typical configuration is given in Figure V-6. Locations extending across the flume are equidistant from each other with the middle point on the centerline. These cross sections refer to sections 1, 2 and 4 respectively, Figure II-1.

DEPTH MEASUREMENT

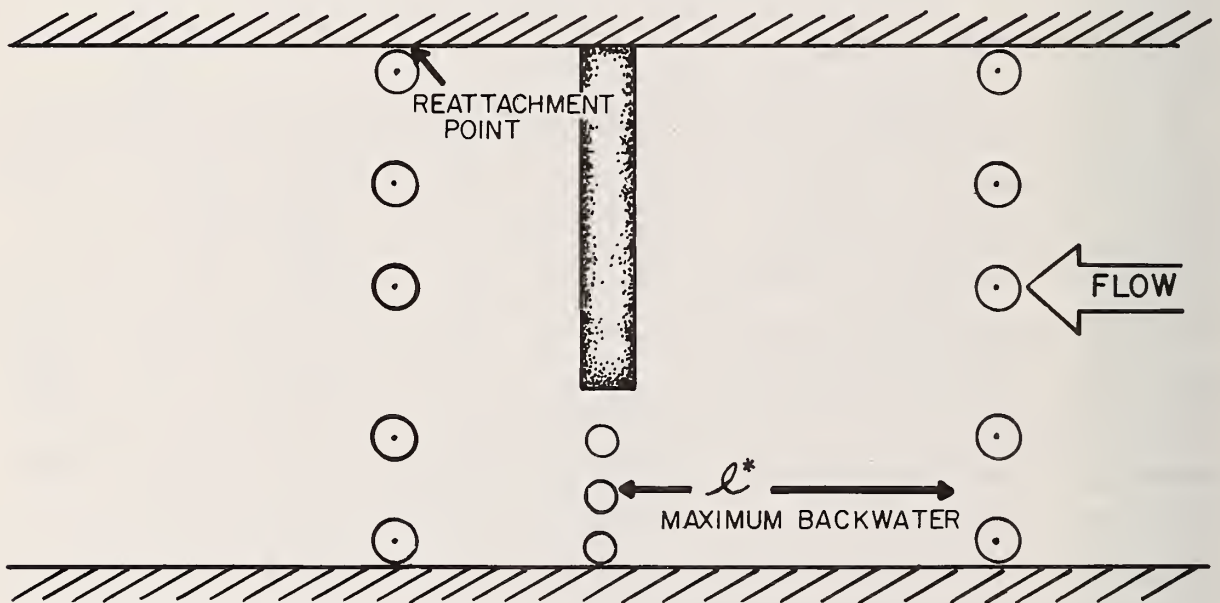
By far the most significant data collected from the large flume were depth measurements. A typical model run recorded depth measurements at approximately 100 separate locations. These locations can be classified as either stationary or moveable. Moveable gage (Table V-8) locations were a function of crossing configuration, opening size and the radius of maximum backwater. These gages were located upstream of the constriction and usually within the cross section bounded by the radius of maximum backwater. The stationary gages numeric code and their location are given in Table V-9. The stationary gages were gages locked in place and located both upstream and downstream of the crossing. Figure V-7 is a description of the typical gage employed at the flume. The smallest scale gradation was 0.001 ft.

Water surface elevation was calculated by adding the bottom elevation to the depth of the water in the flume. Depth was calculated as the difference



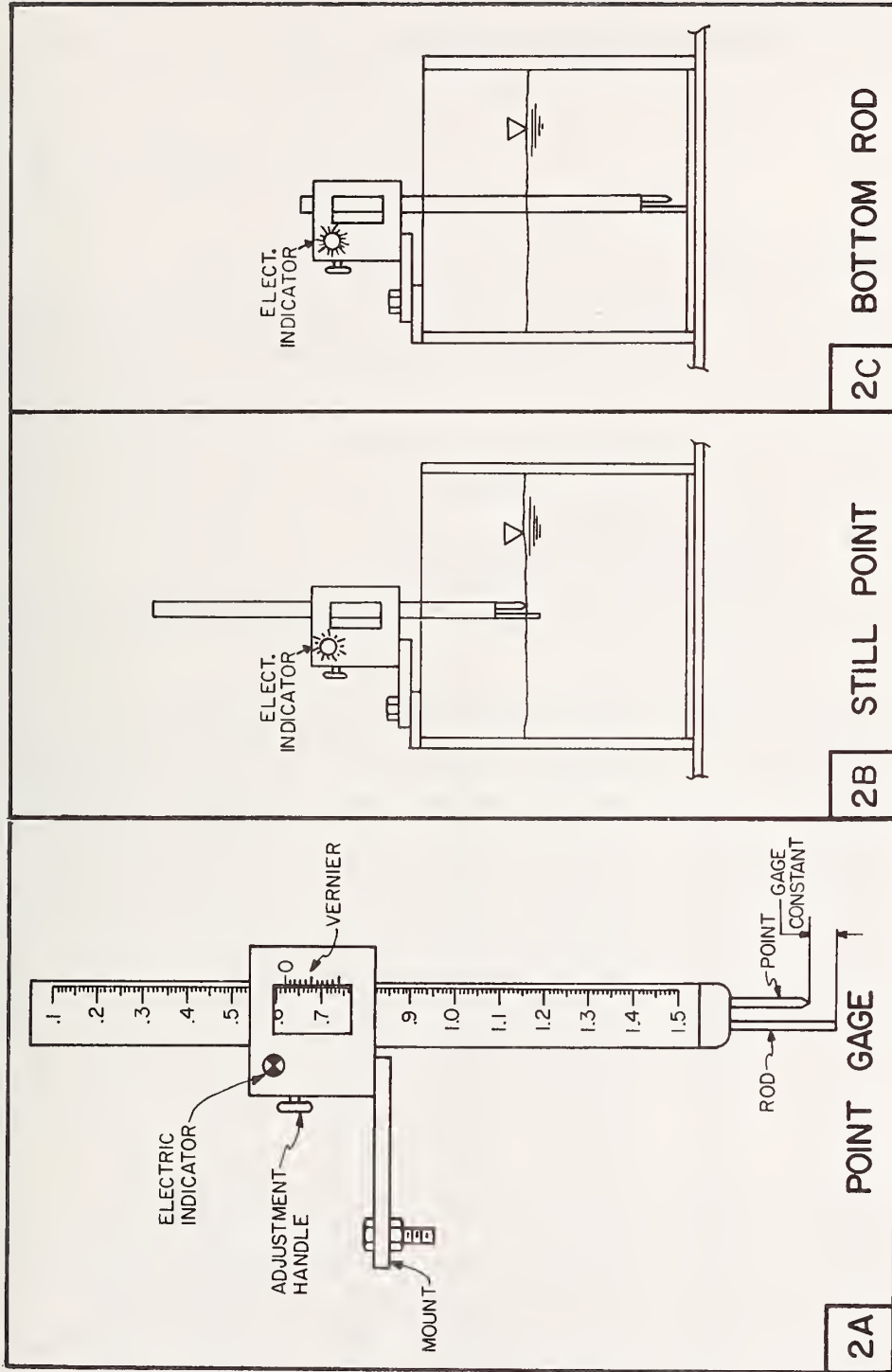
SKewed MODEL VELOCITY MEASUREMENT LOCATIONS

FIGURE V- 5



ECCENTRIC MODEL VELOCITY MEASUREMENT LOCATIONS

FIGURE V-6



POINT GAGES

FIGURE V-7

TABLE V-8
NUMBERS OF MOVEABLE GAGES

42	58	56	63	77
55	74	60	69	82
80	75	62	76	
88	67	57	81	
59	68	61	70	

TABLE V-9
STATIONARY GAGE LOCATIONS

Gage	X	Y	Gage	X	Y	Gage	X	Y
1	90.0	10.3	33	180.0	10.3	87	140.0	20.7
2	100.0	10.3	34	190.0	10.3	89	149.0	20.7
3	110.0	10.3	35	200.0	10.3	90	151.0	20.7
4	120.0	10.3	36	215.0	10.3	94	170.0	20.7
5	131.5	10.3	37	90.1	0.0	95	180.0	20.7
6	135.0	10.3	38	100.0	1.0	96	190.0	20.7
7	137.5	10.3	39	120.0	0.0	97	200.0	20.7
8	140.5	10.3	40	131.5	11.6	98	215.0	20.7
9	142.5	10.3	41	140.0	0.0	153	153.0	10.3
10	143.5	10.3	43	100.0	0.0	154	154.0	10.3
11	144.0	10.3	44	151.0	0.0	155	155.0	10.3
12	144.5	10.3	48	170.0	0.0	156	156.0	10.3
13	145.0	10.3	49	180.0	0.0	157	157.0	10.3
14	145.5	10.3	50	190.0	0.0	158	158.0	10.3
15	146.0	10.3	51	200.0	0.0	159	159.0	10.3
16	146.5	10.3	52	215.0	0.0	160	160.0	10.3
17	147.0	10.3	53	135.0	5.3	161	161.0	10.3
18	147.25	10.3	54	140.0	5.3	162	162.0	10.3
19	148.0	10.3	78	135.0	15.7	163	163.0	10.3
20	149.0	10.3	79	140.0	15.5	164	164.0	10.3
21	150.0	10.3	83	90.0	20.7	165	160.0	20.3
22	151.0	10.3	84	105.0	18.7	166	160.0	16.4
23	152.0	10.3	85	120.0	20.7	167	160.0	4.3
32	170.0	10.3	86	131.5	19.1	168	160.0	0.3

between the surface reading and bottom reading, plus the gage constant, which was the distance between the tip of the point and the tip of the rod shown in Figure V-7. This depth, when added to bottom elevation, known previously, yielded surface elevation.

FLOW MEASUREMENTS

Initially, the flow was measured using annubar flow meters installed in the discharge pipes near the control valves. These flow measurement devices were found to be insensitive. The flow was then measured using a stilling well connected to the upstream side of the overflow weir located at the head of the flume (Figure IV-1). Depth in the standpipe was measured using a hook gage, and then calibrated using the volumetric tank at the base of the flume to determine flow. The volumetric tank was a large tank of known constant cross sectional area in which the depth could be accurately determined. This permitted the calculation of flow rate to two significant decimal places.

After three months of operation, it was clear that the stilling well method did not yield the required accuracy as flows could not be duplicated exactly. This, of course, was due to the large variation in flow caused by a slight change in head over a long weir. A light liquid manometer was subsequently connected to the annubar flow meters placed earlier and an additional valve installed near the discharge pipe outlet. The manometer was calibrated against the volumetric tank readings. The manometer was connected to a manifold valve system attaching to the annubar meter in each discharge pipe. Some fluctuation in manometer readings was observed during the course of the experiment.

This was taken to mean that the flow being observed did not correspond to the expected flow, i.e., the flow at which the normal depths were measured. This was partially solved by regressing flow on depth for the normal runs corresponding to a roughness configuration and thus adjusting all the normal

depths accordingly. A detailed description of this problem is found in Chapter VI and the Appendix.

QUALITY CONTROL

As described earlier, the bridge backwater is the incremental rise in stage over the natural water surface elevation due to constriction of flow passage for a given flow rate. Thus, laboratory determination of backwater requires that a constant flow rate in the test flume be maintained before and after the crossing models are placed. Since the placement of crossing models in the flowing water was not feasible, model tests for the unconstricted and constricted conditions could be performed only on separate occasions. Thus, the accurate duplication of flow rates in the flume during test conditions was the paramount criterion for determining quality of test data. Other factors such as the fluctuation of voltage in the power supply to the pumps, human error, instrumentation malfunction, and change of floor elevations also affected the quality of data. Since some of these errors are local in nature, they cannot be controlled effectively. An inconsistency in discharge, however, can cause the stage to vary throughout the test flume, representing dissimilar flow regimes. The degree of duplication, therefore, was the criterion used as the basis for assessing data quality.

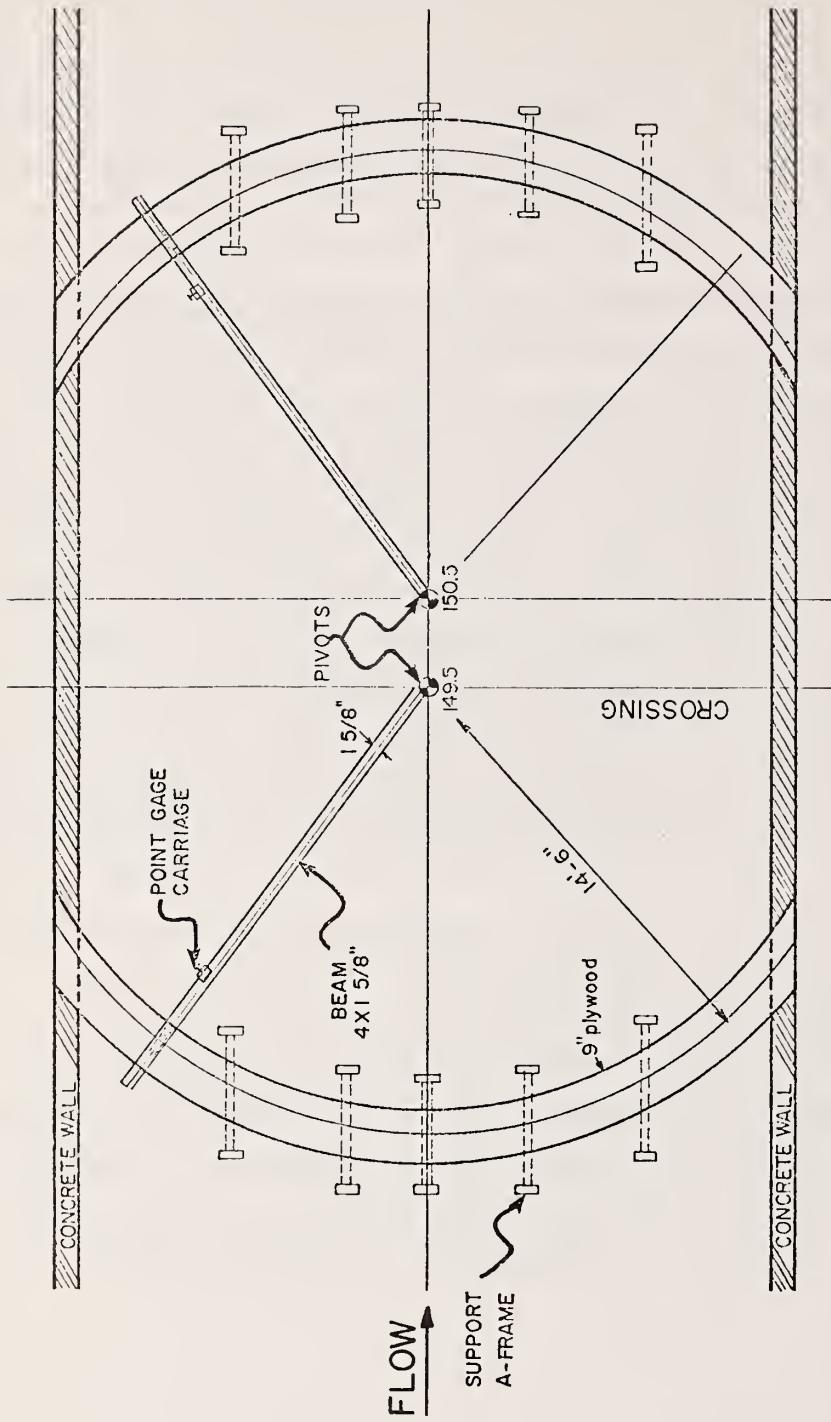
Unexpected shifts in elevation, changes in expected point scatter, and unusual shifts in the location or height of the maximum backwaters were indicated by this method quickly enough to allow corrective action to be taken immediately before moving on to other areas of the testing. This assured reasonable quality in the large amounts of data to be collected in the short period of time the flume was in operation.

OPERATIONAL PROBLEMS

A number of operational problems and decisions significantly affecting the experiment are listed here in an effort to provide insight into the data reliability, particularly in any aspects which might materially affect conclusions drawn from the data.

All elevations measured in the flume were based on a bench mark which was assigned an elevation of 10.000-ft. A flow of approximately 4-6 cfs was maintained when bottom elevations were taken in the flume. A problem which affected depth measurement was the presence of standing waves in the test flume. This was alleviated by the placement of a layer of 6-in. rubberized horsehair mats along both sides of the test flume. Despite the installation of the energy-absorbing mats slight fluctuations in water surface elevation still existed. Minimum fluctuations of 0.002 ft to maximum of about 0.022 ft in double amplitudes were recorded. The wave was probably generated by the placing of the roughness elements aggravated by a slight slope of the flume in the north to south axis. The regular spacing of the elements allowed amplification of vortex strengths and resonance of these vortices interacted with vertical flume walls.

One of the difficulties involved in the experiment was the accurate estimation of the location of the maximum backwater. Previous studies at Colorado State University suggested that its location is at a distance of one bridge length away from the crossing. The search for its location was made from a beam (Figure V-8) having an adjustable slope and a moveable point gage. The slope was set equal to the slope of the flume's bottom surface. Thus by sliding the point gage along the beam the location of the greatest depth was determined. This method was used for all centered and eccentric crossing configurations.



BEAM APPARATUS USED FOR LOCATING MAXIMUM BACKWATER

FIGURE V-8

VI. PRESENTATION AND ANALYSIS OF DATA

INTRODUCTION

This chapter, which is divided into five major subsections, describes the data analysis relating to the objectives of the experiment listed in Chapter I. Among these are the determination of the effect of Froude number, opening ratio, abutment shape, roughness pattern, skewness and eccentricity on the magnitude and location of maximum backwater. Due to the unusual nature of the roughness elements (i.e., protruding through the free surface), an important aspect of this analysis was to determine their relative effectiveness in relation to the modeling of prototype behavior.

The first section of the chapter, "Dimensional Analysis," presents the theoretical basis for the data analysis. The dimensionless dependent variables l^*/b and h^*/y_0 are expressed as a function of the major independent variables varied in the experiment. This analysis is extended to the backwater coefficient, K^* , presented in the third section.

The "Analysis of Water Surface Elevation" presented in the second section has a two-fold purpose: to describe the sensitivity of the most basic parameter recorded, water surface elevation, to the independent variables in the experiment; and to introduce the statistical tool, Analysis of Variance (ANOVA), used in this and later analyses presented in the chapter.

The ANOVA statistically estimates the presence of effects in the measured data caused by changes in the independent variables, assuming certain specific conditions of the data are met. ANOVA demonstrates the effect caused by changing the independent variables on the dependent variable being measured

or calculated, i.e., the effect of Froude number on maximum backwater location. It also provides an estimate of the reliability of the conclusions drawn and the ability to easily handle discontinuous variables such as abutment shape and roughness patterns. However, due to time exigencies in the collection of data, only a small portion (12 percent) of the data can be analyzed by this method. In sections four and five, ANOVA is used as a preliminary screening tool to identify trends and effects in the analysis.

The fourth section presents an analysis of the maximum backwater location and the fifth concludes with an analysis of the height of maximum backwater. Both are conducted in accordance with the concepts developed in the "Dimensional Analysis" section.

DIMENSIONAL ANALYSIS

Any given physical phenomenon is governed by a set of independent quantities or characteristic parameters. The laws relating physical phenomena generally are expressed in the form of mathematical relations among the quantities involved. The principles of dimensional analysis serve as a vehicle for deriving the functional relationships for natural phenomena. This analysis attempts to establish these relationships required to describe the bridge backwater phenomenon among the pertinent parameters through the application of dimensional theory.

DEFINITION OF VARIABLES

Independent Variables

1. Geometry

(a) Channel

Longitudinal Slope (S_0)

Shape Factor (ξ)
Channel Roughness and Distribution (C_f)
Channel Width (B)

(b) Bridge
Abutment Shape (A)
Opening Size (b)
Skewness (γ)
Eccentricity (E)
Bridge Width (w)

2. Flow Characteristics

Discharge (Q)
Depth (y)

3. Fluid Characteristics

Density (ρ)
Viscosity (μ)

4. Constant

Gravitational Constant (g)

Dependent Variables

Maximum Backwater (h^*)
Maximum Backwater Location (l^*)

ANALYSIS

From the variables listed above, the backwater of a highway stream crossing can generally be derived from the following characteristic parameters:

$S_0, \xi, C_f, B, A, b, \gamma, E, w, Q, y, \rho, \mu,$ and g .

And the functional relationship between the dependent and independent variables may be expressed by:

$$h^*, \ell^* = \phi_1(S_0, \xi, C_f, B, A, b, \gamma, E, w, Q, y, \rho, \mu, g) \quad (38)$$

Replacing Q with V yields:

$$h^*, \ell^* = \phi_2(S_0, \xi, C_f, B, A, b, \gamma, E, w, V, y, \rho, \mu, g) \quad (39)$$

Consider the flow conditions at the bridge site prior to the construction of the bridge. A given discharge, Q_0 , can be expressed by B, y_0 and V_0 . Then Equation 39 can be rewritten as

$$h^*, \ell^* = \phi_3(S_0, \xi, C_f, B, A, b, \gamma, E, w, V_0, y_0, \rho, \mu, g) \quad (40)$$

Selecting ρ, y_0 and v_0 as basic quantities (i.e., repeating variables) we obtain the following dimensionless equations:

$$\frac{h^*}{y_0} = \phi^4 \left[S_0, \xi, C_f, \frac{B}{y_0}, A, \frac{b}{B}, \gamma, E, \frac{w}{B}, \frac{V_0 y_0}{v}, \frac{V_0^2}{g y_0} \right] \quad (41)$$

and

$$\frac{\ell^*}{b} = \phi_5 \left[S_0, \xi, C_f, \frac{B}{y_0}, A, \frac{b}{B}, \gamma, E, \frac{w}{B}, \frac{V_0 y_0}{v}, \frac{V_0^2}{g y_0} \right] \quad (42)$$

In the present study, the bottom slope and shape of the flume and the bridge width are fixed. Therefore, the terms $S_0, \xi,$ and $\frac{w}{B}$ may be dropped from Equations 41 and 42, resulting in the following equations:

$$\frac{h^*}{y_0} = \phi_6 \left[\frac{V_0^2}{g y_0}, \frac{V_0 y_0}{v}, \frac{b}{B}, \frac{B}{y_0}, C_f, \gamma, E, A \right] \quad (43)$$

and

$$\frac{\ell^*}{b} = \phi_7 \left[\frac{V_o^2}{gy_o}, \frac{V_o y_o}{v}, \frac{b}{B}, \frac{B}{y_o}, C_f, \gamma, E, A \right] \quad (44)$$

The lower limit of the Reynolds Number (i.e., $\frac{V_o y_o}{v}$) tested was approximately in the order of 5,000, which is in the turbulent flow region; hence the effect of the Reynolds Number can be ignored. Furthermore, a previous study at Colorado State University has shown that the effect of the Reynolds Number on the backwater is negligible. Equations 43 and 44 can be further reduced to:

$$\frac{h^*}{y_o} = \phi_8 \left[\frac{V_o^2}{gy_o}, \frac{b}{B}, \frac{B}{y_o}, C_f, \gamma, E, A \right] \quad (45)$$

and

$$\frac{\ell^*}{b} = \phi_9 \left[\frac{V_o^2}{gy_o}, \frac{b}{B}, \frac{B}{y_o}, C_f, \gamma, E, A \right] \quad (46)$$

Let

$$\pi F_r = \frac{V_o}{\sqrt{gy}}$$

$$M = \frac{b}{B}$$

$$\tau = \frac{B}{y_o}$$

$$\delta = \frac{h^*}{y_o} \quad \text{and}$$

$$\epsilon = \frac{\ell^*}{b}$$

Then Equations 45 and 46 become

$$\delta = \phi_{10}(\pi F_r, M, \tau, C_f, \theta, E, A) \quad (47)$$

and

$$\epsilon = \phi_{11}(\pi F_r, M, \tau, C_f, \theta, E, A) \quad (48)$$

In Equations 47 and 48, τF_r is the Froude Number of the flow, M is the ratio of the bridge opening to the valley width, τ is the width-depth ratio of the stream, C_f is the roughness parameter of the channel, γ is skewness, E is eccentricity, and A is the shape factor of the abutments, as defined previously. Equations 47 and 48 are used as the basis for the data analysis.

Since the test flume provides only a single slope, the interrelation of τF_r and τ cannot be examined explicitly. For example, it is impossible to set a value of τ and vary values of τF_r without changing the slope of the flume and the flow rate. As a result, a change in flow rate will cause the depth and, hence, the value of B/y to change accordingly, since B is a constant.

In the present study, the value of B/y ranges from 13 to 82 in the model flume. Based upon a distortion of 8.3 (i.e., 100/12) the corresponding width-depth ratio for the prototype is 110 to 680. (Existing field data collected at approximately 100 bridge sites have shown that the values of the width-depth ratio vary from 6 to 770.) In view of this analysis, the effect of the width-depth ratio of the model data may be eliminated. Equations 47 and 48 can then be rewritten as

$$\delta, \varepsilon = \phi_{12} (\tau F_r, M, C_f, A, \gamma, E) \quad (49)$$

Equation 49 has six independent dimensionless variables useful for the development of a functional relationship describing δ and ε . Of course, γ and E are only important for skew and eccentric model openings. The elimination of these two leaves four independent parameters. The development of the relationship describing δ and ε are developed from plotting and verified by statistics. Typically in this type of analysis heavy reliance is placed on Analysis of Variance (ANOVA) [17,18] and Regression Analysis.

TWO-DIMENSIONAL ANALYSIS OF WATER SURFACE ELEVATIONS

This section presents the results of an analysis of the effects of Froude number (F), crossing opening ratio (M) and abutment shape (A) on water surface elevations for each gage position used in collecting data over the entire flume for roughness pattern "C," i.e., main channel 25 percent and flood plain 75 percent. This includes 36 runs with the crossing configuration centered in the flume at the 150 ft location. Roughness pattern C was selected because it offers a complete set of the results of varying Froude number through four levels, opening ratio through three levels and abutment shape through three levels. Complete set means every combination of three variables was tested yielding 36 runs ($3 \times 3 \times 4$). Roughness pattern C is the only set of centered runs meeting this definition. Skew and eccentric crossings are also complete sets but with a different set of variables, i.e., they include angle of skewness and eccentricity.

The purpose of this analysis is to:

1. Determine and/or confirm that the major variables affected backwater in a measurable way.
2. Determine the spatial range of the effects of these variables in the flume.
3. Determine where normal depth was re-established.
4. Introduce the concept of Analysis of Variance (ANOVA) used in this and later sections.

This analysis demonstrates that the opening ratio, Froude number, and abutment shape are statistically related to the height of the water surface elevation, each independently of the other. This is, of course, by no means a startling conclusion. However, the analysis extends this over the entire flume for each gage where data were taken. This permits an estimation not only of where opening and abutment shape affect elevation but also of where they do not affect water surface elevation. This by definition represents a return to normal flow conditions.

Implicitly this type of data analysis serves as a very good indicator of the amount and magnitude of data error in the flume along with an indication of the sensitivity of the dependent variable, water surface elevation, to changes in the independent variables (Froude number, opening ratio, and abutment shape). It also provides an indicator, in the F distribution, as to nonrandom error introduced by either the experimenter or model design. The F distribution is a statistic used in testing for effects and specifically represents a ratio of mean squares. This is not to be confused with Froude number (F). In all cases the meaning should be clear from the text.

Since the ANOVA is used in following sections, we will digress with a brief nontechnical description of the method, its advantages and disadvantages and how it was employed here. For a theoretical presentation the reader is referred to Reference 17. The purpose of the following section is merely to acquaint the reader with the principles of ANOVA.

ANALYSIS OF VARIANCE

An analysis of variance is a statistical analytical method which can be used on certain kinds of experimental data (i.e., data meeting certain well defined criteria) in order to reveal the importance of effects of individual independent variables on some dependent variable. In this problem is answered the question "Does the data demonstrate at a given confidence level whether Froude number, opening ratio (M), or abutment shape have a direct effect on water surface elevation or does any combination of these variables have an effect on water surface elevation?"

Since Froude number is directly linked to flow, an obvious expected result is that the differing Froude numbers have an effect on surface elevation. It is also expected that differing M ratios should show significant effects at least upstream of the constriction. It is not so obvious whether the difference in abutment shapes, i.e., wingwall and spillthrough, is great enough to cause

a statistically significant effect on water surface elevation. It is also not obvious what the spatial distribution of these effects is in the flume. For example, the ANOVA can demonstrate how far upstream from the flow constriction the opening ratio affects depth. If the opening ratio affected depth over an area, that area would be classified as a Zone 2 flow region (Figure II-3).

The same can be demonstrated for the flume below the constriction, i.e., "Does Zone 3 extend the length of the flume or is Zone 4 (normal flow and depth) attained?" The answer to this question determines the location where normal depth is attained. Throughout this report any question answered by ANOVA is assumed to be prefaced with "According to the statistical model used does the data collected demonstrate...?"

The ANOVA used in this section and generally throughout the data analysis is a three-variable, factorial design with one replication. "Three-variable" refers to the independent variables, i.e., Froude number, opening ratio, and abutment shape. Roughness element pattern was not included as a variable in the analysis due to incompleteness of the data matrix. Each variable is divided into levels. In the analysis there are four levels for Froude number, each representing one of the four flows used, three levels for opening ratio, corresponding to 3, 5 and 8ft openings and three levels representing abutment shape (wingwall, spillthrough and spur dike). For ease of discussion the two abutment shapes, wingwall, **spillthrough**, and spur dikes are collectively referred to as abutment shapes. Each represents a specified level of the variable "A". Factorial design refers to the combinations of the levels, in this case the (4x3x3) 36 flume runs. This means there are 36 water surface elevations for each point. Ideally, the ability to discern effects is greatly increased by replications; however, due to the expense of the data this was not done.

An important difference in independent variables is whether they are fixed or random. Fixed variables are variables whose levels are arbitrarily chosen by the experimenter. In this example, abutment shape and opening ratio are fixed variables. As originally planned, flow would also have fallen into

this category but due to the difficulty of generating the same exact flow, as previously described, flow was classified as a random variable. As will be seen when the model is discussed, this is generally a conservative bias. An ANOVA which uses random and fixed variables is referred to as a Mixed Model.

The statistical model that tests effects and interactions for the mix of random and fixed variables is developed using standard procedures described in most advanced texts [20]. A list of the variables and the test for each is shown in Table VI-1. The components of variance represent the theoretically possible variance attributable to each source of variance. This is shown under the heading "Components of Variance" by the random error component, sigma, and a second and/or third component attributable to the effect being tested.

The effects are tested by calculating the various ratios shown under the column "Test." The parameter MS represents a mean square, which in turn is calculated by dividing the sums of squares by the degrees of freedom. Each mean square theoretically can contain the components of variance attributable to it by the design, as shown in Table VI-1. Sums of squares and mean squares are the most mechanistic part of an analysis of variance. The calculating formulas for each sum of squares representing each component can also be found in an advanced text describing an ANOVA (see Myers, Ref. 17). The calculating procedure is exactly the same regardless of the classification of variables as fixed or random. Note that in the development of the testing ratios each major variable is isolated from the effect of the others. In essence, the effect of opening ratio on surface elevation can be tested with the effects of Froude number and abutment shape removed.

For example, the mean square for Froude number, MS_F , contains a random error, sigma, and possibly a variance component due to the differences in the effects of Froude number on the dependent variable, water surface elevation. The determination of whether there is an effect of Froude number is demonstrated by the ratios shown under the heading "Test" in Table VI-1. If the conditions of normality, independence and homogeneity hold, the ratio of two mean squares can be shown to have an F distribution. Consequently, the

TABLE VI-1
ANALYSIS OF VARIANCE

Source of Variance	Type	df	Components of Variance	Test
Froude (F)	Random	3	$\sigma^2 + Bn\theta^2_F$	MS_F/MS_{FA}
Abutment Shape (A)	Fixed	2	$\sigma^2 + Qn\theta^2_A + Bn\theta^2_{FA}$	MS_A/MS_{FA}
Opening Ratio (M)	Fixed	2	$\sigma^2 + Qn\theta^2_M + Mn\theta^2_{FM}$	MS_M/MS_{FM}
FxA Interaction	Mixed	6	$\sigma^2 + Bn\theta^2_{FA}$	No Test
FxM	Mixed	6	$\sigma^2 + Mn\theta^2_{QB}$	MS_{FM}/MS_{FA}
MxA	Mixed	4	$\sigma^2 + Qn\theta^2_{MA} + n\theta^2_{FAM}$	MS_{MA}/MS_{FAM}
FxAxM	Mixed	12	$\sigma^2 + n\theta^2_{FAM}$	MS_{FAM}/MS_{FA}

Where:

- x = interaction,
- df = degrees of freedom,
- sigma = random error component of variance,
- B = number of levels of openings,
- M = number of levels of abutment shapes,
- Q = number of levels of Froude number,
- θ = variance (either fixed or random),
- MS = mean square,
- n = number of replicates

probability of obtaining various F values for a given confidence level and thus the presence of an effect can be determined. For example, if the effect of Froude number is negligible on water surface elevation (which it is not), the hypothesis that $BMn\theta_F^2=0$ would be true. The F test would be:

$$F_{(3,6)}^{(.05)} = \frac{\sigma^2 + BMn \theta_F^2}{\sigma^2 + BMn \theta_{FA}^2} \quad (51)$$

A prior assumption in this design is that $BMn\theta_{FA}^2=0$. The reasons for this assumption are described in a later part of this section. Rewriting Equation 51,

$$F_{(3,6)}^{(.05)} = \frac{\sigma^2 + BMn \theta_F^2}{\sigma^2} \quad (52)$$

If the hypothesis is true, i.e., $\theta_F^2=0$, Equation 52 reduces to

$$\frac{\sigma^2}{\sigma^2} = 1$$

Of course, in reality the above ratio is never exactly 1, whether the hypothesis is true or false. However, if the hypothesis is false and $BMn\theta_F^2=0$, the ratio is greater than 1. How much greater than 1 determines the level of confidence that can be placed in the result. The 95 percent level of confidence for the above F test is 4.76. For the hypothesis that differing Froude numbers do not have an effect on water surface elevation to be rejected at the 95 percent confidence level, the ratio of the two calculated mean squares must be less than 4.76. The 95 percent confidence level should be interpreted as there is a 95 percent chance that if the ratio equals 4.76 that the hypothesis is false ($H_0:BMn\theta_F^2=0$) and Froude number does have an effect on water surface elevation. A similar process is used to test the other effects as shown in Table VI-1 under the heading "Test."

The term σ^2 in each component of variance requires special mention. This term ideally contains only random error and as such has an expected mean of 0 and variance of 1. In the F test presented above, note that σ^2 appears in the denominator. Intuitively this would indicate that the larger the random error term becomes, the more difficult it is for a hypothesis to test false (i.e., an effect exists). In experimental problems the estimate of σ^2 is probably one of the most important and difficult problems that must be answered. If random measuring error or nonrandom error is too large in comparison to the effect being measured, positive results cannot be drawn from the data. The efficacy of the F test lies in the fact that this problem is recognized in the analysis.

In the analysis presented in this chapter the ANOVA is often used as a screening mechanism to determine whether sufficient reliability can be placed in the data to justify further analysis using regression techniques. It is recognized that regression analysis alone can provide results similar to those of the ANOVA but since ANOVA more easily handles the noncontinuous type of variables required for this experiment, that analysis was performed initially.

ANALYSIS OF DATA FOR ROUGHNESS PATTERN C

The following conditions were tested for roughness pattern C (75 percent in flood plain, 25 percent in main channel):

<u>Froude Number</u>	<u>Opening Ratio (M)</u>	<u>Abutment Shape (A)</u>
.107	.387	Wingwall
.082	.242	Spillthrough
.072	.145	Spur Dike
.059		

The analysis of variance took the form previously shown in Table VI-1.

It is standard procedure to use within-cell variance as an estimate of random error, σ , if replicates of the experiment are possible. If this proves impossible, as in this case, either a two- or three-way interaction can be used as a conservative estimate of σ .

The data base for this analysis consisted of 36 runs, each consisting of approximately 100 gage points. Thus at each point 36 measurements of water surface elevations were expected. An examination of the data base revealed that for most gage points, the data matrix (4x3x3) was complete. However, occasionally between one and three points were missing. The missing values were estimated since for the most part there was only one datum lacking and although it is possible to analyze the matrix of data with a limited amount of missing data, substantial changes in technique must be made or the analysis will be biased. The data were highly linear for opening size and flow, so that a linear regression estimate of missing data would not seriously bias results and the error introduced would be minimal. A "front end" was constructed and added to the program which performed a linear regression over the three directions of the matrix to generate three estimates of a missing value. The correlation coefficient (R^2) was computed for $n > 3$, and the best value was selected from three estimates. Generally, R^2 (for the regression on flow) was very close to unity, and estimates were based on that fitted line.

Figure VI-1 presents the analytical results in a gage map of the flume. As may be seen from the first gage map, the water surface elevation at any point in the flume is affected by flow at the 95 percent confidence level. Since flow is a significant variable everywhere, even at the 99.9 percent level, it is not shown on the gage map.

Opening ratio (M) was found to significantly affect surface elevation everywhere above the constriction, demonstrating that the backwater clearly extended back beyond the upper limit of the flume. Note also that the effects of opening ratio essentially are limited to above the constriction. This is, of course, to be expected.



- OPENING RATIO (M) SIGNIFICANT
- ABUTEMENT SHAPE (A) SIGNIFICANT
- ABUTEMENT-OPENING SIZE INTER-ACTION SIGNIFICANT (A X M)
- FROUDE - OPENING SIZE INTER-ACTION SIGNIFICANT (F X M)
- FROUDE - ABUTEMENT OPENING SIZE INTERACTION SIGNIFICANT (F X M)
- CONFIDENCE LEVEL 95 %
- ALL GAGES SHOWN HAD SIGNIFICANT FROUDE EFFECTS
- THE M REFERS TO GAGE POINTS

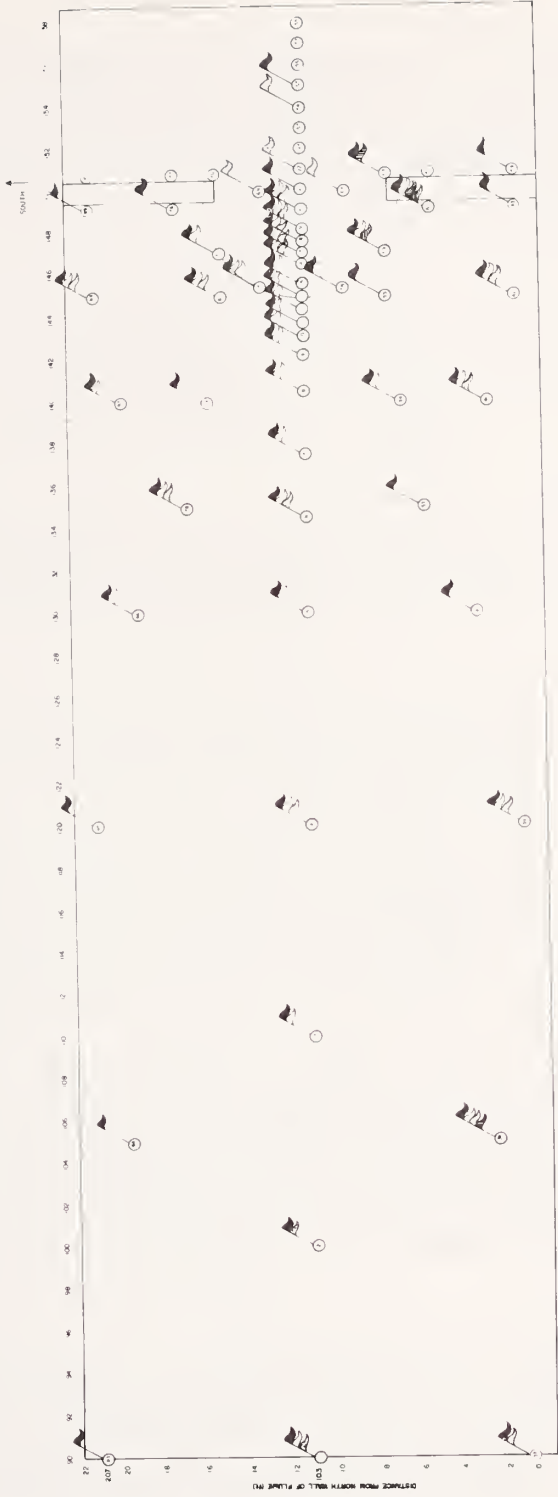


FIGURE VI-1
ANALYSIS OF VARIABLES AFFECTING WATER SURFACE ELEVATION

The variable abutment shape was found to affect stage in a region bounded for practical purposes by the 120-ft line (30 ft above the constriction) although the demarcation is not clear cut and some other gages above this line appeared to have been affected.

The only interactive effect which was significant for a large number of gages was AxM. This is the interactive effect on water surface elevation of abutment shape and opening, independent of both of their already noted main effects. Interestingly, in general terms these appear to congregate within the constriction; there appears to be a region on the centerline above the constriction where the interaction is not significant; and finally, above the 120-ft line and on the north side of the flume, all gage depths appear to be affected.

Except for a few anomalous two-way interactions, no effects of opening or abutment shape are observed below the constriction.

This leads to the conclusion that normal depth has been reestablished below the constriction well within the flume. The line of reasoning follows: Assume normal depth has not been established. If this were the case the various stages below the constriction would show an effect of either opening or abutment shape since these are the principal changing variables affecting depth in this experiment other than Froude number. Certainly the reattainment of normal depth would be affected by opening ratio if this were the case. However, the analysis demonstrates that below the constriction only Froude number has an effect on elevation. This would indicate normal depth has been reattained.

Establishing that normal depth has been attained allows the method to be applied for establishing flow based on specific gages as described in the Appendix. Only those gages on the centerline where normal depth was shown to occur were used as estimators of average depth for a particular run.

It should also be noted that the analysis of variance, like every other probability-based statistical analysis using a confidence level, provides a finite probability of not only making a correct decision, but a wrong decision as well. In the case of a 95 percent confidence level, it should be noted that there is a 5 percent chance that the significant ratio is coincidental, that is, anomalous, and the effect thus indicated as being significant actually is not. This will occasionally cause the analyst to assume that an effect has been manifested when it has not. This may be partially responsible for the occasionally apparently anomalous significant interactive effects.

Another possible explanation, and one which accounts for gage locations where several interactive effects are anomalously significant, is a lack of validity of one or more of the assumptions, especially that error is independent of the variables, i.e., the error introduced in the surface elevation measurement for changes in flow is the same as for changes in abutment shape. This is especially true under the present circumstance of using one of the interactive effects to estimate error. If error was indeed small for the interaction but large over other variables, this would be manifested as anomalous groups of significant variables and interactions. Such a situation may well have given rise to the condition at gages 38 and 1 and those downstream showing a significant effect other than flow.

The strong effect of the abutment variable on water surface was selected for special duty, in view of the very close geometric similarity of two of the abutment shapes (spillthrough and wingwall) and the very much different spur dike. It was hypothesized that the strong effect was caused by the disparity between spur dike and the other two shapes.

There are two straightforward ways to test this hypothesis using analysis of variance. One, commonly called "orthogonal contrasts," allows the analyst to extract the maximum amount of information from the data as dictated by the number of degrees of freedom. The other method, which was

considered more practicable under the circumstances, was to remove from the statistical analysis that part of the data base relating to spur dike and to proceed to determine whether abutment shape was or was not a significant independent variable relative to surface elevation at the various gages. Since the analysis had already been performed with spur dike data included, such an analysis would provide for two related pieces of information. First, were the strong effects of the abutment variable due to the large structural differences between the spur dike and the other two abutment shapes, and second, if so, just how much impact did the difference between spillthrough and wingwall have on surface readings.

The results of this analysis are presented in Figure VI-2 in the form of a second gage map of the flume. Comparing the results of this analysis with those for two abutment shapes and spur dikes combined, certain interesting conclusions may be drawn. First, it appears that the spur dike did in fact cause some of the significant effects of the variable abutment on surface elevation, particularly between the 130-ft line and the constriction and off the centerline. Interestingly, however, the gages situated on the centerline and between the 130-ft line and the constriction appear to be affected by the difference between spillthrough and wingwall. Also interesting is the apparently substantial reduction of the number of gages exhibiting the MxA interactive effect, particularly in and near the constriction. It would appear that the strong interactive effect observed in the analysis described earlier was due to a considerable extent to the presence of spur dike data. Thus, interpreting this observation, we may conclude that while spur dike alters the impact of opening size on depth the direct effect of either abutment shapes or spur dike is strong for even minor differences in geometry.

These results must be interpreted carefully, however, Because of the approach taken for investigating the impact of spur dike, the total degrees of freedom and the degrees of freedom for the abutment variable and all abutment-incorporating interactions are reduced. This reduces the sensitivity of the analysis to the presence of effects. This means that we may accept without



- OPENING RATIO (M) SIGNIFICANT
- ABUTMENT SHAPE (A) SIGNIFICANT
- ABUTEMENT-OPENING SIZE INTER-ACTION SIGNIFICANT (A X M)
- FROUDE -OPENING SIZE INTER-ACTION SIGNIFICANT (F X M)
- FROUDE -ABUTEMENT OPENING SIZE INTERACTION SIGNIFICANT (F X M)
- CONFIDENCE LEVEL 95 %
- ALL GAGES SHOWN HAD SIGNIFICANT FROUDE EFFECTS
- MODEL TESTED WITH SPUR DIKE DATA REMOVED

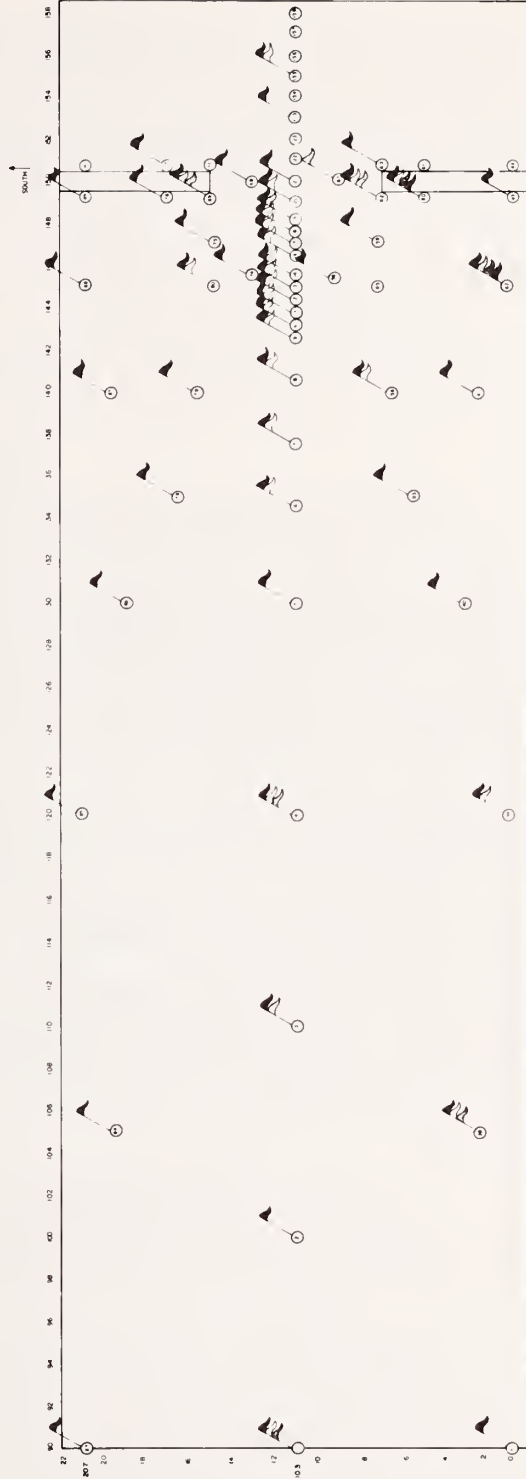


FIGURE VI-2
ANALYSIS OF VARIABLES AFFECTING WATER SURFACE ELEVATION-EXCLUDING SPUR DIKES

reservation those gages which continue to show some effect, but have reservations with those observations where effects have been minimized or are not observed. In terms of the results of these two analyses, it is reasonable to accept the premise that spur dike was not the sole reasons for the impact of the abutment variable on surface readings near the constriction. However, the observation that the interactive effect ($A \times M$) is reduced may be due in part to a reduced data base.

The conclusions from an analysis of roughness pattern C (FP-75, MC-25) are:

1. Opening ratio (M) affected surface elevation the entire length of the flume above the constriction. No effects were noted more than 5 ft below the constriction.
2. Normal depth was reattained within 5 ft below the constriction for the flows and openings studied. Individual effects of flow with a given opening size in regard to the attainment of normal depth were not investigated.
3. Water surface measurement was sensitive enough to detect differences in wingwall and spillthrough abutment shapes (A).
4. Froude number (F) was a significant factor in water surface elevation measurement.
5. Interactive effects between abutment shape and opening ratio, though significant in some cases, are generally inconclusive due to their scatter. This interaction might be interpreted as an effect of turbulence due to abutment shape and constriction.
6. The use of spur dikes was responsible for a large portion of the water surface elevation effects attributed to the variable abutment shapes.

In general, the ANOVA analysis demonstrates that the primary parameter recorded, water surface elevation, was sufficiently sensitive as measured to demonstrate the effects of each of the independent variables, Froude number, opening ratio, and abutment shape in the data collected.

ANALYSIS OF TOTAL BACKWATER COEFFICIENT, K^*

The backwater equation as developed by Liu and Bradley [1], solved for K^* is given as:

$$K^* = \frac{h^*_1}{\alpha_2 V_{n2}^2 / 2g} - \frac{\alpha_1}{\alpha_2} \left[\left(\frac{A_{n2}}{A_4} \right)^2 - \left(\frac{A_{n2}}{A_1} \right)^2 \right] \quad (53)$$

A_{n2} = Cross-sectional area of the opening at normal flow

V_{n2} = Velocity in the opening at normal flow

In terms of application where the upstream and downstream areas, A_1 and A_4 , vary little, the calculation of K^* is essentially a function of the velocity head, $V_{n2}^2/2g$. In the flume experiments of the present study, A_1 and A_4 are the same since the flume was of a regular shape with both A_1 and A_4 reflecting normal depth. Alpha 2 (α_2), which gives a weighted average of the kinetic energy distribution across the opening, was essentially equal to one for the flume runs reported. However, Equation 53 was used for the calculation of all backwater coefficients presented in this section.¹

Previous studies [1] have established the experimental relationship that K^* varies primarily with

1. Stream constriction ratio (M),
2. Type and shape of bridge abutment (A),
3. Number, size and shape of piers in the constriction (P),
4. Asymmetric position of the crossing in relation to the flow (E),
5. Angle of skewness (γ), and
6. Froude number (F).

¹Data for the analysis described in this section are in the Appendix under the heading "KB" in the Consolidated Data Table.

$$K^* = f(M, A, P, E, \gamma, F, C_f)$$

In the flume experiments the effect of piers was not a variable and the effect of skewness and eccentricity was measured using only one abutment shape and roughness. These conditions allow the estimation of K^* for centered models:

$$K^* = f_1(M, A, F, C_f) \text{ and}$$

and for skewed and eccentric models:

$$K^* = f_2(M, F, E, \gamma).$$

It is important to note that these independent variables are not theoretically related to K^* with the exception of Froude number, F . The backwater coefficient can thus be rewritten as:

$$K^* = \frac{2h_1^*}{F_{n2} h_n}$$

ignoring α_2 , where F_{n2} and h_n are theoretical values related to normal flow. In most cases the degree of interdependence between independent variables does negate the usefulness of each independent variable in predicting the dependent variable, K^* .

BACKWATER COEFFICIENT (K^) FOR CENTERED CROSSING*

Analysis of Variance (ANOVA)

The purpose of the analysis of variance as used in this and following sections is to serve as a preliminary screening device using a small portion of the data base (approximately 12 percent). Since the data base encompasses a reasonable distribution of the abutment shapes, openings, and flows, results derived from this portion of the analysis can be considered to hold for the entire data base within limits. Reasonably strong positive or negative

results can be extrapolated with a degree of certainty while marginal results should, of course, be viewed with caution.

In any case, the analysis of variance will complement the graphical exposition, and these in turn will complement the regression analysis.

The K^* was analyzed by ANOVA using the same data as used in the section on "Analysis of Water Surface Elevations." The dependent variable, water surface elevation, was replaced with K^* . This provided (4x3x3) 36 estimates for K^* . Each estimate represented a particular combination of Froude number (calculated in the flood plain), opening ratio and abutment shape.

Table VI-2 presents the output of the ANOVA and Table VI-3 the results of testing for effects. The abutment shape variable is the only observed significant effect at the 95 percent confidence level (Table VI-3). This means that the only variable whose various categories measurably affected K^* at the stated level was abutment shapes. Removing spur dikes from the data base eliminated this effect. This indicates the effect on K^* was significant for spur dikes but not for wingwall or spillthrough. The testing also indicates that the effect of the various categories of M or F on K^* was not statistically significant. For example, the effect on K^* of differing opening ratios was not observed in the data at the 95 percent significance level. The effect of Froude number on K^* was not statistically significant at the stated level. This does not deny the existence of a relationship but rather states that the data analyzed do not confirm its existence at the given level of confidence.

In order to further test for significance, the conservative estimate of the error mean square, σ^2 , was relaxed. By observing the ratio of mean squares in Table VI-3, it can be noted that the three-way interaction mean square is considerably less than the interaction mean square FA. FA was used as an estimate of σ^2 . However, after the three-way mean square was substituted and the proper test ratios calculated, no significant differences were noted other than those previously indicated.

TABLE VI-2
ANOVA OF K* WITH AND WITHOUT SPUR DIKES

WITH SPUR DIKES				WITHOUT SPUR DIKES		
Levels of Variables				Levels of Variables		
F	4			F	4	
M	3			M	3	
A	3			A	2	
<u>Grand Mean</u>		<u>1.70</u>		<u>Grand Mean</u>		<u>1.55</u>
Source of Variance	Sums of Squares	Degrees of Freedom	Mean Squares	Sums of Squares	Degrees of Freedom	Mean Squares
Froude (F)	0.39	3	0.13	0.24	3	0.08
Opening Ratio (M)	1.13	2	0.56	0.44	2	0.22
F X M	0.77	6	0.12	0.36	6	0.06
Abutment (A)	1.68	2	0.84	0.13	1	0.13
F X A	0.83	6	0.13	0.75	3	0.25
M X A	0.45	4	0.11	0.25	2	0.12
F X M X A	0.59	12	0.04	0.38	6	0.06
TOTAL	5.88	35		2.59	23	

TABLE VI-3
 TESTING OF K* WITH AND WITHOUT SPUR DIKES
 AT 95 PERCENT CONFIDENCE LEVEL

Source of Variance	Test	With Spur Dikes		Without Spur Dikes	
		F Statistic	Req. for Signif.	F Statistic	Req. for Signif.
Froude (F)	MS_F/MS_{FA}	4.76	0.95	No	No
Opening Ratio (M)	MS_M/MS_{FM}	5.14	4.39	No	No
Abutment (A)	MS_A/MS_{FA}	5.14	6.01	Yes	No
FxM	MS_{FM}/MS_{FA}	4.28	0.92	No	No
FxA	No Test	--	--	--	--
MxA	MS_{MA}/MS_{FMA}	3.06	2.28	No	No
FxMxA	MS_{FMA}/MS_{FA}	4.00	0.36	No	No

The conclusion drawn from this analysis is that the opening ratio, abutment shape and Froude number do not show a strong effect, if any, on K^* using data collected for 36 runs with roughness configuration C. It does not state there is no relationship, but rather these data do not demonstrate a relationship at a reasonable level of significance. The error is considered to lie in the large data scatter as shown in the following graphical analysis.

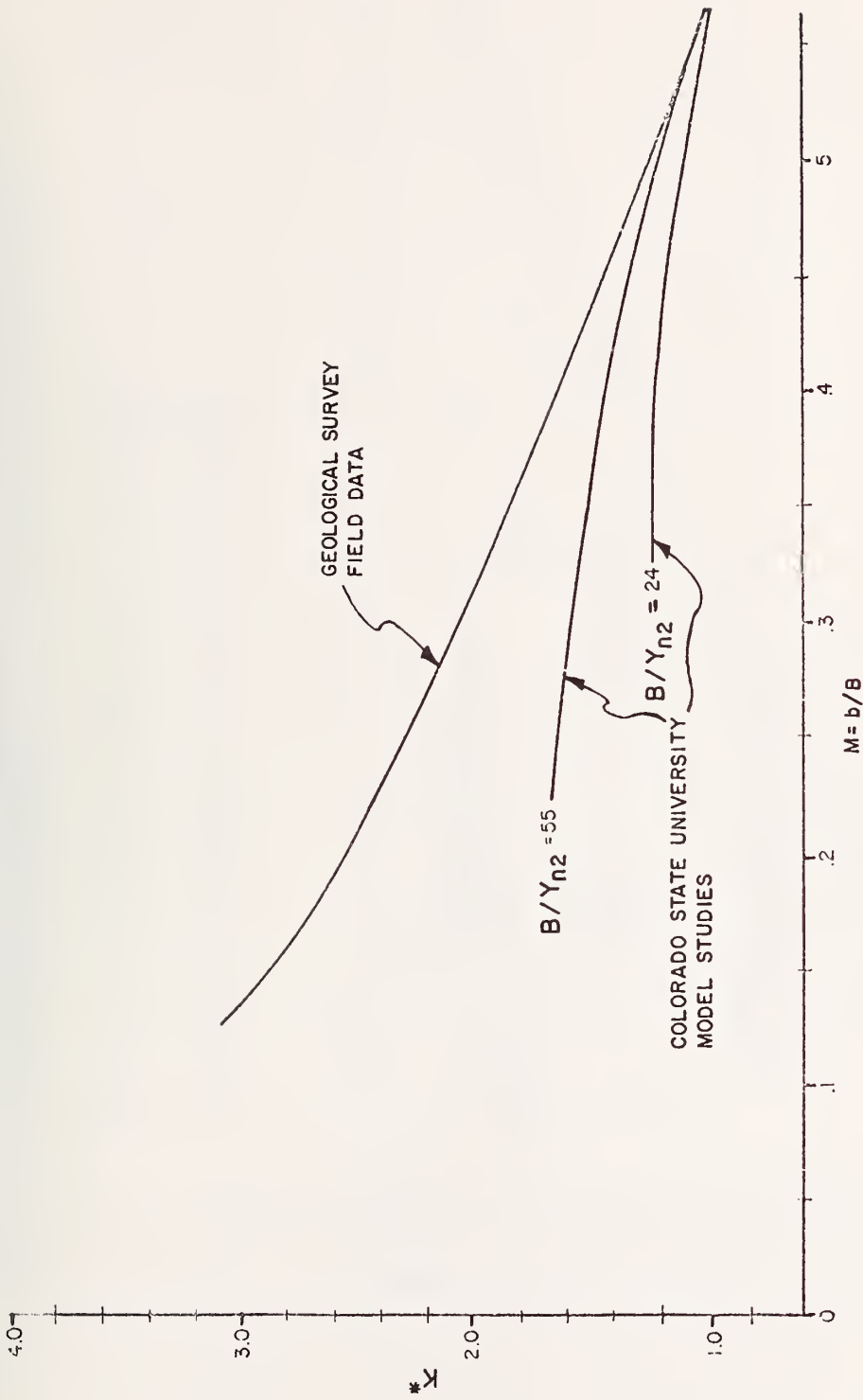
Graphical Analysis

A graphical analysis of all the backwater coefficient data divided by abutment shape, spur dike and roughness configuration is presented in Figures VI-3 to VI-16.

For comparative purposes, the plot of K^* vs M for Type I, subcritical flow, taken from Hydraulic Design Series Bulletin No. 1, is superimposed on the flume data. Also included are previous curves developed by Colorado State University flume studies. Plotting position M, which is the ratio of the length of the opening to the width flood plain, is the same for both sets of data. For convenience, the five patterns and their roughness densities are repeated below:

<u>Pattern</u>	<u>Density</u>	
	<u>Flood Plain</u>	<u>Main Channel</u>
P	100%	100%
A	100	50
B	75	75
C	75	25
D	50	50

Numbers shown beside points on Figures VI-4 to VI-16 are theoretical Froude numbers calculated in the opening at normal depth, taken from the Consolidated Data Tables under the heading "FROUDE." Note these are not the

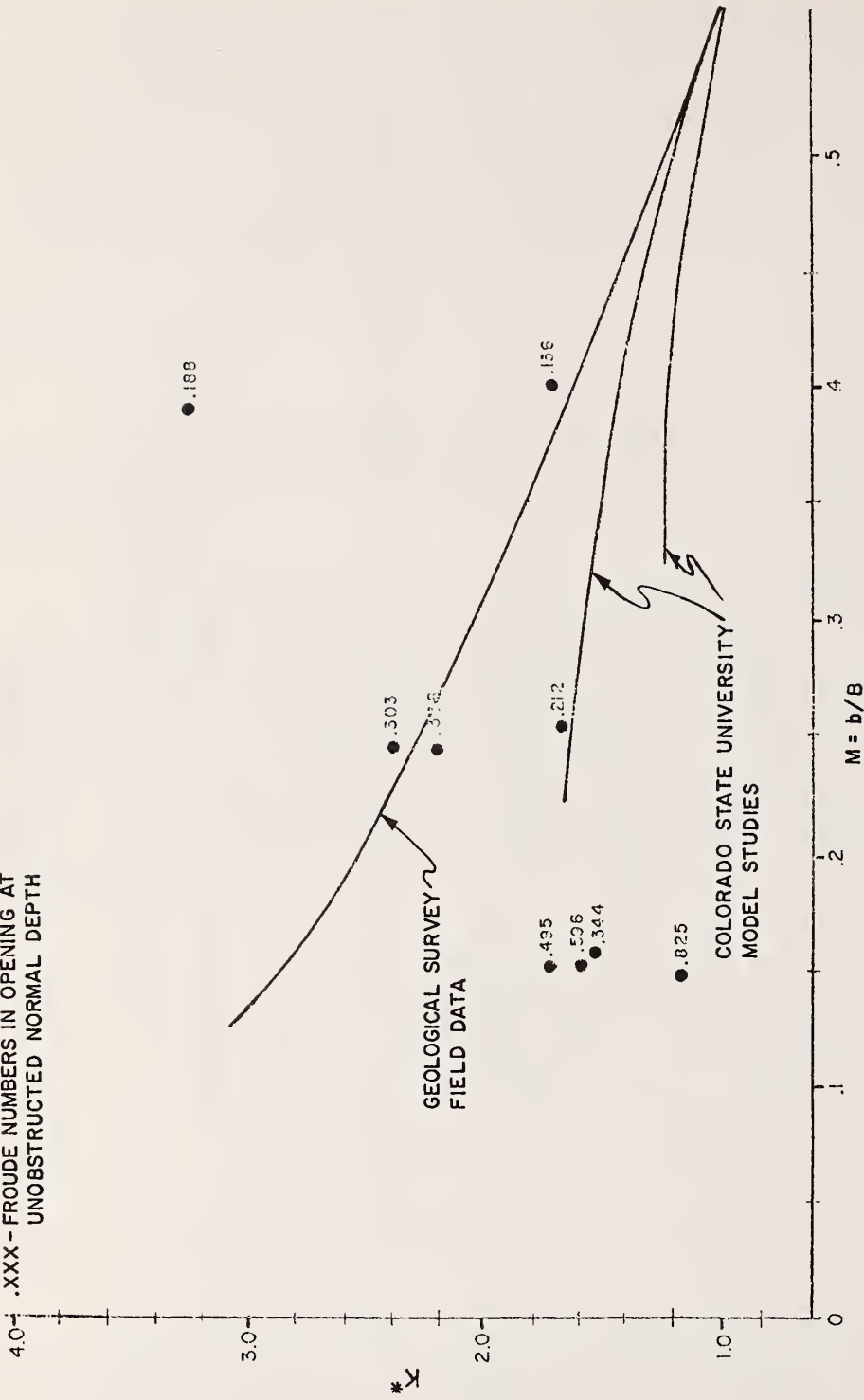


MAXIMUM BACKWATER COEFFICIENT (K^* vs M)

Ref: HYDRAULIC DESIGN SERIES BULLETIN no. 1

FIGURE VI-3

.XXX - FROUDE NUMBERS IN OPENING AT UNOBSTRUCTED NORMAL DEPTH

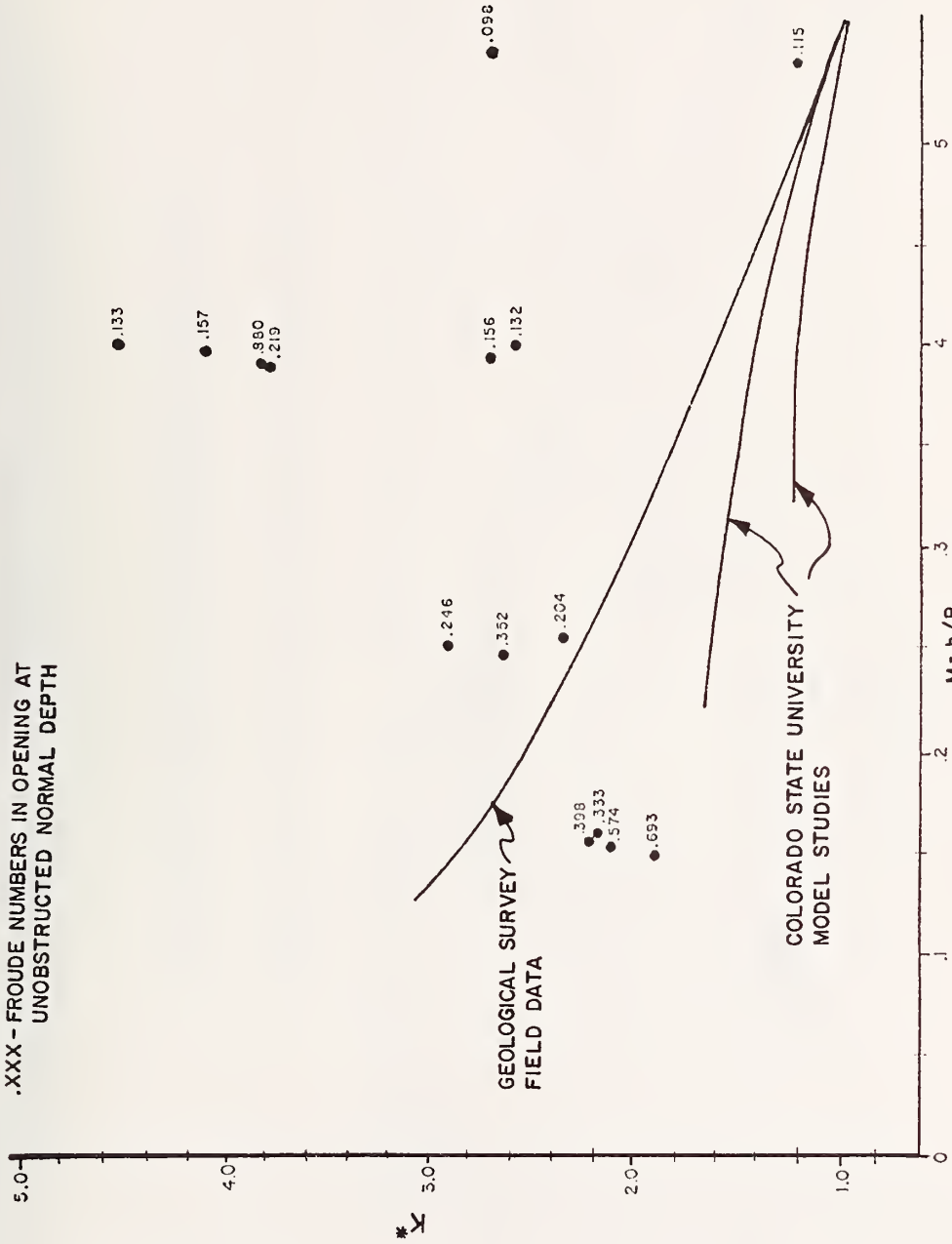


MAXIMUM BACKWATER COEFFICIENT (K^* vs M)

FOR SPILLTHROUGH ROUGHNESS PATTERN A

FIGURE VI-4

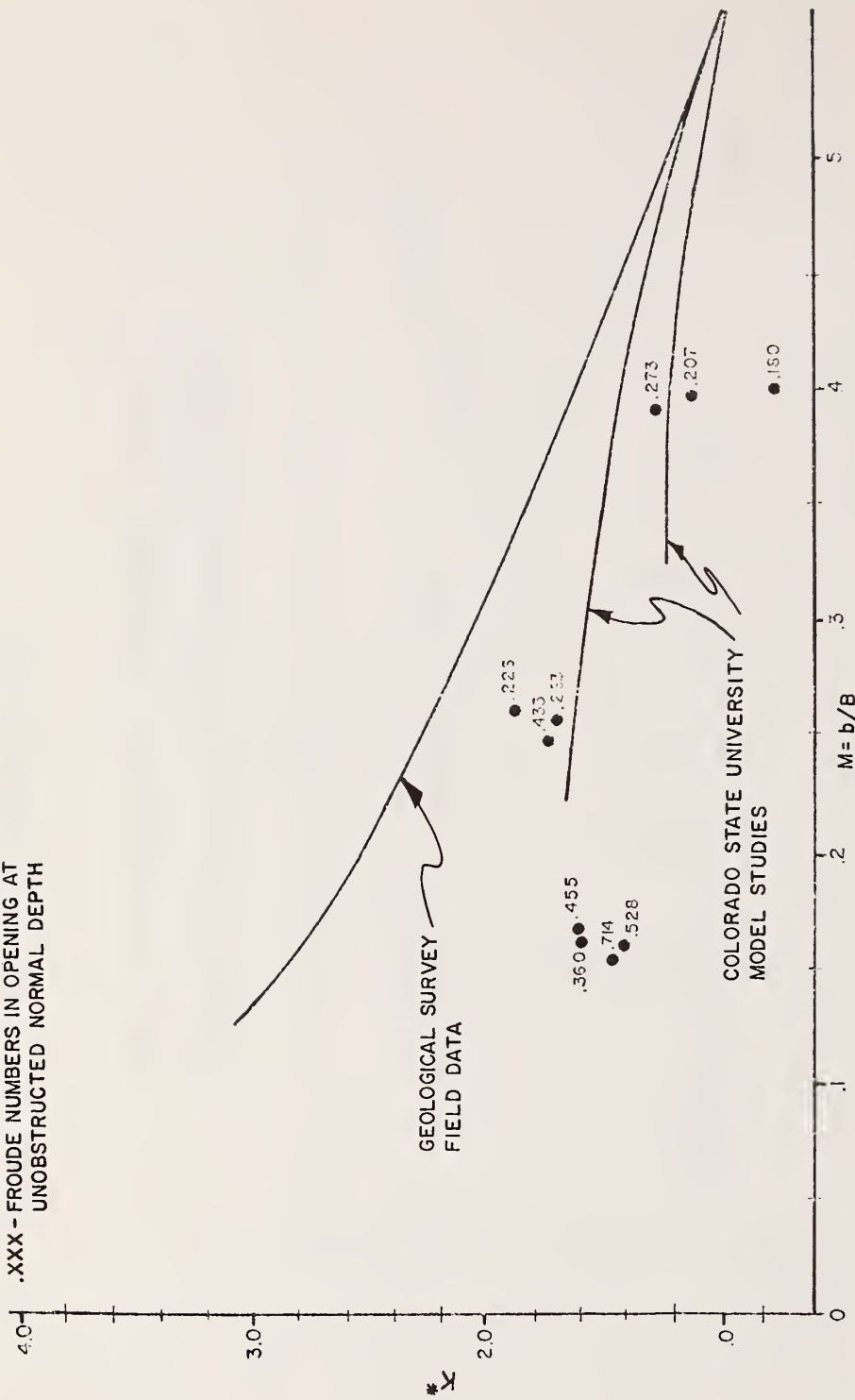
.XXX - FROUDE NUMBERS IN OPENING AT UNOBSTRUCTED NORMAL DEPTH



MAXIMUM BACKWATER COEFFICIENT (K^* vs M)
FOR SPILLTHROUGH ROUGHNESS PATTERN B

FIGURE VI-5

.XXX - FROUDE NUMBERS IN OPENING AT UNOBSTRUCTED NORMAL DEPTH

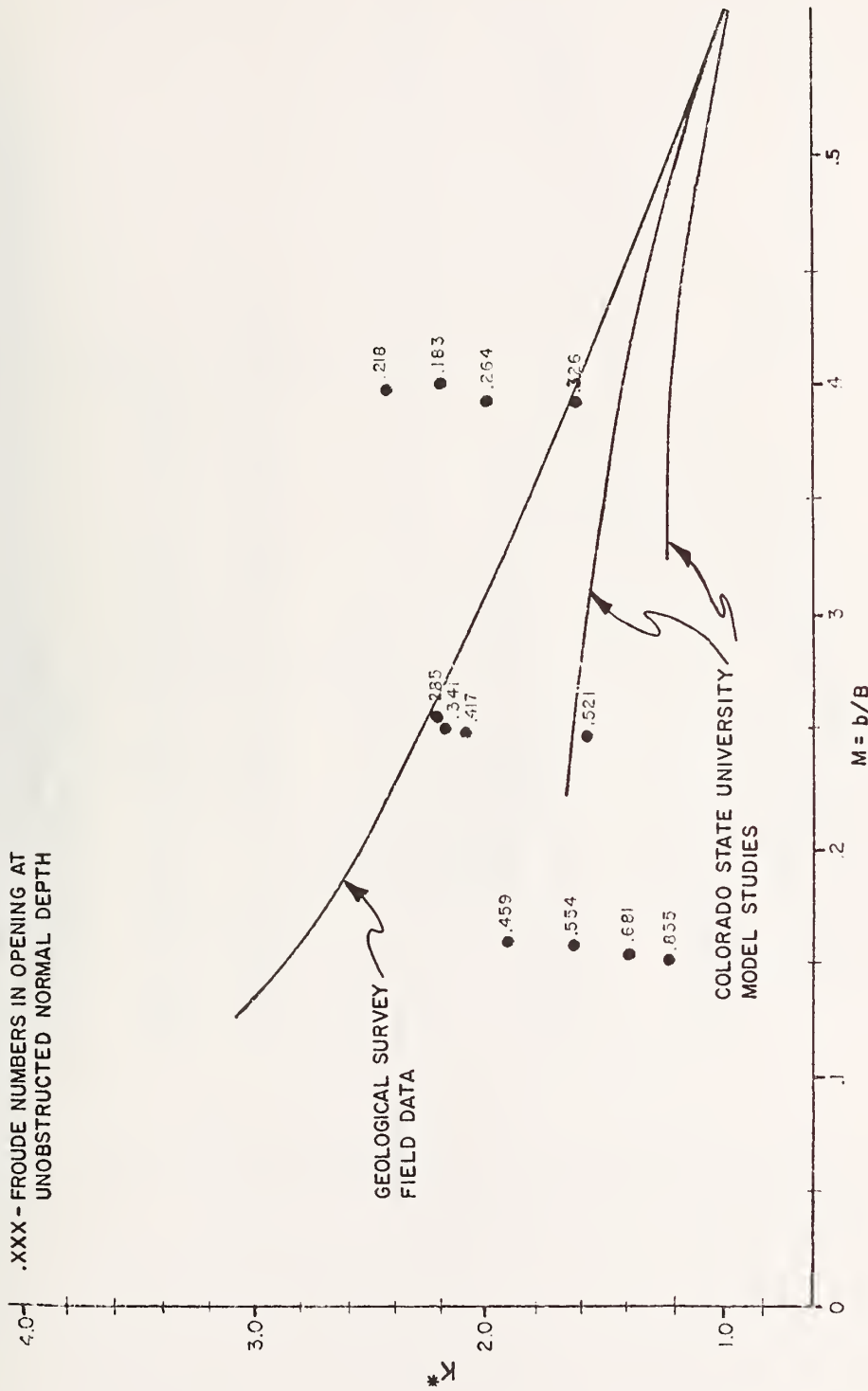


MAXIMUM BACKWATER COEFFICIENT (K* vs M)

FOR SPILLTHROUGH ROUGHNESS PATTERN C

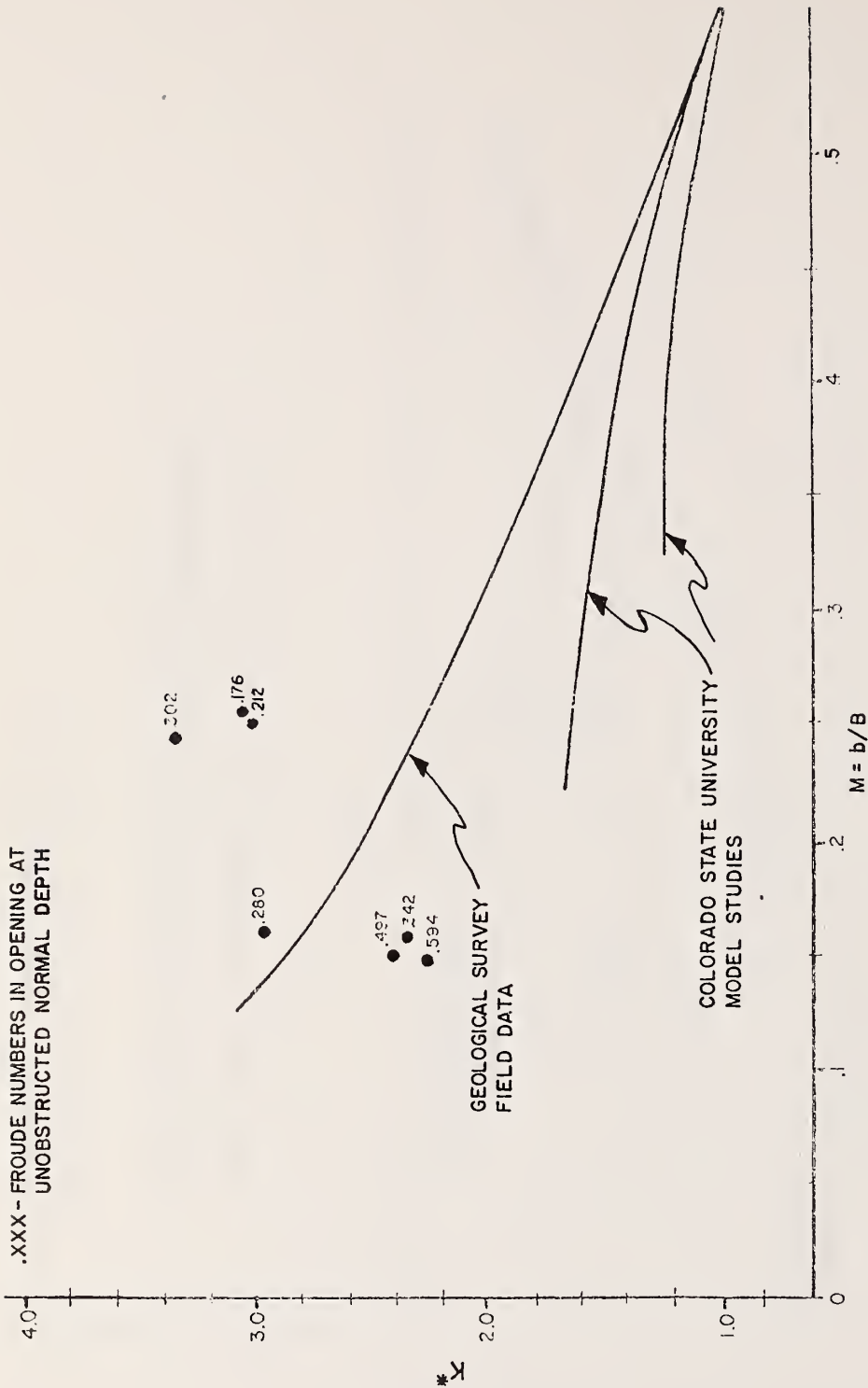
FIGURE VI-6

.XXX - FROUDE NUMBERS IN OPENING AT UNOBSTRUCTED NORMAL DEPTH



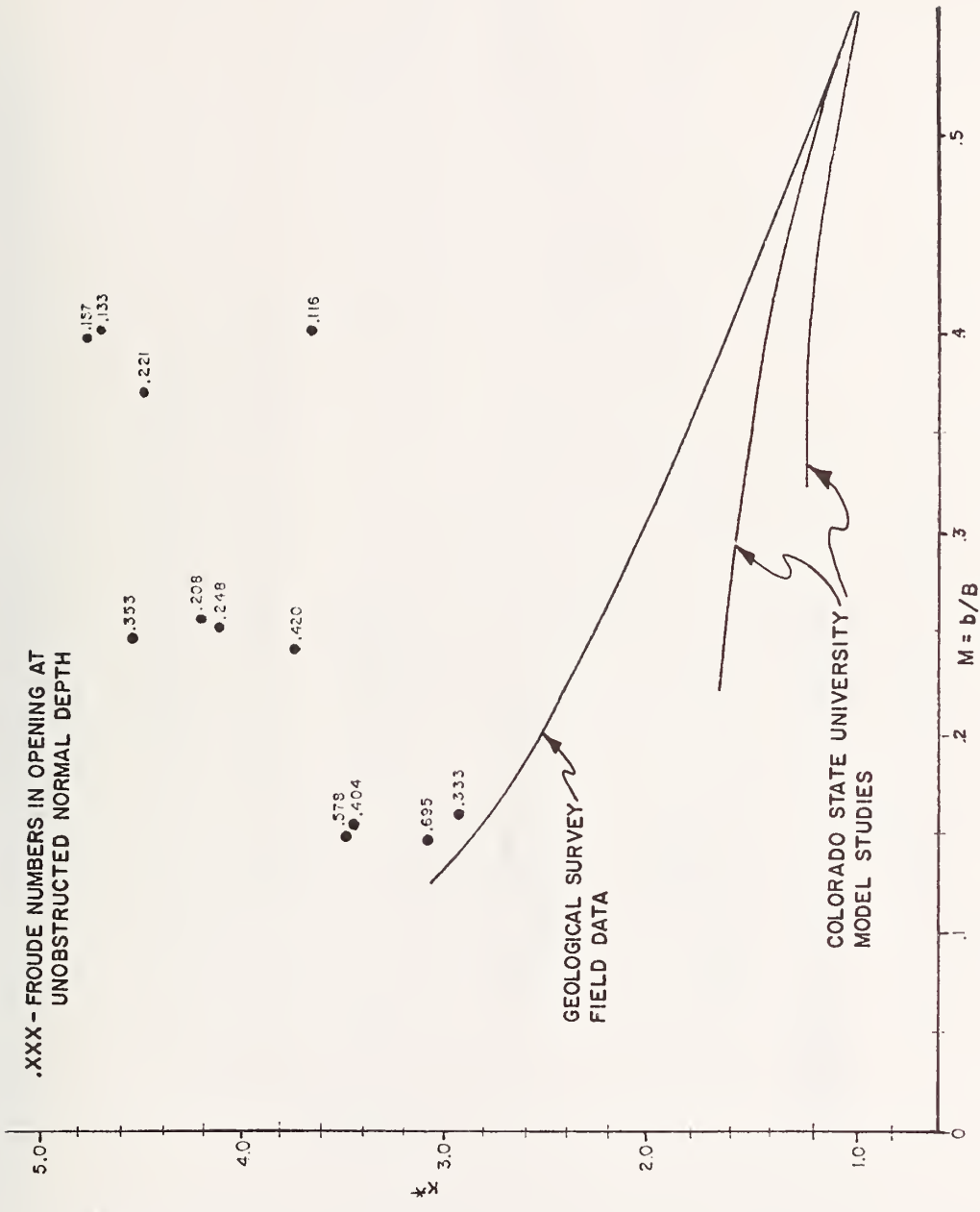
MAXIMUM BACKWATER COEFFICIENT (K^* vs M)
FOR SPILLTHROUGH ROUGHNESS PATTERN D

FIGURE VI-7



MAXIMUM BACKWATER COEFFICIENT (K^* vs M)
FOR SPUR DIKE ROUGHNESS PATTERN A

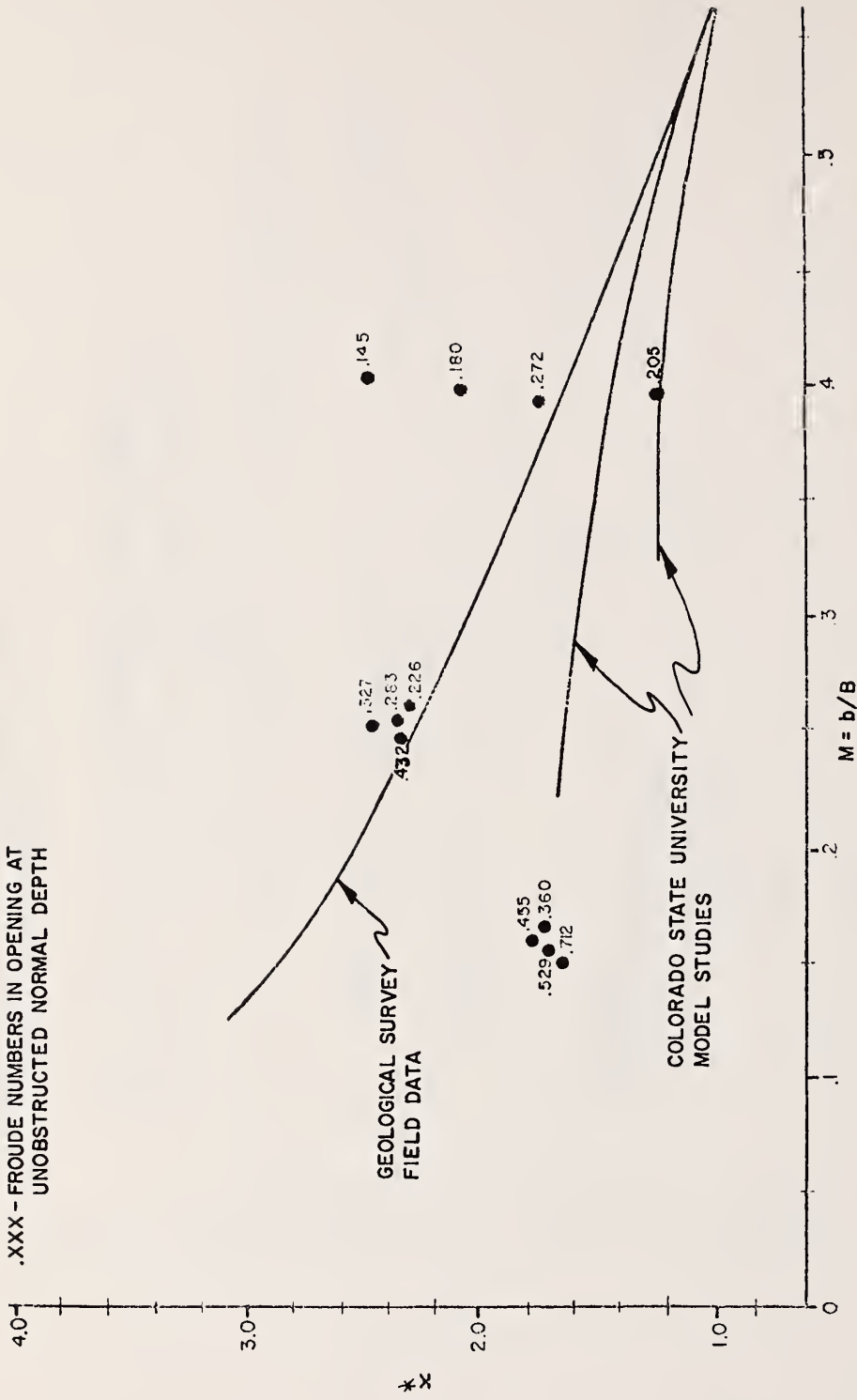
FIGURE VI-8



MAXIMUM BACKWATER COEFFICIENT (K^* vs M)
FOR SPUR DIKE ROUGHNESS PATTERN B

FIGURE VI-9

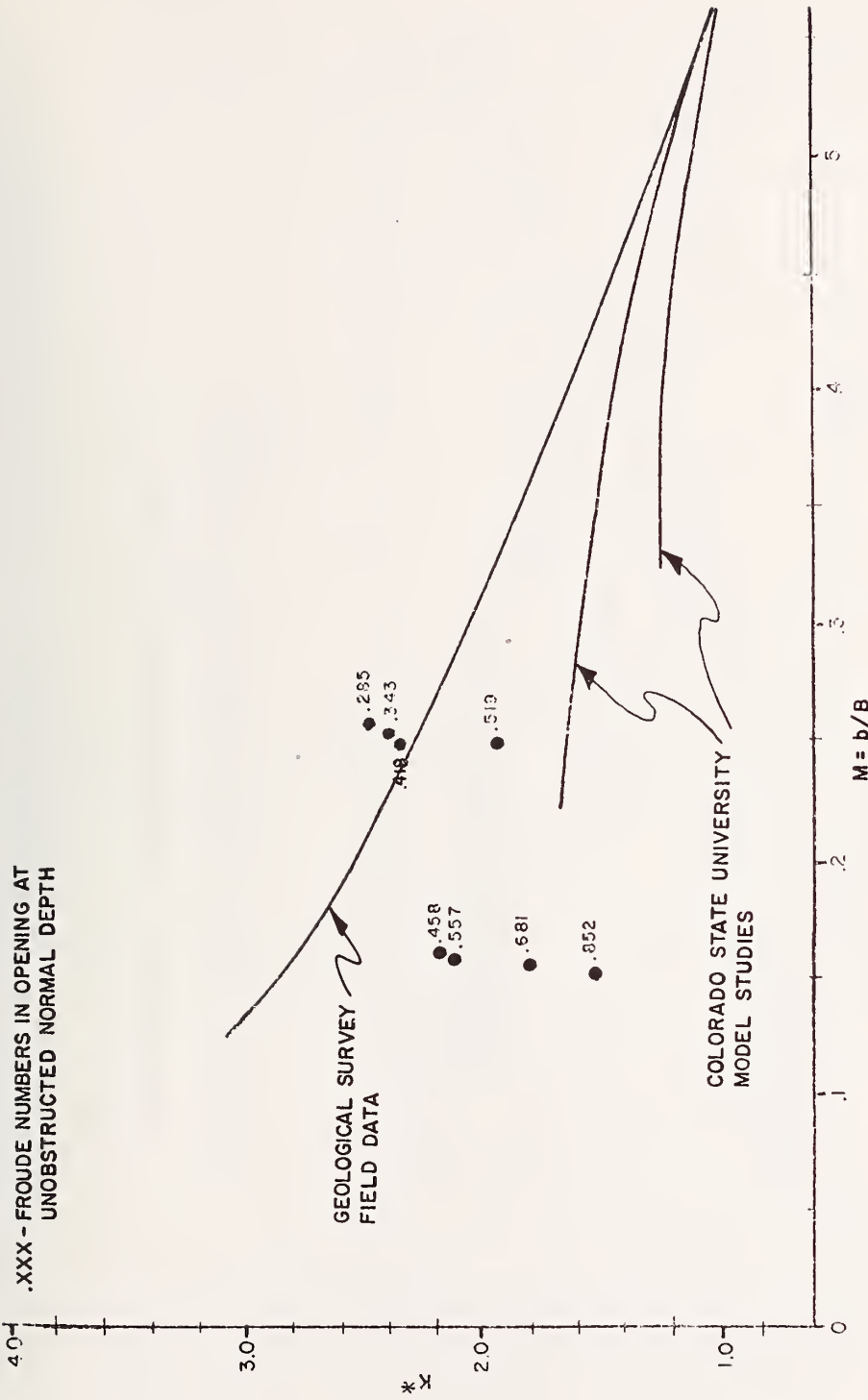
.XXX - FROUDE NUMBERS IN OPENING AT UNOBSTRUCTED NORMAL DEPTH



MAXIMUM BACKWATER COEFFICIENT (K vs M)
FOR SPUR DIKE ROUGHNESS PATTERN C

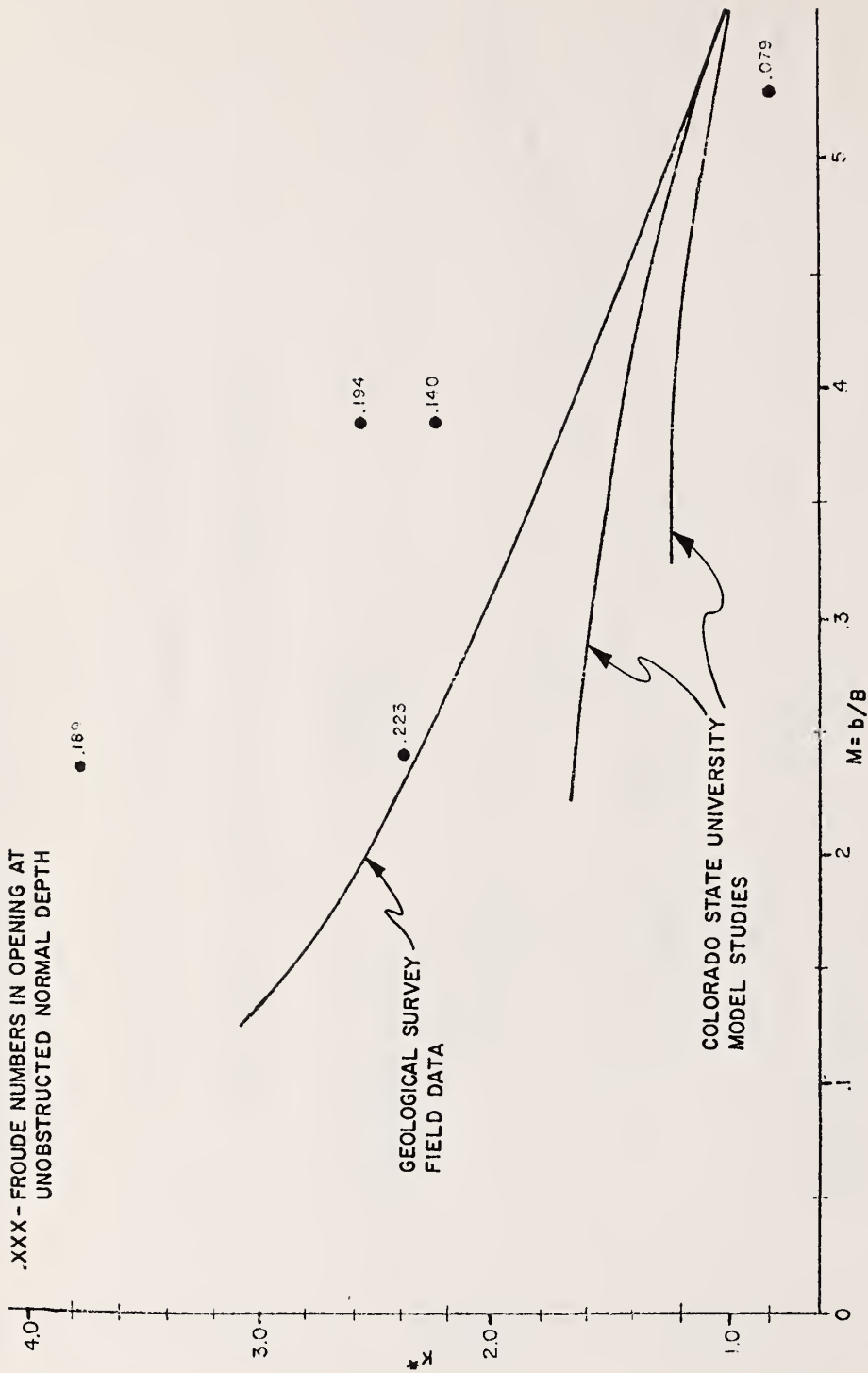
FIGURE VI-10

.XXX - FROUDE NUMBERS IN OPENING AT UNOBSTRUCTED NORMAL DEPTH



MAXIMUM BACKWATER COEFFICIENT (K^* vs M)
FOR SPUR DIKE ROUGHNESS PATTERN D

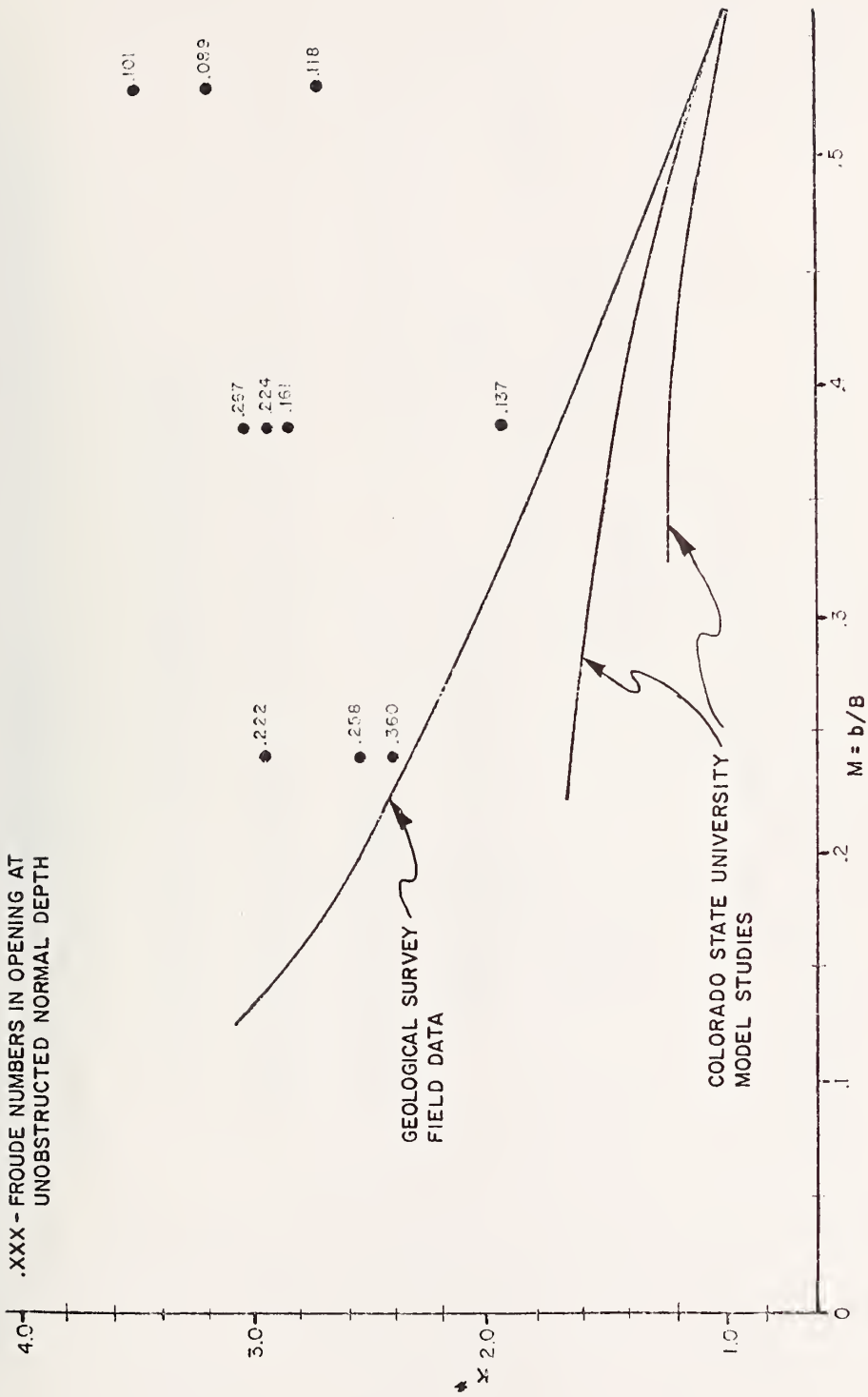
FIGURE VI-11



MAXIMUM BACKWATER COEFFICIENT (K^* vs M)
 FOR WINGWALL ROUGHNESS PATTERN A

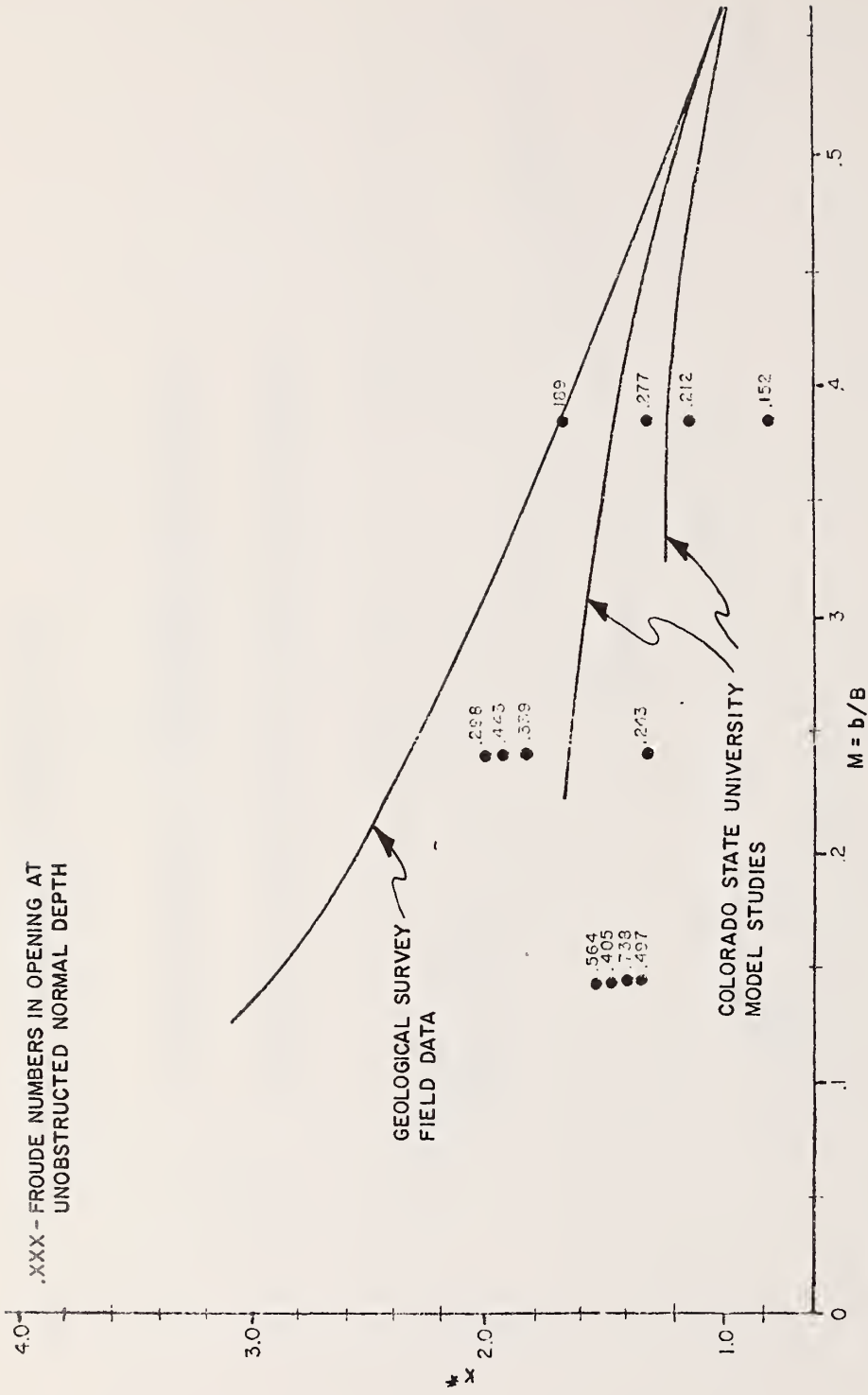
FIGURE VI-12

.XXX - FROUDE NUMBERS IN OPENING AT UNOBSTRUCTED NORMAL DEPTH



MAXIMUM BACKWATER COEFFICIENT (K^* vs M)
FOR WINGWALL ROUGHNESS PATTERN B

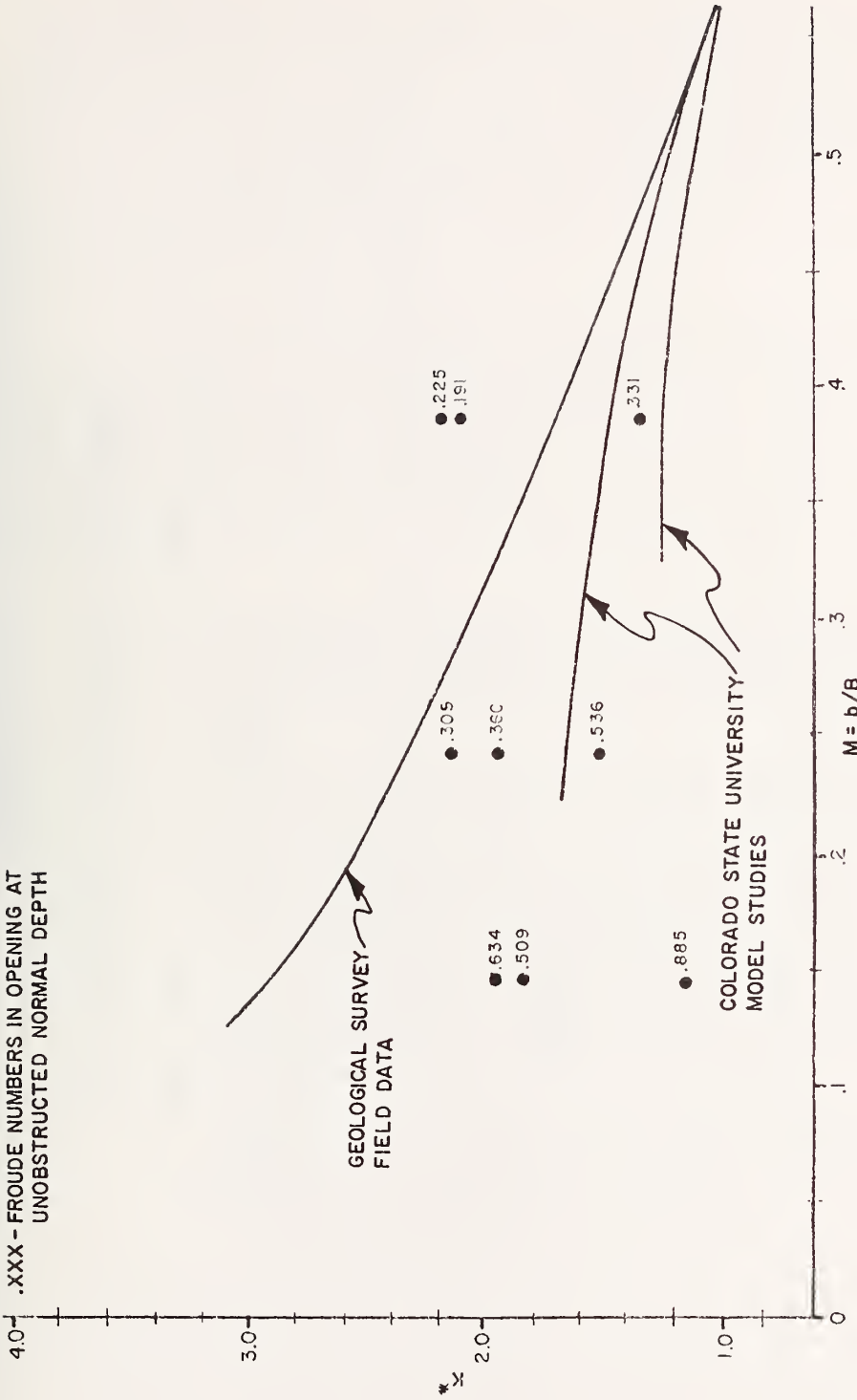
FIGURE VI-13



MAXIMUM BACKWATER COEFFICIENT (K^* vs M)
FOR WINGWALL ROUGHNESS PATTERN C

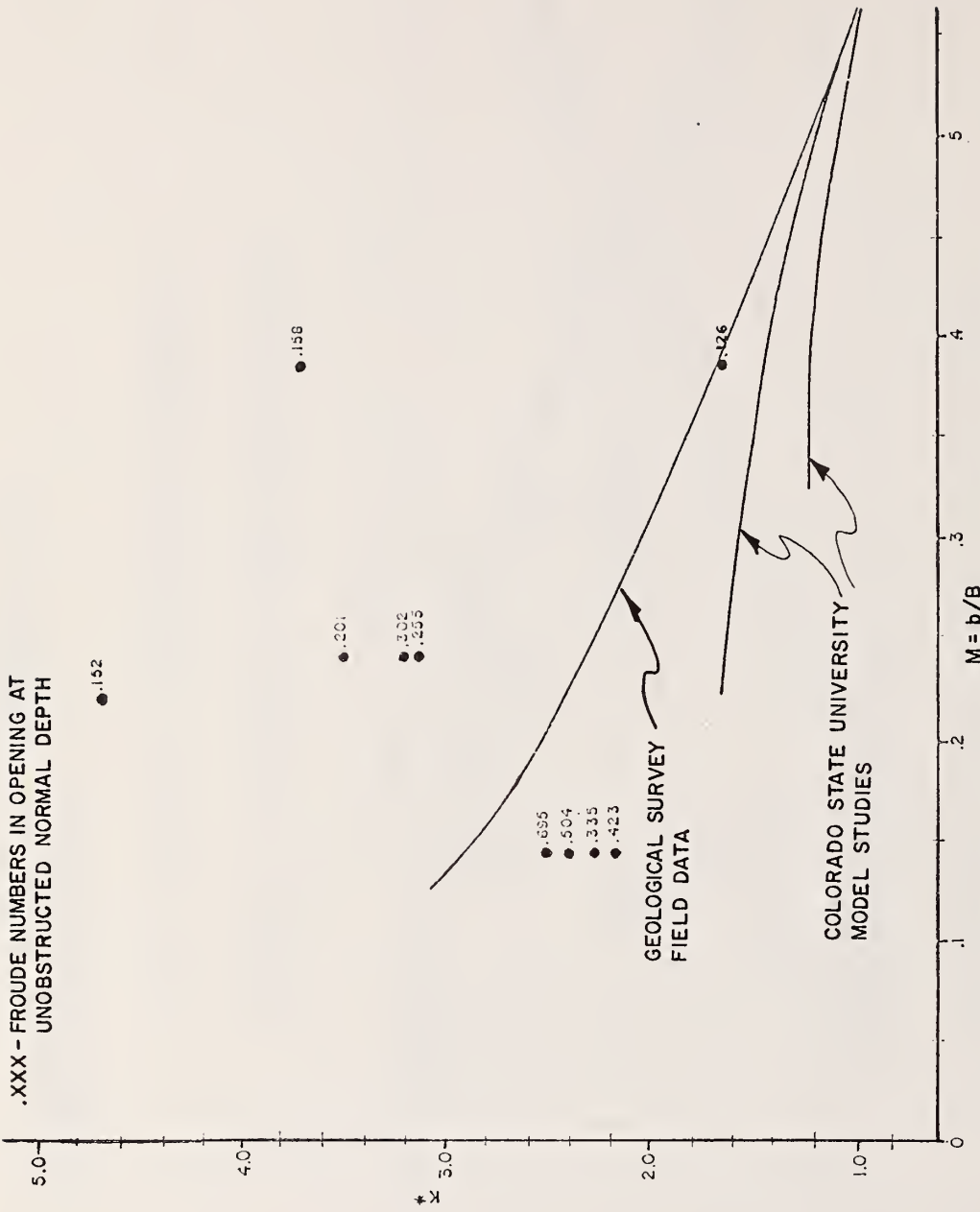
FIGURE VI-14

.XXX - FROUDE NUMBERS IN OPENING AT UNOBSTRUCTED NORMAL DEPTH



MAXIMUM BACKWATER COEFFICIENT (K^* vs M)
FOR WINGWALL ROUGHNESS PATTERN D

FIGURE VI-15



MAXIMUM BACKWATER COEFFICIENT (K^* vs M)
FOR WINGWALL ROUGHNESS PATTERN P

FIGURE VI-16

same experimental Froude numbers used in the ANOVA. The lines shown on each graph are from top to bottom: USGS field data, and two lines showing Colorado State University flume data. These are shown separately on Figure VI-3. Of the K^* values reported in the Appendix, only those less than 0.5 and greater than 5.0 are now shown. All runs which had a Froude number greater than 1.0 were also excluded.

The data do not show the consistency required for definitive conclusions and quantitative assessments of major variables. As indicated by the ANOVA the plotting parameter ($M=b/B$) as shown on the figures does not indicate a strong relationship, if any, to K^* for most of the figures. Nevertheless, certain qualitative assessments can be made:

1. The effect of varying roughness patterns is indeterminate in regard to the maximum backwater coefficient. This might be alleviated by a subjective sorting of the plotted data, not done here.
2. An inverse relationship between Froude number as calculated in the opening and K^* appears to exist for any opening ratio. Note here that due to the resistance of the roughness elements the higher Froude numbers correspond to lower flows. Effective Manning roughness in the flume increased with flow.
3. As expected, scatter tended to decrease with decreasing opening ratio. This was due to the small backwater produced by large openings and therefore the difficulty in accurately measuring this parameter.
4. Finally, as also indicated by the ANOVA, any future analysis of K^* could combine wingwall and spillthrough data into one set of data due to the similarity of results for each roughness pattern.

BACKWATER COEFFICIENT (K^*) FOR SKEWED CROSSING

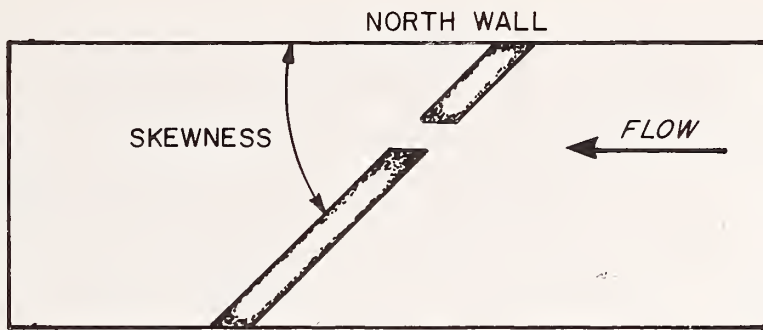
Analysis of Variance

All skewed crossing runs were made with roughness pattern D (flood plain 50 percent and main channel 50 percent), using 45° wingwall abutment faces. Categorization by Froude number was based on the Froude numbers calculated using the entire flume at the given flow and normal depth. Eccentric categories were divided into north, central or south, depending on the opening orientation to the north or south sides of the flums. The definition of eccentricity defined earlier in this report is not used here as it does not adequately assess the direction of eccentricity from the centerline. Eccentricity as used in this part of the analysis is defined in Figure VI-17. This definition is applied in order to take into account the expected differences in the maximum backwater height and location caused by energy losses due to eddies generated by the opening location. Calculations of eccentricity for each run are contained in the Appendix.

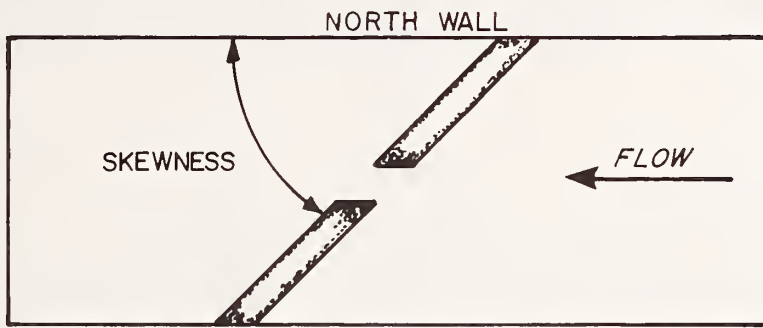
Opening ratios were categorized according to that portion of the opening perpendicular to the flow for both sizes of opening. Data were further divided into 15° and 45° levels. Levels for each variable are:

Variable	15°			45°		
Froude (F)	.077	.091	.129	.077	.091	.129
Eccentricity (E)	North	Central	South	North	Central	South
Opening Ratio (M)	2.89	7.73		2.12	5.66	

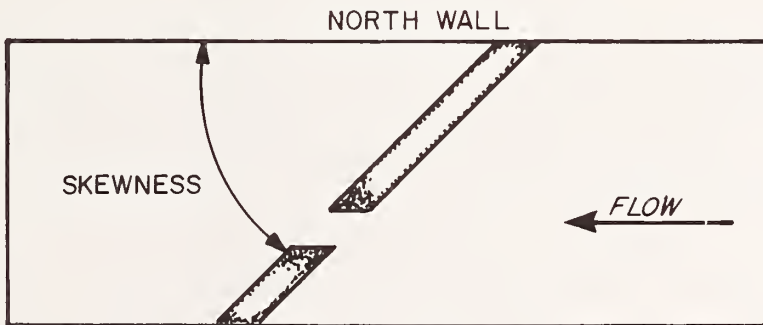
The angle of skewness was not analyzed because the opening ratio categories varied with the angle of skew. This made it impossible to statistically test for variances in K^* due to the angle of skew. An examination of Table VI-4 shows that 18 ($3 \times 3 \times 2$) estimates of K^* are needed for both the 15° and 45° skewed crossings



SOUTH WALL
a) NORTH ECCENTRICITY



SOUTH WALL
b) CENTRAL ECCENTRICITY



SOUTH WALL
c) SOUTH ECCENTRICITY

EXPERIMENTAL ECCENTRICITY DEFINITION
FIGURE VI-17

TABLE VI-4
ANOVA OF K* FOR 15° AND 45° SKEW CROSSINGS

15° SKEW CROSSINGS				45° SKEW CROSSINGS			
Levels of Variables				Levels of Variables			
	F	3		F	3		
	E	3		E	3		
	M	2		M	2		
	<u>Grand Mean</u>		1.68	<u>Grand Mean</u>		1.57	
Source of Variance	Sums of Squares	Degrees of Freedom	Mean Squares	Sums of Squares	Degrees of Freedom	Mean Squares	
Froude (F)	1.93	2	0.96	.93	2	0.46	
Excenctricity (E)	1.20	2	0.60	1.48	2	0.74	
F x E (FE)	.64	4	0.16	0.93	4	0.23	
Opening Ratio (M)	1.09	1	1.09	0.29	1	0.29	
F x M (FM)	.34	2	0.17	0.32	2	0.16	
E x M (EM)	1.59	2	0.79	5.88	2	2.94	
F x E x M (FEM)	1.71	4	0.42	0.43	4	0.10	
TOTAL	8.54	17	.	10.30	17		

Table VI-4 presents the sums of squares, degrees of freedom and mean square calculations for the skew runs. Table VI-5 presents the results of testing each factor at the 95 percent confidence level. No significance could be attributed to any of the main effects for either 15° or 45° skew runs. The one interactive effect of eccentricity and opening ratio for the 45° skew runs is considered an anomaly since neither of their main effects tested as significant. The conclusion drawn from the ANOVA is that the data show no statistically significant effect at the 95 percent confidence level which may be attributable to Froude number (as calculated in the entire flume), opening ratio, or eccentricity. Effects between 15° and 45° crossing configuration angles were not testable because of insufficient data.

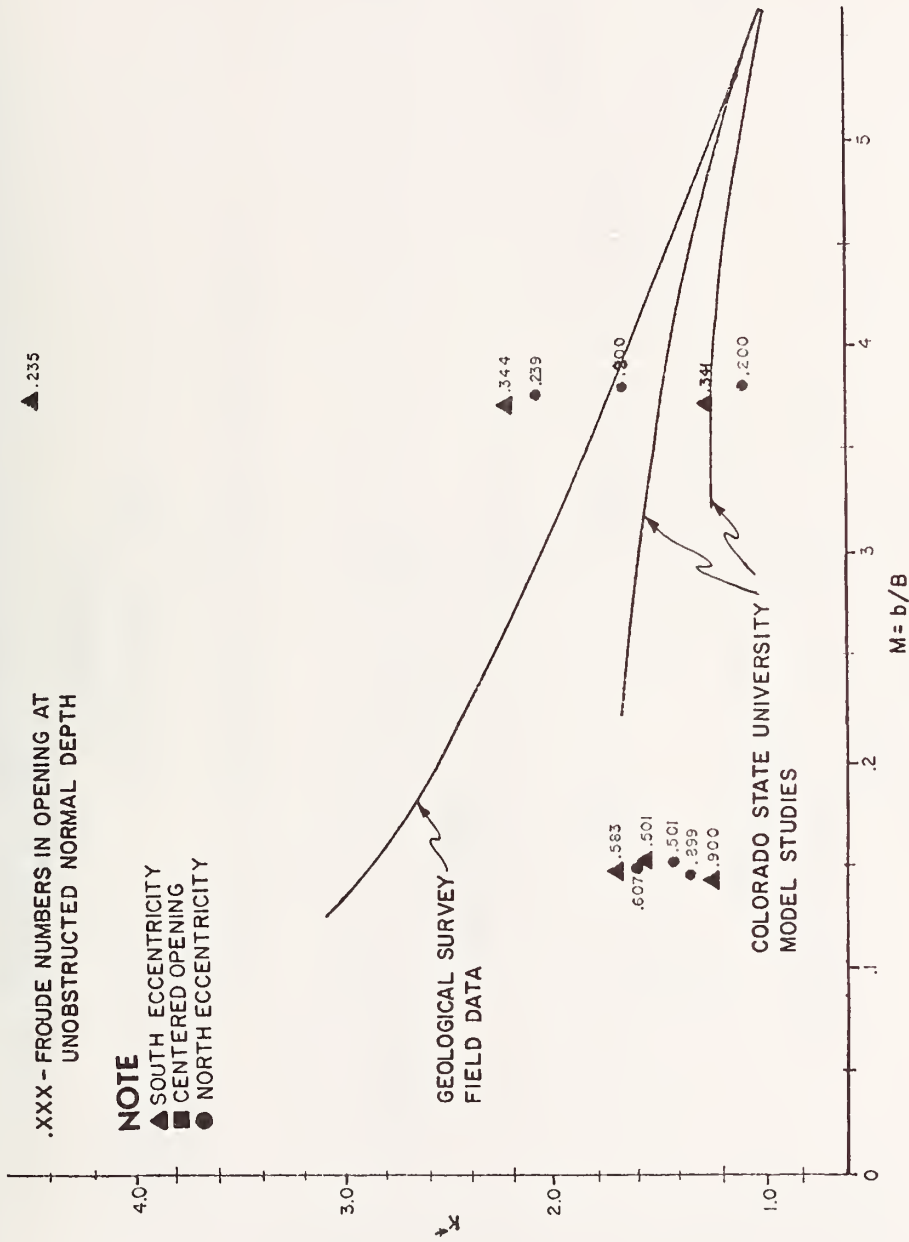
Graphical Analysis

Plots of K^* vs M are given in Figures VI-18 to VI-20. Numbers associated with each point refer to the theoretical Froude number calculated in the constriction at normal depth. Triangles refer to a south eccentricity and squares to a north eccentricity. All others were centered in the flume at the angle of skew shown.

Graphically, the same difficulties regarding measurement error are evidenced in the skew runs as were found in the centered crossings, perpendicular to flow. Measurement error decreases with increasing backwater as noted by the clustering of points at smaller M ratios. As indicated by the ANOVA, the effects of opening ratio cannot be graphically quantified at a reasonably significant level. The clustering of points shows that the Froude value calculated in the opening perpendicular to flow using the normal unobstructed depth has an inverse relationship to the backwater coefficients. However, this relationship has not been quantified by any further regression analysis.

TABLE VI-5
 TESTING OF K* FOR SKEW CROSSING
 AT 95 PERCENT CONFIDENCE LEVEL

<u>Source of Variance</u>	<u>Test</u>	<u>Req. for Signif.</u>	<u>F Statistic</u>		<u>Significant</u>	
			<u>15°</u>	<u>45°</u>	<u>15°</u>	<u>45°</u>
Froude (F)	MS_F/MS_{FEM}	6.94	2.26	4.24	No	No
Eccentricity (E)	MS_E/MS_{FE}	6.94	3.72	3.18	No	No
FxE	MS_{FE}/MS_{FEM}	6.39	0.38	2.13	No	No
Opening Ratio (M)	MS_M/MS_{FM}	18.5	6.30	1.83	No	No
FxM	MS_{FM}/MS_{FEM}	6.94	0.40	1.48	No	No
ExM	MS_{EM}/MS_{FEM}	6.94	1.86	26.7	No	Yes
FxExM	No Test	--	--	--	--	--



MAXIMUM BACKWATER COEFFICIENT (K vs M)

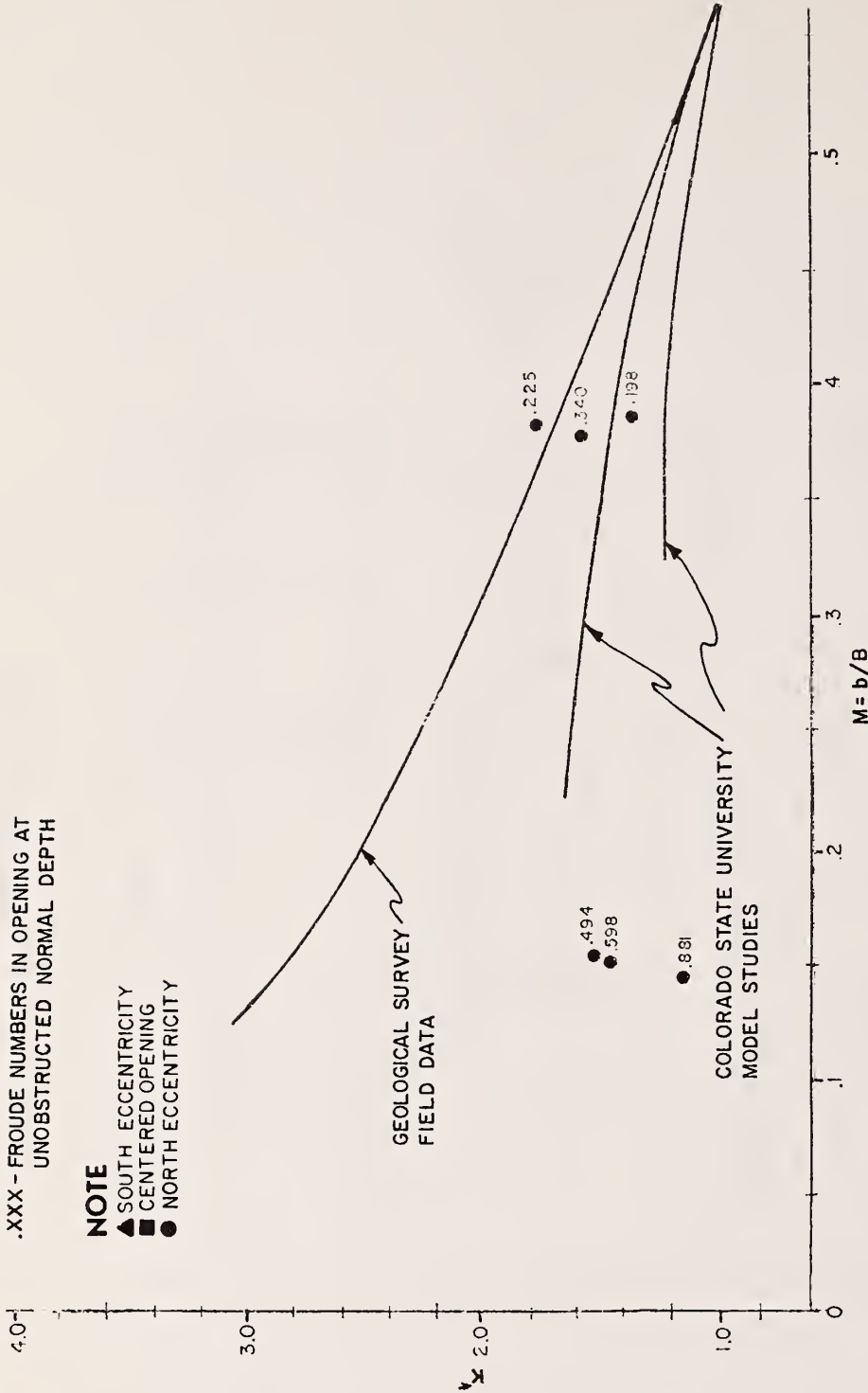
FOR SKEW $\gamma = 15^\circ$

FIGURE VI-18

.XXX - FROUDE NUMBERS IN OPENING AT UNOBSTRUCTED NORMAL DEPTH

NOTE

- ▲ SOUTH ECCENTRICITY
- CENTERED OPENING
- NORTH ECCENTRICITY

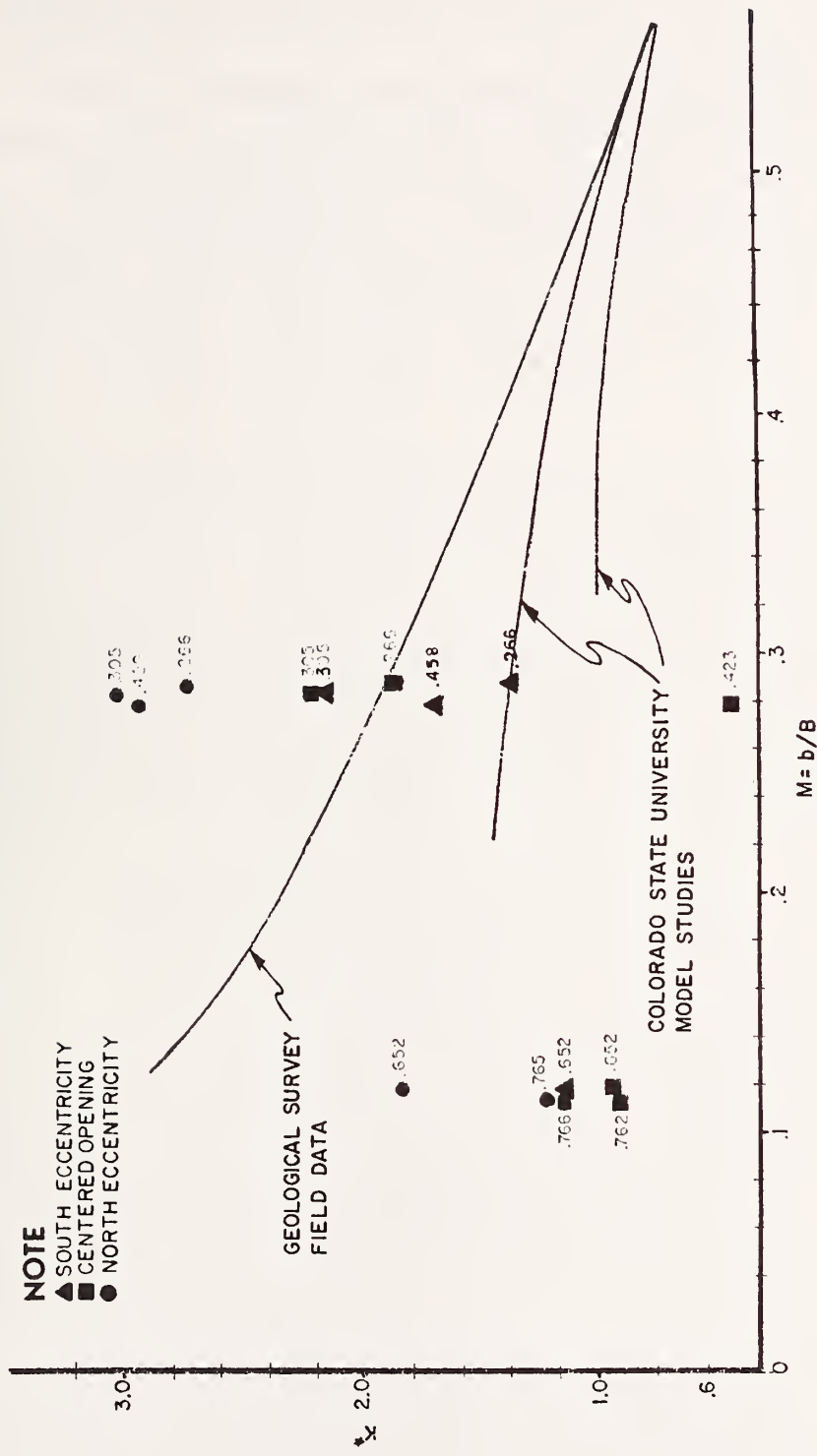


MAXIMUM BACKWATER COEFFICIENT (K^* vs M)

FOR SKEW $\gamma = 15^\circ$
(centered)

FIGURE VI-19

.XXX - FROUDE NUMBERS IN OPENING AT UNOBSTRUCTED NORMAL DEPTH



MAXIMUM BACKWATER COEFFICIENT (K^* vs M)

FOR SKEW $\gamma = 45^\circ$

FIGURE VI-20

The parameter h^* used in the calculation of K^* represents the height above normal water surface elevation at the location of the maximum backwater. This involves three sources of error: estimating the location for measurement, the water surface elevation and the height of the normal water surface elevation. In collecting and analyzing the data, emphasis has been placed on finding the maximum backwater position and estimating the most accurate normal water surface elevation possible. These errors have been minimized to the extent possible. The remaining error is considered attributable to the small calculated values of h^* due to the combination of flows and opening ratios.

ANALYSIS OF MAXIMUM BACKWATER LOCATION (ℓ^*/b)

The location of the maximum backwater, ℓ^* , was defined as the distance from the upstream crossing embankment to the location of the maximum water surface elevation above normal surface elevation. The location of this point was found experimentally using the apparatus and methodology described in Chapter IV.

ANALYSIS OF VARIANCE (ℓ^/b)*

As has been done previously, an analysis of variance was performed on the 36 runs comprising roughness pattern C, 75 percent flood plain and 25 percent main channel. The purpose of this test was again to provide some statistical screening of the data in order to establish a level of significance for the important variables. The dependent variable tested was ℓ^*/b . An ANOVA was performed with and without the spur dike data. The variables tested were Froude number as calculated in the flood plain (F), opening ratio (M), and abutment shape (A) (Figure V-3). The levels of each variable are given below:

Froude Number (F)	.059	.072	.083	.134
Opening Ratio (M)	.145	.242	.387	
Abutment Shape (A)	wingwall	spillthrough		spur dike

Output of the ANOVA and significance testing of the major variables and interactions is given in Tables VI-6 and VI-7. Note the estimate of the residual mean square, σ , is the interaction mean square, FA. This was done in order to give a slight conservative bias over the three-way interaction mean square, FMA. No differences in significance results from the choice of either as an estimate of σ .

Results of significance testing demonstrate that all three major variables affect the dependent parameter, ℓ^*/b . The effect noted for the variable abutment shape appears attributable to spur dike alone. Conversely, no differing effect

TABLE VI-6
ANOVA OF ϵ^*/b WITH AND WITHOUT SPUR DIKES

WITH SPUR DIKES				WITHOUT SPUR DIKES		
Levels of Factors				Levels of Factors		
	F	4		F	4	
	M	3		M	3	
	A	3		A	2	
	Grand Mean		1.31	Grand Mean		1.17
Source of Variance	Sums of Squares	Degrees of Freedom	Mean Squares	Sums of Squares	Degrees of Freedom	Mean Squares
Froude (F)	1.64	3	0.54	1.44	3	0.48
Opening Ratio (M)	9.56	2	4.78	4.94	2	2.47
F x M	0.43	6	0.07	0.43	6	0.07
Abutment (A)	1.40	2	0.70	0.01	1	0.01
F x A	0.20	6	0.03	0.12	3	0.04
M x A	1.05	4	0.26	0.27	2	0.13
F x M x A	0.12	12	0.01	0.05	6	0.01
TOTAL	14.43	35		7.29	23	

TABLE VI-7
 TESTING OF ℓ^*/b WITH AND WITHOUT SPUR DIKES
 AT 95 PERCENT CONFIDENCE LEVEL

Source of Variance	Test	With Spur Dikes		Without Spur Dikes	
		F Statistic	Req. for Signif.	F Statistic	Req. for Signif.
Froude (F)	MS_F/MS_{FA}	4.76	16.1	Yes	Yes
Opening Ratio (M)	MS_M/MS_{FM}	5.14	66.4	Yes	Yes
Abutment (A)	MS_A/MS_{FA}	5.14	20.6	Yes	No
FxM	MS_{FM}/MS_{FA}	4.28	2.09	No	No
FxA	No Test	--	--	--	--
MxA	MS_{MA}/MS_{FMA}	3.06	26.5	Yes	Yes
FxMxA	MS_{FMA}/MS_{FA}	4.00	0.294	No	No

on λ^*/b at the 95 percent confidence level is noted for wingwall and spillthrough alone. The interactive effect of opening ratio and the variable abutment shape may be due to their interactive effect on turbulence.

GRAPHICAL ANALYSIS (λ^/b)*

Figures VI-21 to VI-27 present plots of all the λ^*/b data generated by the experiment. Plotting numbers are flood plain Froude numbers. The graphs give further evidence to that indicated by ANOVA for roughness element patterns C. Opening ratio and Froude number do appear functionally related to λ^*/b and the addition of spur dikes to the embankment faces does affect the magnitude of the λ^*/b parameter. These facts appear to be significant for all the data taken, though except for roughness pattern C they have not been proven statistically significant. Again any future analysis of λ^*/b could combine wingwall and spillthrough data with only a slight increase in data scatter.

Due to the few points taken for any set of combinations and the difficulty in pooling the data onto one or two graphs, a regression analysis is presented below using the same data shown in the figures. This difficulty arises because of the impossibility of keeping Froude numbers in the experimental setup constant between roughness patterns and the incomplete testing due to time exigencies.

REGRESSION ANALYSIS (λ^/b)*

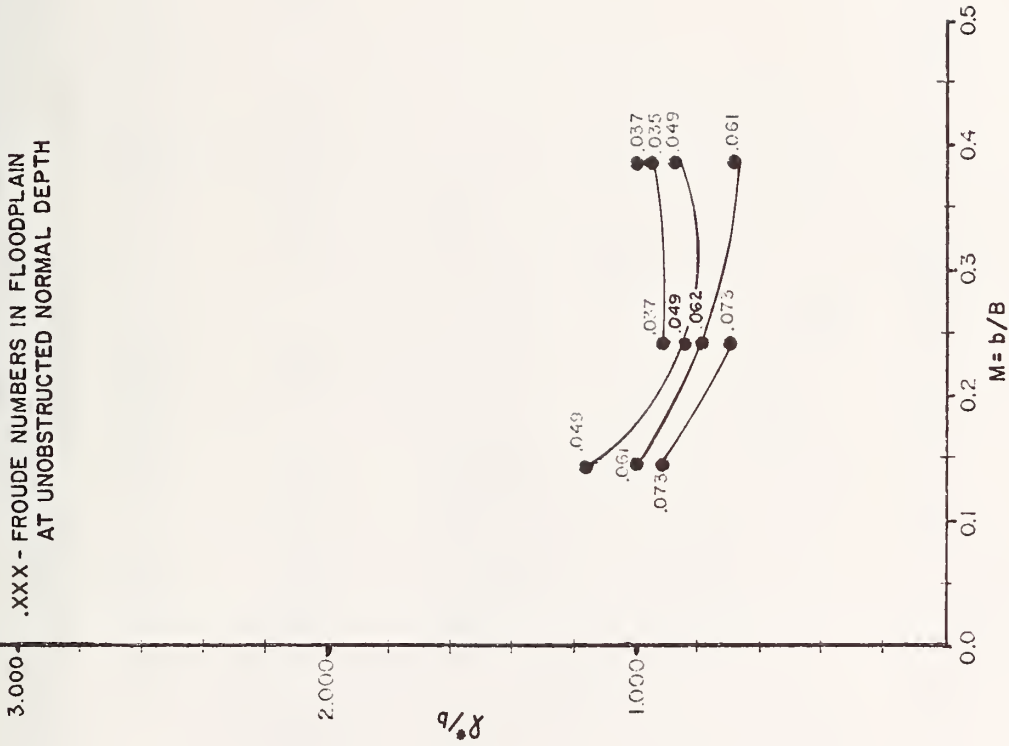
The notation describing the regression, taken from the dimensional analysis, is given below:

$$\lambda^*/b = f(M, A, F, C_f) \quad (54)$$

where

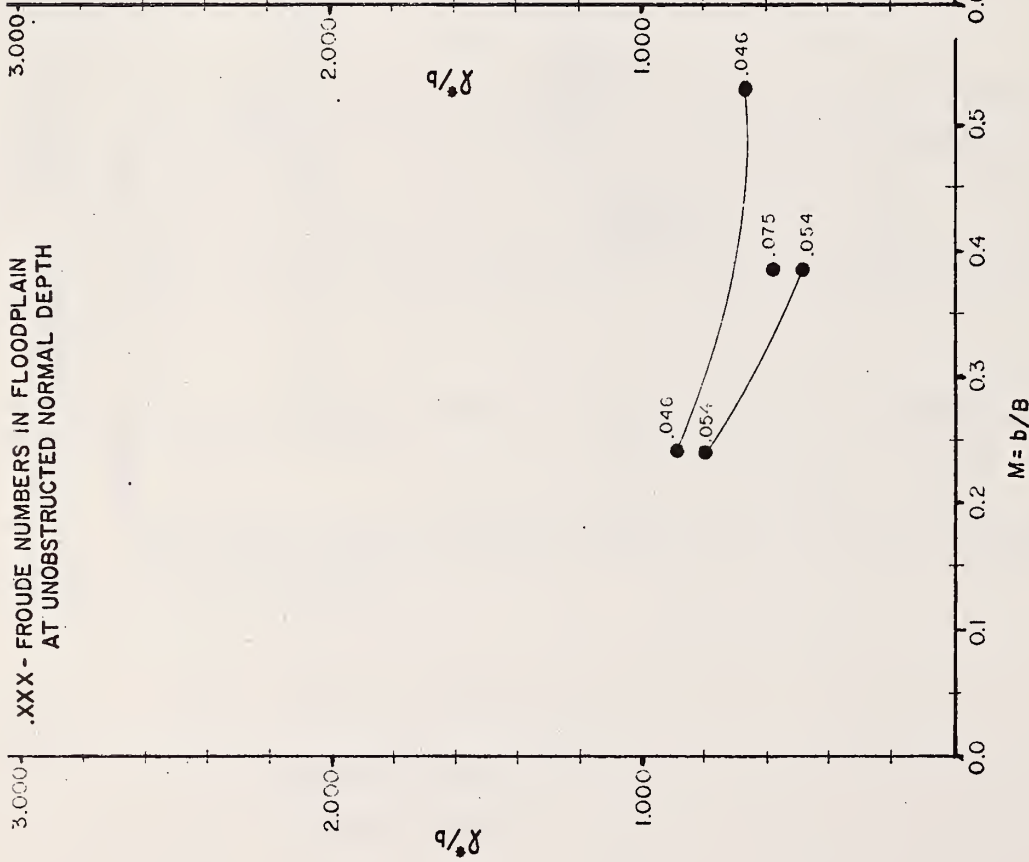
M = Opening ratio, b/B

A = Abutment shape

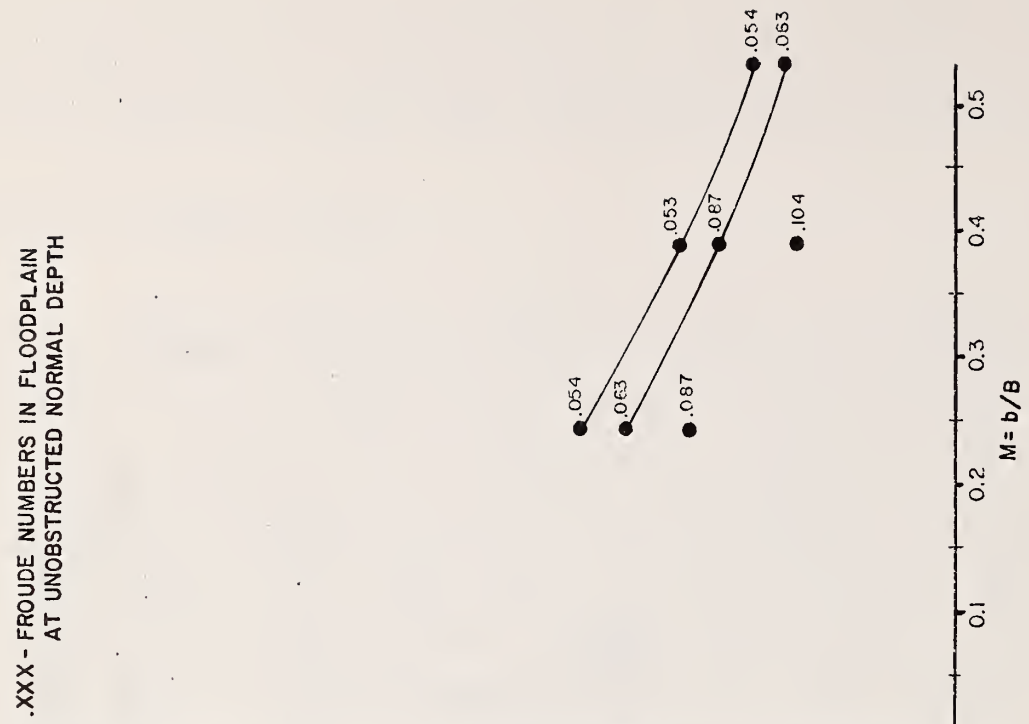


MAXIMUM BACKWATER LOCATION (X^*/b vs M)
FOR WINGWALL ROUGHNESS PATTERN P
FIGURE VI-21

.XXX - FROUDE NUMBERS IN FLOODPLAIN
AT UNOBSTRUCTED NORMAL DEPTH



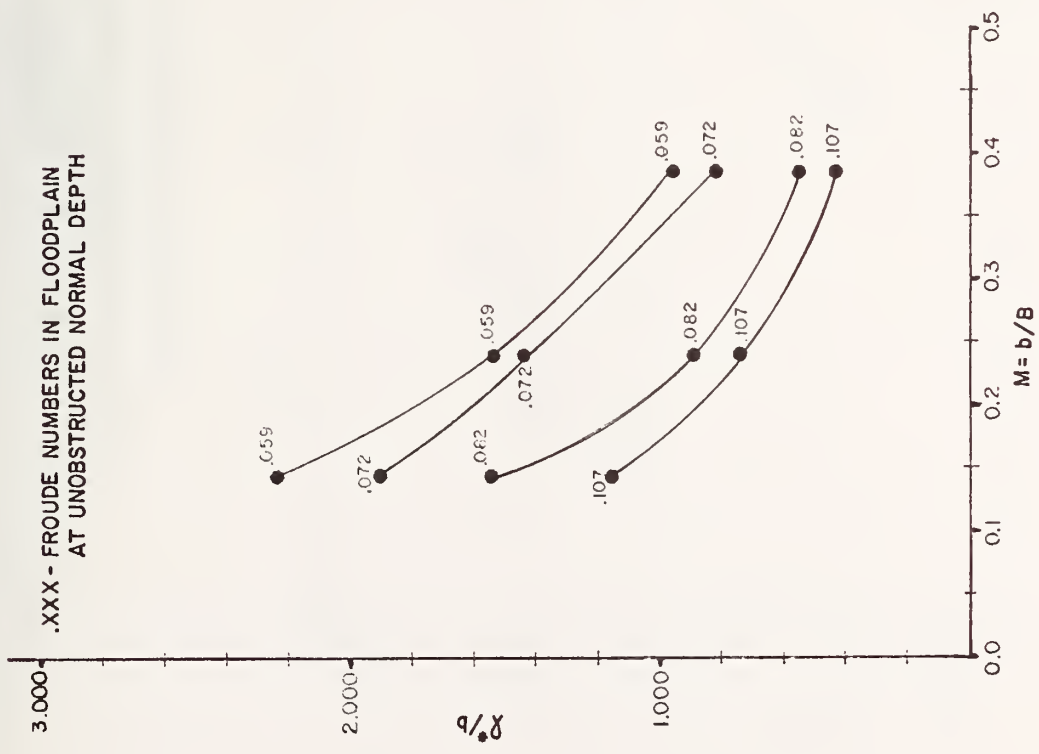
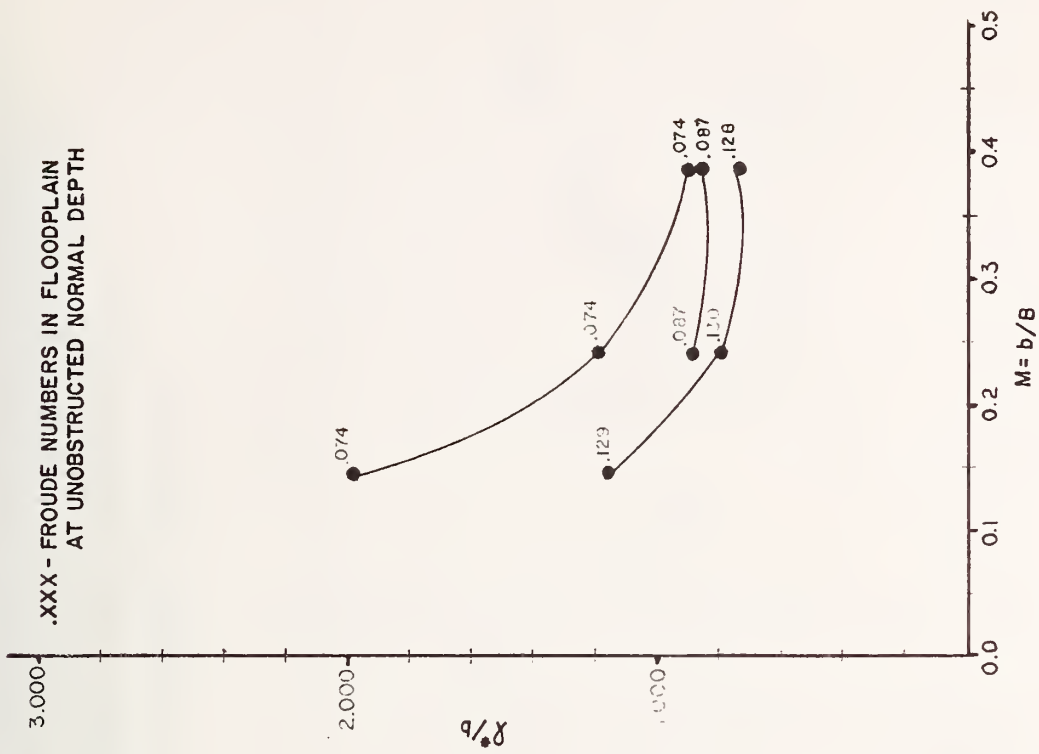
.XXX - FROUDE NUMBERS IN FLOODPLAIN
AT UNOBSTRUCTED NORMAL DEPTH



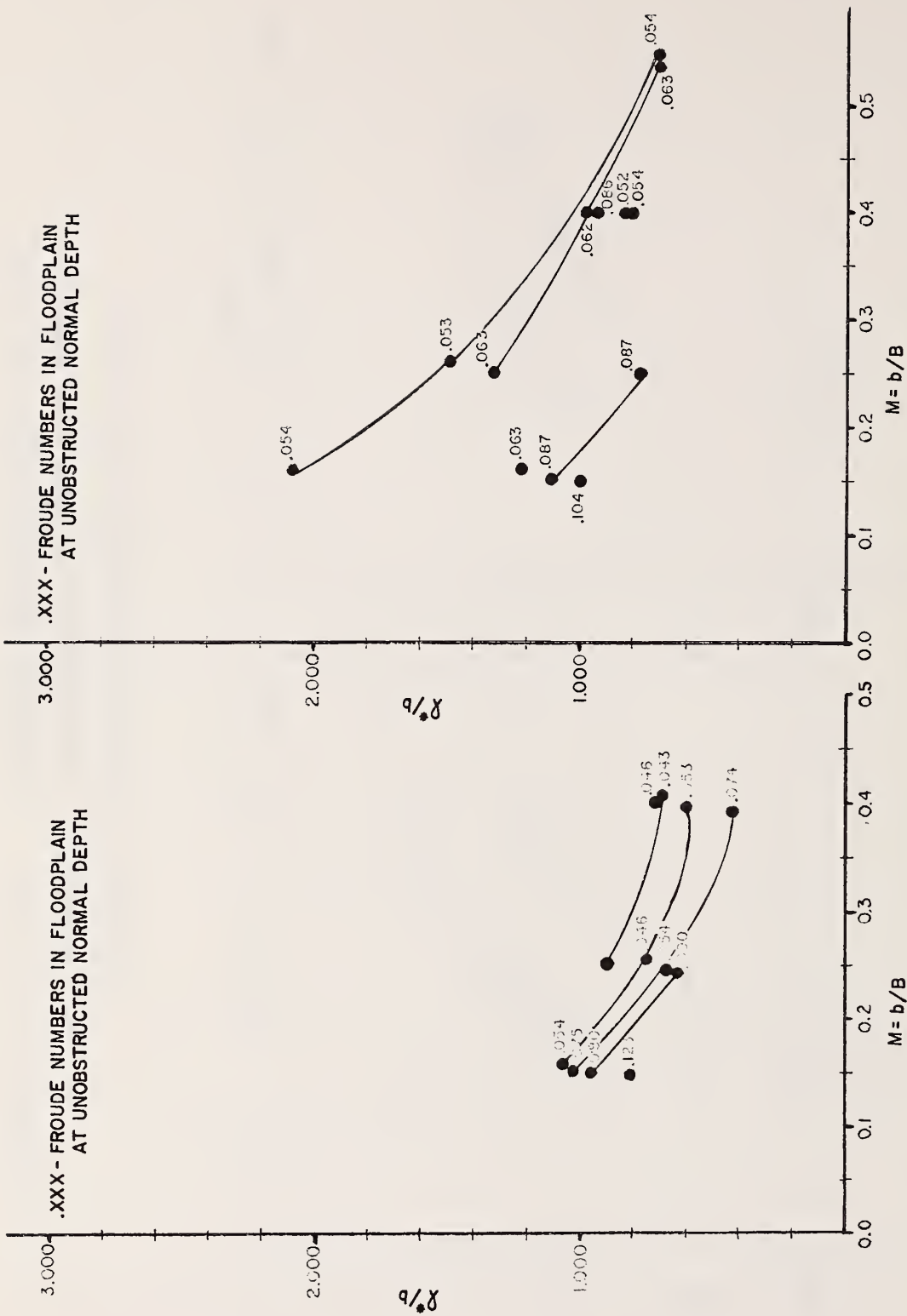
MAXIMUM BACKWATER LOCATION (X^*/b vs M)

FOR WINGWALL ROUGHNESS PATTERNS A and B

FIGURE VI-22

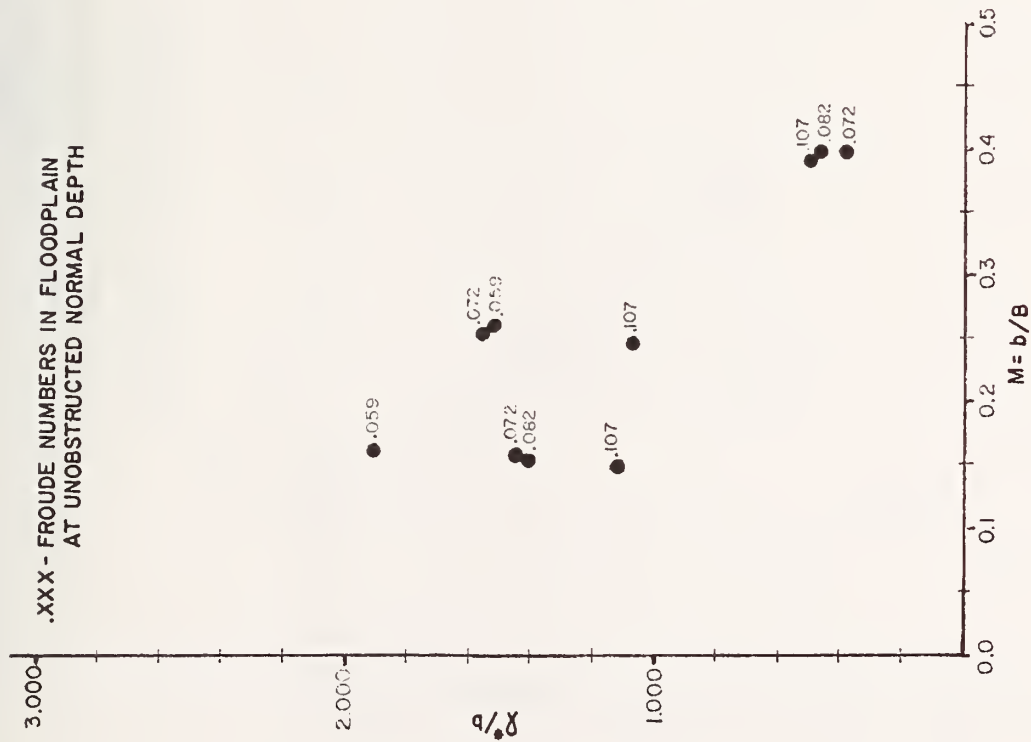
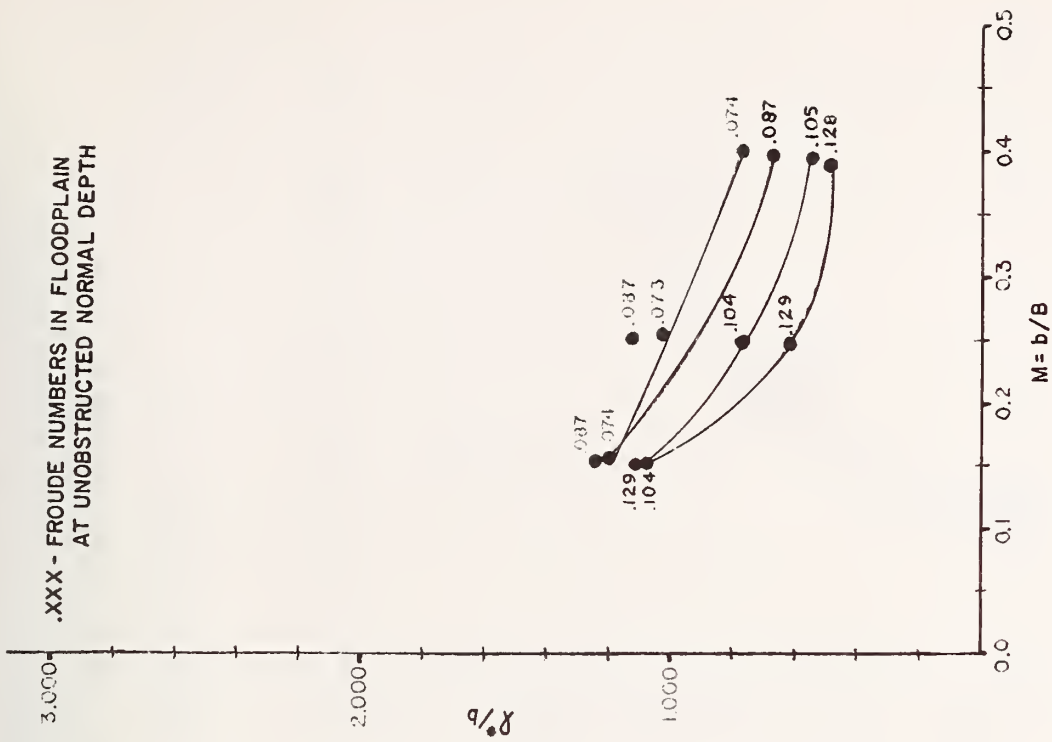


MAXIMUM BACKWATER LOCATION (δ^*/b vs M)
 FOR WINGWALL ROUGHNESS PATTERNS C and D
 FIGURE VI-23

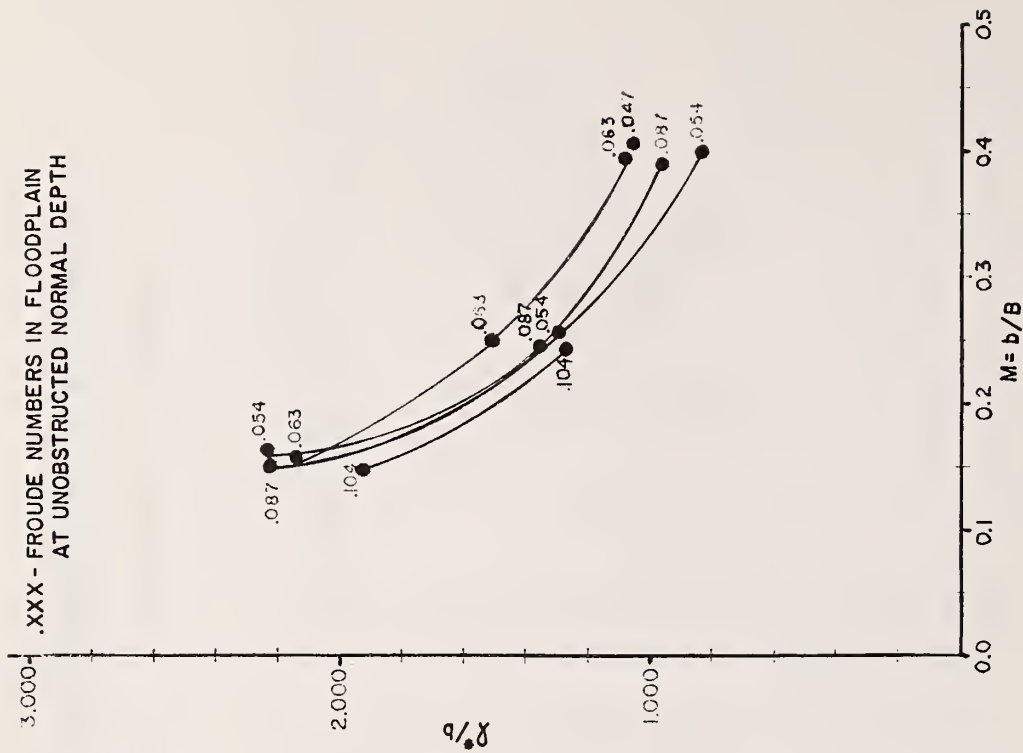
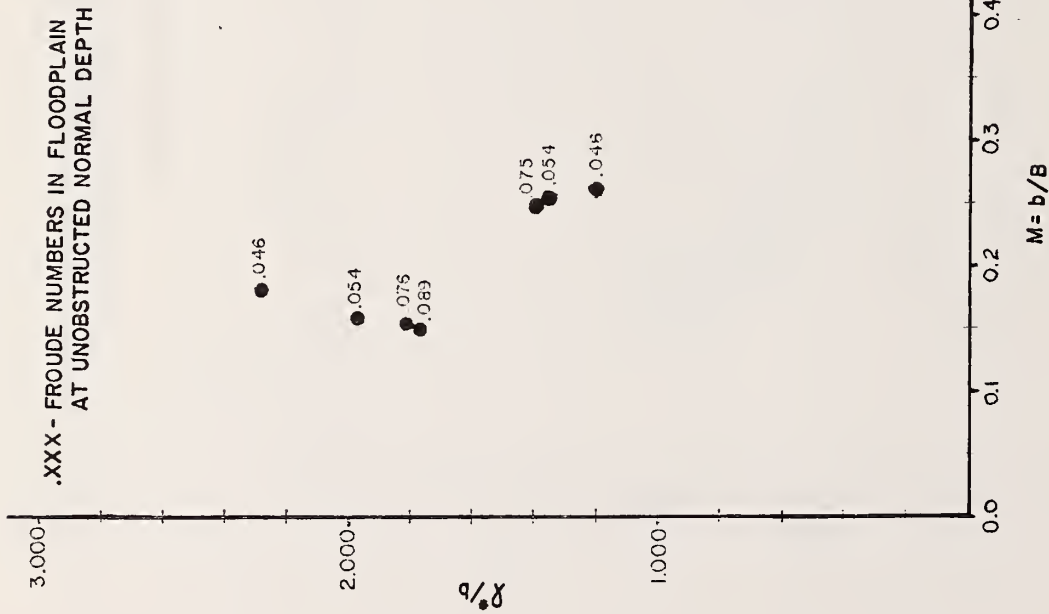


MAXIMUM BACKWATER LOCATION (λ^*/b vs M)
FOR SPILLTHROUGH ROUGHNESS PATTERNS A and B

FIGURE VI-24

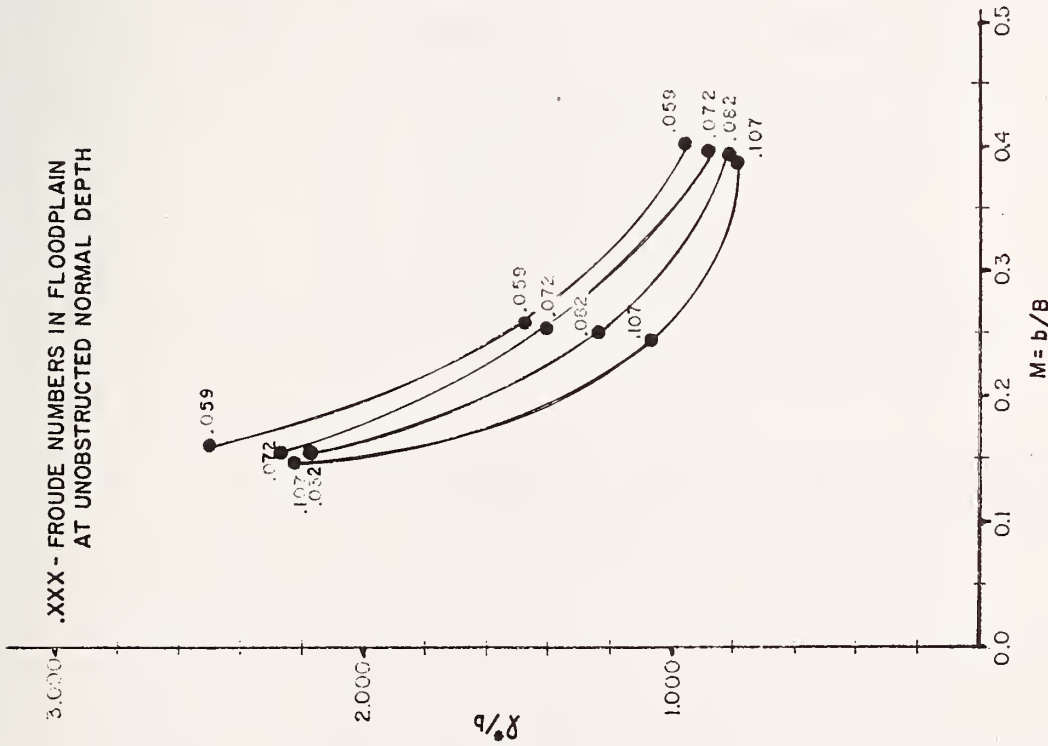
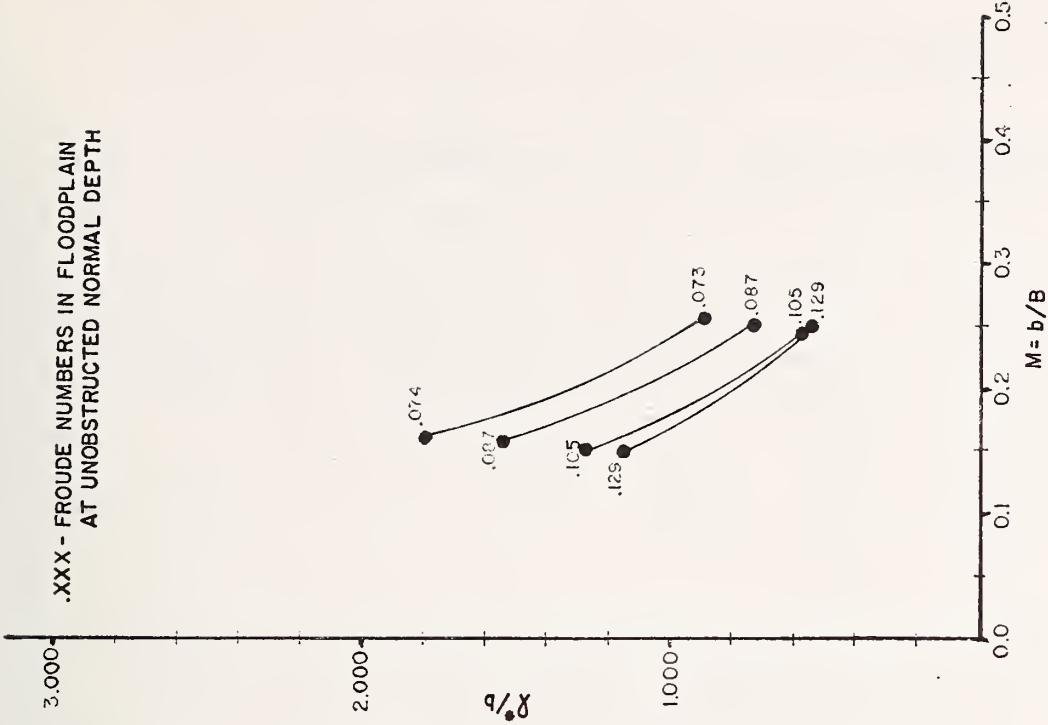


MAXIMUM BACKWATER LOCATION (λ^*/b vs M)
 FOR SPILLTHROUGH ROUGHNESS PATTERNS C and D
 FIGURE VI-25



MAXIMUM BACKWATER LOCATION (ℓ^*/b vs M)
FOR SPUR DIKE ROUGHNESS PATTERNS A and B

FIGURE VI-26



MAXIMUM BACKWATER LOCATION (λ^*/b vs M)
 FOR SPUR DIKE ROUGHNESS PATTERNS C and D

FIGURE VI-27

F = Froude number (flood plain)

C_f = Roughness element pattern (A through D)

Regression requires a general form of the equation to be defined before proceeding. In this analysis only linear and log-linear were considered. These were chosen since the data appeared to follow a log-linear to linear pattern as shown in the preceding section. Though both were analyzed only the log-linear is presented here due to its generally superior performance. The form of the log-linear equation is given below:

$$\frac{Q^*}{b} = b_1 M^{b_2} A^{b_2} F^{b_3} R^{b_4} \quad (55)$$

Table VI-8 shows multiple correlation coefficients (R) for the four independent variables in the experiment. The data in this table have been log transformed. Note that abutment shape is treated as a categorical variable. In the regressions that follow this means that abutment shapes (wingwall, spill-through and spur dike) are coded. These are given below:

Abutment Variable		
	<u>X₄</u>	<u>X₅</u>
Wingwall	1	1
Spillthrough	1	10
Spur dike	10	1

Roughness patterns are also coded by using λ values defined in Chapter IV. These are repeated here for reference.

TABLE VI-8
CORRELATION COEFFICIENTS FOR INDEPENDENT VARIABLES

Variable Number	1	2	3	4	5	6
1	1.000	-0.049	-0.691	0.536	-0.281	-0.151
2		1.000	-0.205	0.071	0.081	-0.553
3			1.000	-0.177	0.048	0.010
4				1.000	-0.495	-0.116
5					1.000	-0.112
6						1.000

where Variable 1 = ℓ^*/b
 2 = Froude Number (flood plain) (F)
 3 = Opening Ratio (M)
 4 = Abutment Variable (categorical)
 5 = Abutment Variable (categorical)
 6 = Roughness Element Pattern

<u>Roughness Element Pattern</u>	<u>Lambda (λ)</u>
P	0.0242
A	0.0198
B	0.0160
C	0.0144
D	0.0107

The effect of coding is to identify categories into which the dependent variable can be classified in an attempt to "explain" variance. The numerical coding in no way affects the tests of significance or conclusions drawn. However, it does modify coefficients and/or exponent values.

Table VI-9 presents results of four log-linear regressions completed on the λ^*/b data. Regression equation 1 is the best least squares fit to the data obtainable from the data presented previously for λ^*/b . Approximately 77 percent of the total variance is "explained" by these four independent variables. All the exponents test significant at the 95 percent confidence level. Figure VI-28 is a plot of the log residuals vs log of λ^*/b . Note that no unusual distribution of the residuals is obtained. Approximately one-half the residuals are positive and one-half negative.

Analysis 2, Table VI-9, is the functional relationship between λ^*/b on M and F alone. Fifty-two percent of the total variance is accounted for. This would indicate the abutment shape variable and roughness element pattern accounts for 25 percent more of the variance when added to the equation at this time. Note that the amount of variance explained by a variable is dependent on the order in which independent variables enter the regression.

The problem of estimating the relative importance of the independent variables to the regression equation is a problem that cannot be directly assessed. This is due to the interrelationships (correlations) between the independent variables (Table VI-8). If all cross correlations were zero, the

TABLE VI- 9
LOG-LINEAR REGRESSIONS FOR λ^*/b

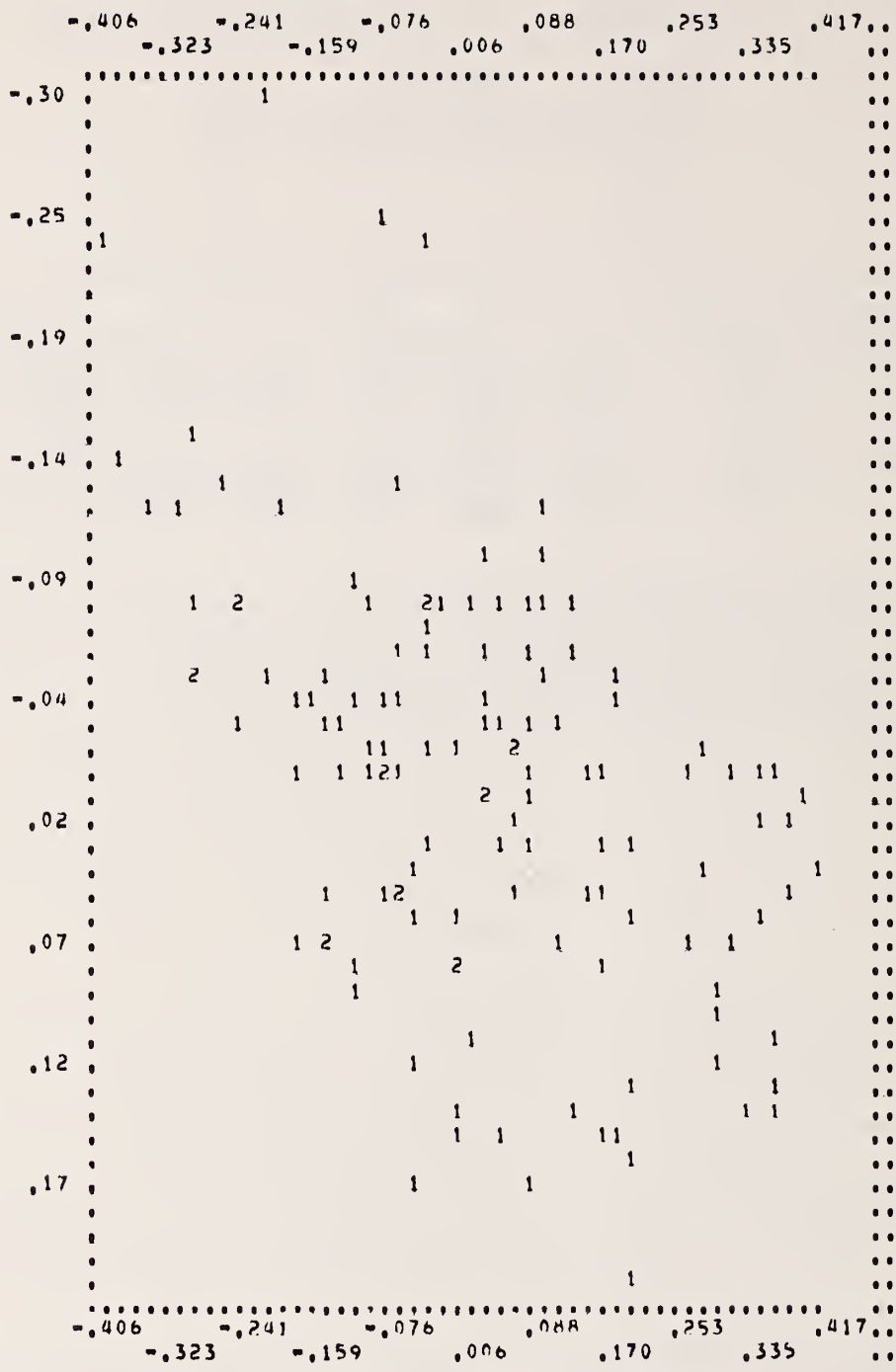
Analysis	Constant	M	F	A ₁	A ₂	R	F _{stat}	R ²
1	7.2*10 ⁻³	0.193	0.275	1.41	0.939	0.263	82.9	0.77
2	0.173	0.179	0.521	--	--	--	68.0	0.52
3 ^a	0.100	0.196	0.288	1.35	0.943 ^b	0.932 ^b	72.2	0.87
4 ^c	0.057	0.138	0.221	1.31	0.977 ^b	0.980 ^b	65.0	0.84

^aOnly Roughness Element Patterns B and D.

^bDoes not contribute significantly to the regression.

^cOnly Roughness Element Patterns B and C.

PLOT OF RESIDUALS (Y-AXIS)
 VS. VARIABLE 1 (X-AXIS)



PLOT OF RESIDUALS vs Q^*/b
 FIGURE VI-28

multiple correlation coefficient (R^2) would be the sum of the correlations shown in Table VI-10 under R^2 . In regression equation 1 this sum is .867 as compared with the actual R^2 for the regression given in Table VI-9 of 0.77. The amount of variance "explained" by the addition of a variable in this problem is directly linked to the order of the addition.

This problem can be partially alleviated by the calculation of Beta weights (Table VI-10). Beta's are standardized partial correlation coefficients that can be used in a regression if all variables are in standard form. Standard form means each variable is subtracted from the mean of that variable and divided by its deviation.

$$\text{Standard Form: } Z_x = \frac{x - \bar{x}}{S_x}$$

Beta variables can be viewed as a standardized form of b_1 . This removes the problem of various scales and units between independent variables. The disclaimer "partial" refers to the fact that the effects of variables other than the one to which the weight applies are held constant. With these facts in mind, it can be said qualitatively that opening ratio is the most important variable, abutment variable 1 (spur dike), Froude number, and the roughness pattern are of lesser importance, and abutment variable 2 is of least importance for the prediction of Q^*/b .

Regression equation 3 is an attempt to test for significant differences between roughness patterns B and D. These patterns represent uniform distributions of decreasing density (75 percent to 50 percent). More specifically the question that can be answered is "Does the knowledge of which element roughness pattern (B or D) explain any additional variance after the other three independent variables have been included." In this case the additional variance is an increase in R^2 of .005. For any practical purpose this increase is negligible.

TABLE VI-10
BETA WEIGHTS

	b_j	B_j	R_j^2
Froude Number	-0.56	-0.393	0.002
Opening Ratio	-0.713	-0.702	0.477
Abutment Variable 1	0.150	0.366	0.287
Abutment Variable 2	-0.027	-0.069	0.079
Roughness Pattern	-0.580	-0.33	0.022

Regression equation 4 was used to examine the effect of element roughness patterns B and C on the prediction of ℓ^*/b . These have flood plain and main channel differences of 75-75 and 75-25 percent, respectively. The results were essentially the same as for equation 3. The knowledge of the roughness pattern after the other variables are taken into account is of marginal practical use.

The results of equation 3 and 4 can be accounted for in two ways:

1. The effect of changes in pattern densities which changes effective Manning's roughness, is accounted for by Froude number, or
2. The parameter ℓ^*/b is not sufficiently sensitive to show the change.

However, due to the correlation (R) of Froude number to roughness pattern of -0.553 (Table VI-8) the former is considered more likely.

A summary of conclusions from the regression analysis of ℓ^*/b on F, M, A, C_f follows:

1. Regression equation 1 provides an accurate representation of the ℓ^*/b data.
2. The use of Froude number and opening ratio alone explain a little over 50 percent of the variance.
3. Froude number accounts for the effect of changing roughness densities for patterns B and D.
4. The effect of a main channel of lesser density after the variables F, M, and A are included is marginal for predicting ℓ^*/b . The knowledge of the main channel differences adds little to a regression relationship beyond that added by the other variables. This can definitively be said for only patterns B and D and has not been extended to the entire data base.
5. The inclusion of spur dikes has a significant effect on ℓ^*/b .

The regression analysis has attempted to assess the significance of varying roughness patterns on the parameter ℓ^*/b . This approach is restricted due to the difficulty of assessing absolute importance of independent variables and the lack of sensitivity inherent in the parameter ℓ^*/b . Possible future analysis of different variables might eliminate the latter problem while the former is solved only by further experimentation.

ANALYSIS OF MAXIMUM BACKWATER HEIGHT (h^*/y_0)

Maximum backwater height, defined as the maximum difference in backwater surface elevations over normal elevation (h^*), is calculated as described in the Appendix. The normal depth y_0 is the average of the three normal depths taken over the north, central and south sides of the flume. The values of the parameters h^* and y_0 used in this part of the analysis can be found in the Appendix under headings "HSTAR" and "YTILD," respectively.

ANALYSIS OF VARIANCE (h^/y_0)*

An analysis of variance was performed on the 36 runs comprising the complete set for roughness pattern C (flood plain 75 and main channel 25 percents). The major variables and levels are the same as given in the previous section on backwater location. The dependent variable is, of course, h^*/y_0 .

Table VI-11 is output of the ANOVA for the data both with and without spur dike results, respectively. Testing (Table VI-12) shows that Froude number, opening ratio, and one interaction FxM are significant for both sets of data at the 95 percent confidence level. The significance of the abutment variable is due to the spur dike data.

GRAPHICAL ANALYSIS (h^/y_0)*

Figures VI-29 to VI-35 are plots of the dependent variable h^*/y_0 and opening ratio (M). Numbers included in the plot are Froude numbers calculated over the entire width of the flume.

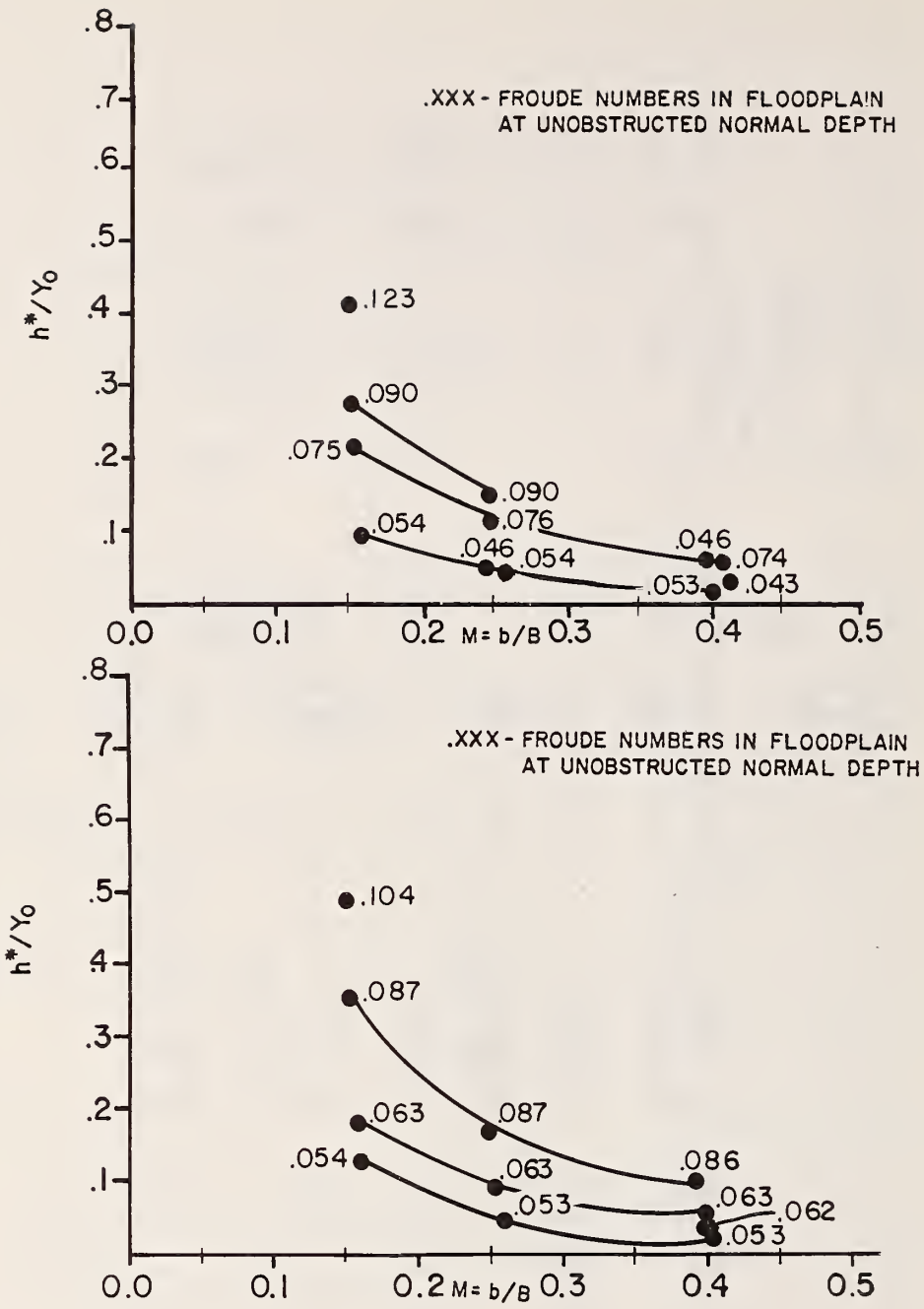
A review of the plots indicates that for the entire data base:

TABLE VI-11
ANOVA OF h^*/y_0 FOR ROUGHNESS PATTERN C
WITH AND WITHOUT SPUR DIKE DATA

WITH SPUR DIKES				WITHOUT SPUR DIKES		
Analysis of Variance $h^* 433$				Analysis of Variance $h^* 432$		
Levels of Factors				Levels of Factors		
F	4			F	4	
M	3			M	3	
A	3			A	2	
Grand Mean .12				Grand Mean .11		
Source Variance	Sums of Squares	Degrees of Freedom	Mean Squares	Sums of Squares	Degrees of Freedom	Mean Squares
Froude (F)	0.11	3	0.03	0.06	3	0.02
Opening Ratio (M)	0.22	2	0.11	0.14	2	0.07
F x M	0.04	6	0.01	0.02	6	0.00
Abutment (A)	0.00	2	0.00	0.00	1	0.00
F x A	0.00	6	0.00	0.00	3	0.00
M x A	0.00	4	0.00	0.00	2	0.00
F x M x A	0.00	12	0.00	0.00	6	0.00
TOTAL	0.39	35		0.24	23	

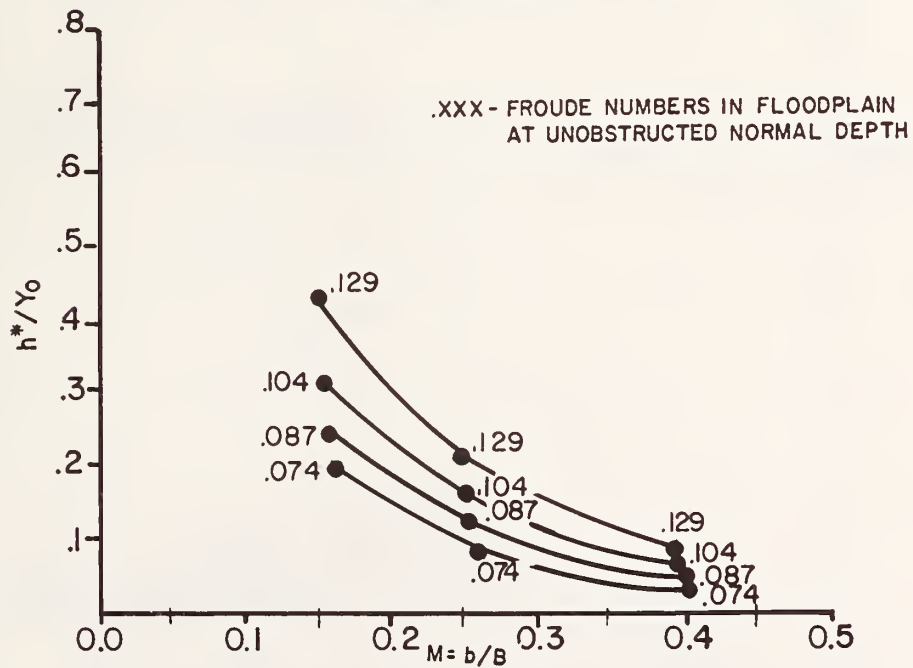
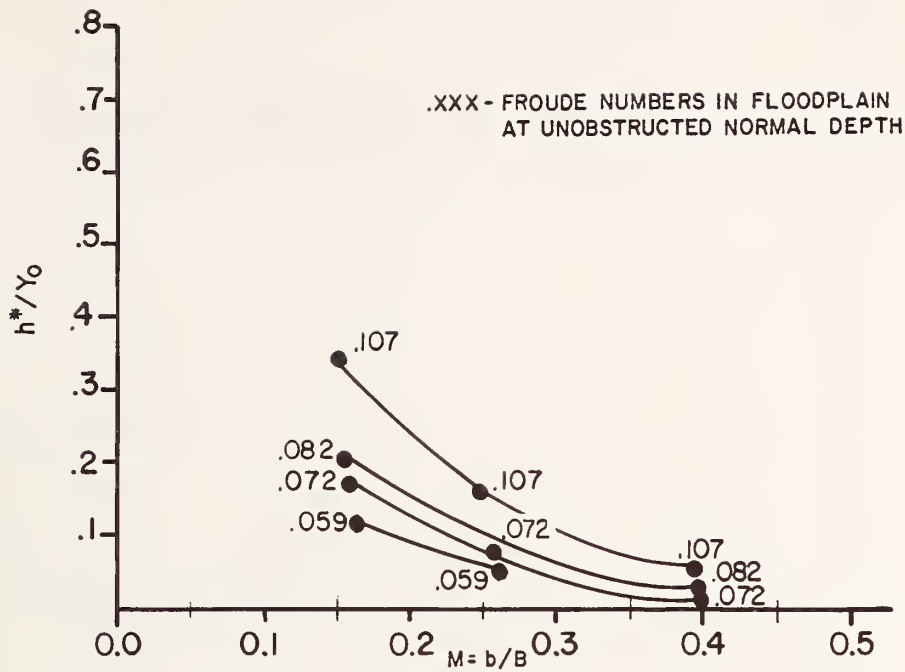
TABLE VI-12
 TESTING OF h^*/y_0 FOR ROUGHNESS PATTERN C
 AT 95 PERCENT CONFIDENCE LEVEL

Source of Variance	Test	With Spur Dikes		Without Spur Dikes			
		F Statistic	Req. for Signif.	F Statistic	Req. for Signif.		
Froude (F)	MS_F/MS_{FA}	4.76	172.0	Yes	9.28	133.0	Yes
Opening Ratio (M)	MS_M/MS_{FM}	5.14	15.5	Yes	5.14	17.6	Yes
FxM	MS_{FM}/MS_{FA}	4.28	33.4	Yes	8.94	24.8	Yes
Abutment (A)	MS_A/MS_{FA}	5.14	9.55	Yes	10.1	7.76	No
FxA	No Test	--	--	--	--	--	--
MxA	MS_{MA}/MS_{FMA}	3.26	1.54	No	5.14	1.78	No
FxMxA	MS_{FMA}/MS_{FA}	4.00	0.59	No	8.94	1.06	No

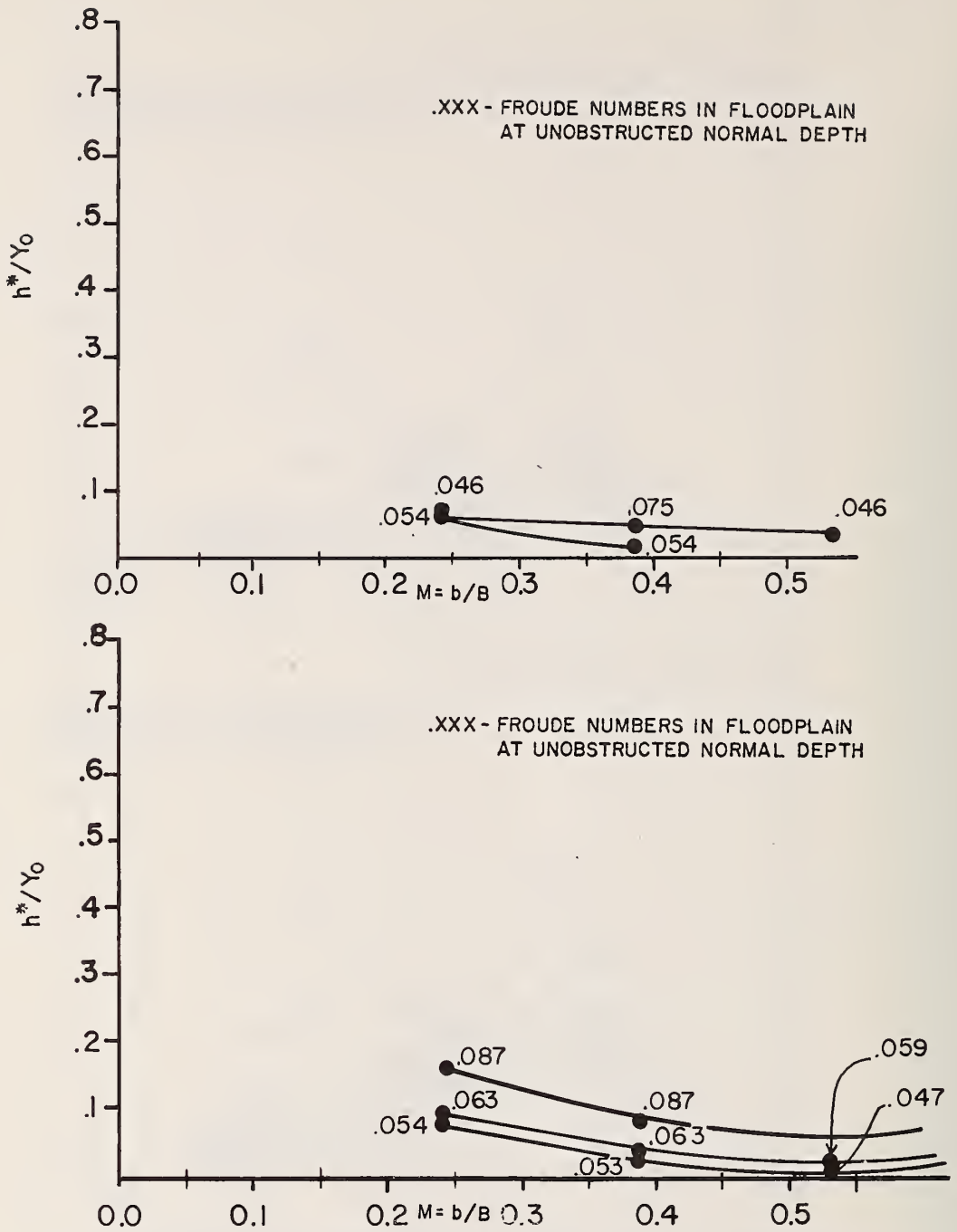


MAXIMUM BACKWATER HEIGHT (h^*/Y_0 vs M)
 FOR SPILLTHROUGH ROUGHNESS PATTERNS A and B

FIGURE VI-29

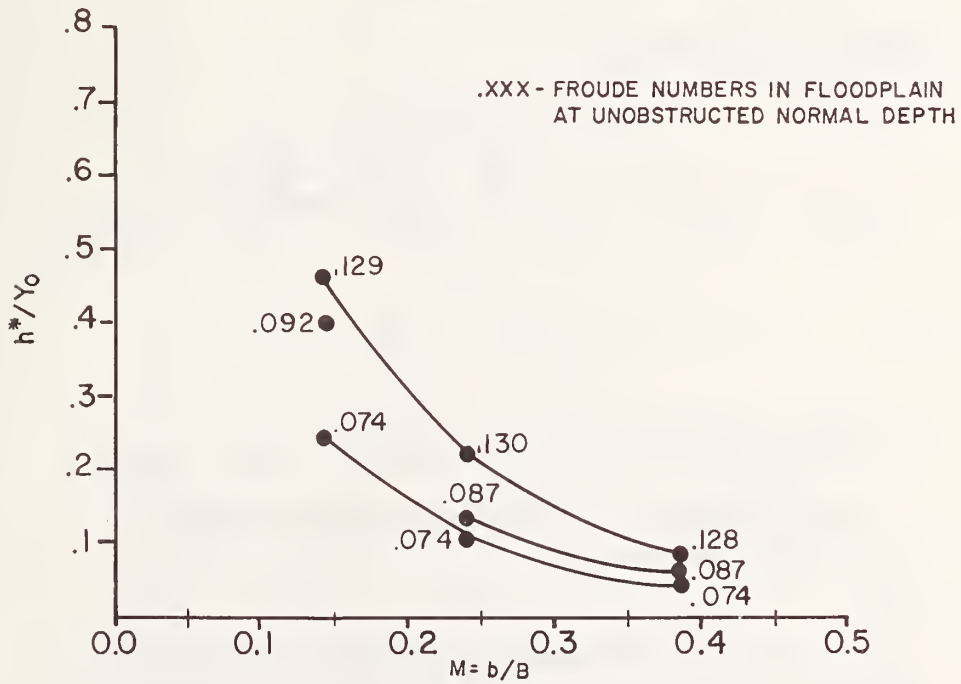
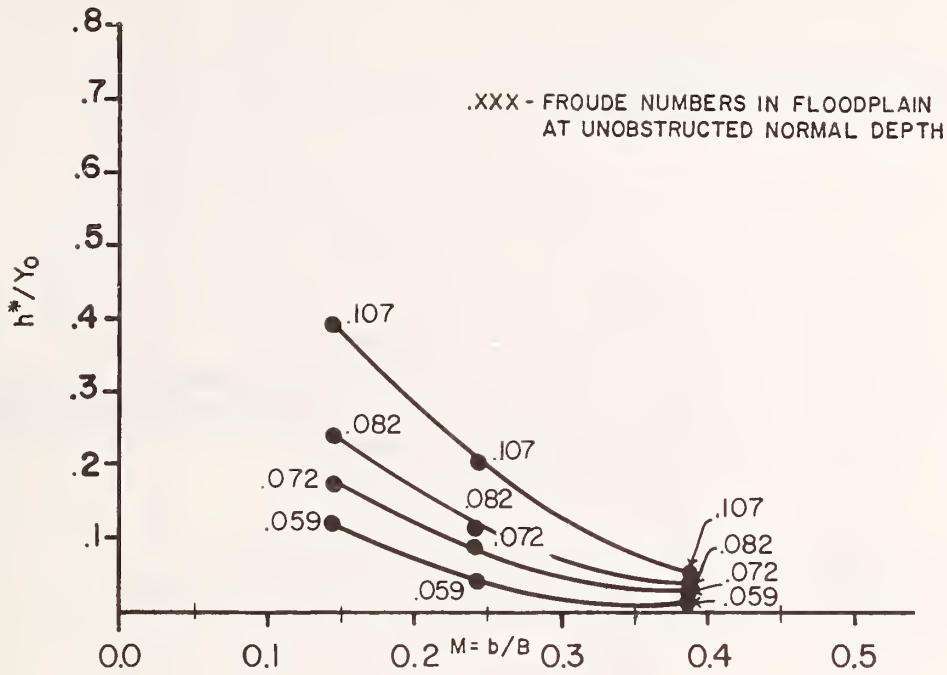


MAXIMUM BACKWATER HEIGHT (h^*/Y_0 vs M)
 FOR SPILLTHROUGH ROUGHNESS PATTERNS C and D
 FIGURE VI - 30

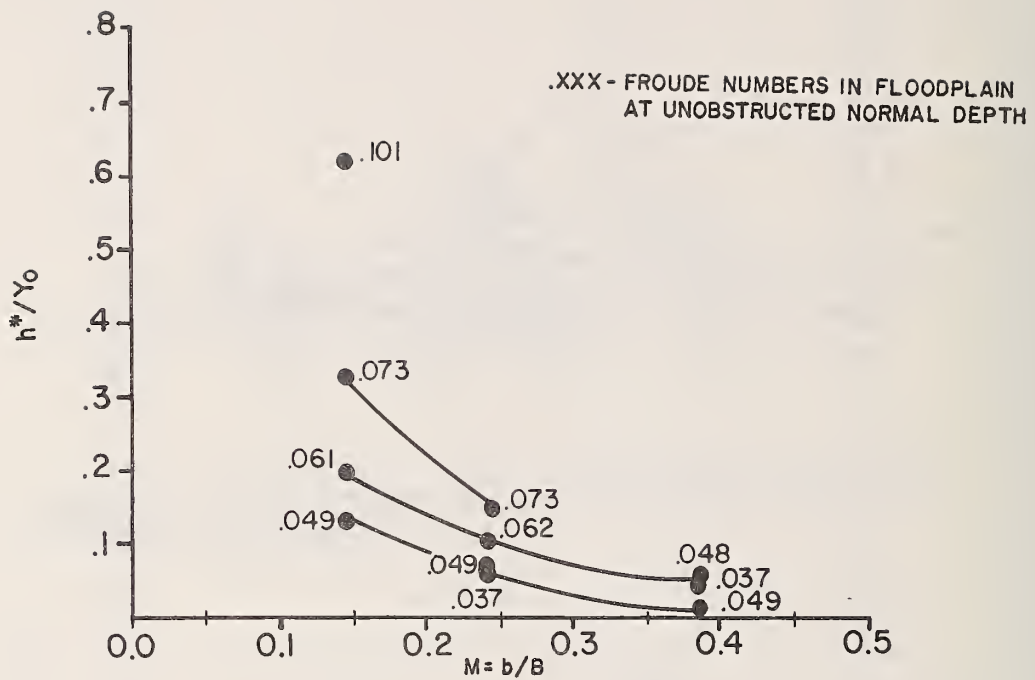


MAXIMUM BACKWATER HEIGHT (h^*/Y_0 vs M)
 FOR WINGWALL ROUGHNESS PATTERNS A and B

FIGURE VI-31

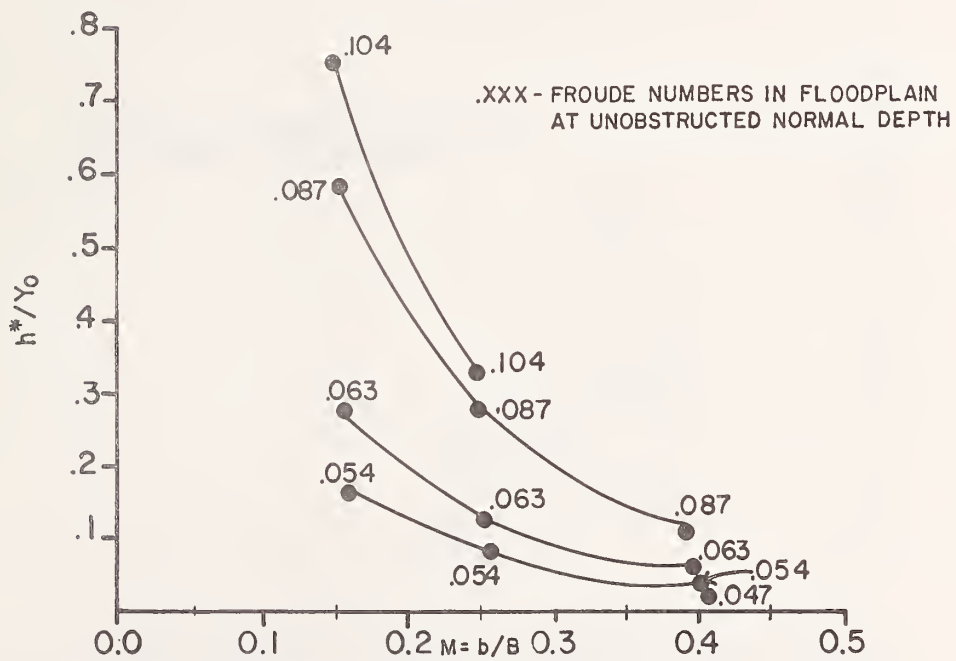
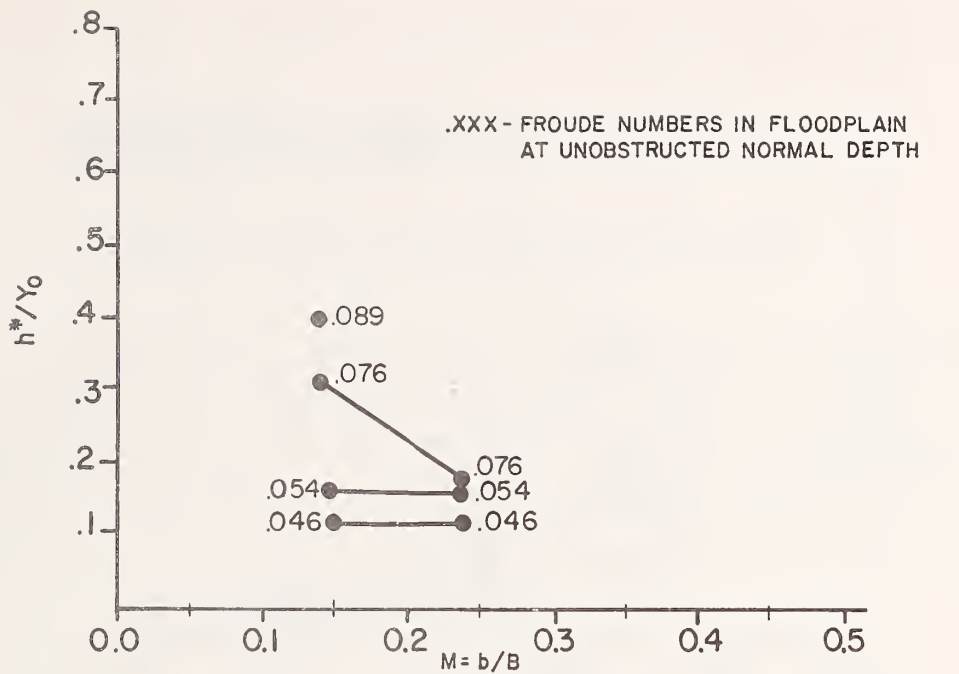


MAXIMUM BACKWATER HEIGHT (h^*/Y_0 vs M)
FOR WINGWALL ROUGHNESS PATTERNS C and D
FIGURE VI - 32



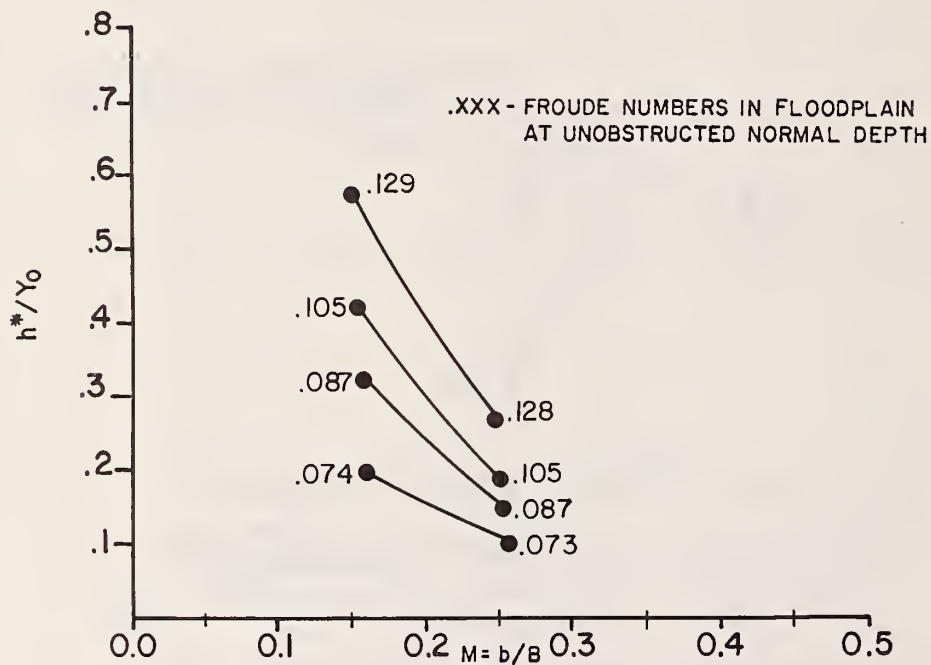
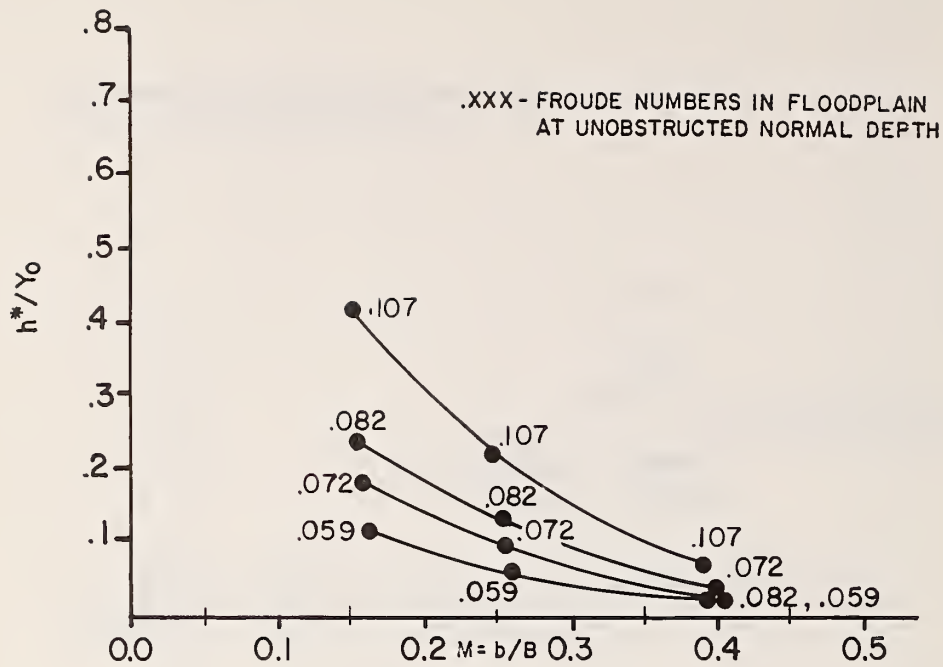
MAXIMUM BACKWATER HEIGHT (h^*/Y_0 vs M)
FOR WINGWALL ROUGHNESS PATTERN P

FIGURE VI-33



MAXIMUM BACKWATER HEIGHT (h^*/Y_0 vs M)
FOR SPUR DIKE ROUGHNESS PATTERNS A and B

FIGURE VI-34



MAXIMUM BACKWATER HEIGHT (h^*/Y_0 vs M)
 FOR SPUR DIKE ROUGHNESS PATTERNS C and D
 FIGURE VI-35

1. H^*/y_0 is strongly related to opening ratio and Froude number.
2. Spur dikes appreciably alter the relationship noted above.
3. The effect of various roughness element patterns appears slight as can be expected, since the value of y_0 varies with roughness.

In regard to any further analysis this would indicate that differing wingwall and spillthrough abutment shapes do not appreciably reflect in h^*/y_0 parameter nor do the various roughness element patterns. The presence or absence of spur dikes must be noted due to its strong effect as shown on Figures VI-31 and VI-34.

VII. CONCLUSIONS

In relation to the volume of data collected, the information thus far obtained can be viewed only as a partial analysis. Topics bearing on the two-dimensionality of the data have not been given the attention possible in relation to the data collected. Important energy transfer mechanisms due to the roughness elements have not been investigated nor has the effect of differing roughness patterns on the basic energy relationships been adequately characterized. These are topics beyond the scope of this contract that can be pursued in later analysis.

Conclusions reached in the present analysis are:

1. The primary parameter recorded, water surface elevation, was sensitive to every level of the independent variables. The independent variables were Froude number, opening ratio, and abutment shape.
2. For any use of the data other than an analysis of water surface elevations, data describing wingwall and spill-through abutment shapes can be pooled with little increase in data scatter.
3. The presence of spur dikes constitutes a strong influence on the location and height of maximum backwater. Any general purpose prediction equation for these and other parameters must make allowances for their effect.
4. A return to normal depth was shown to occur approximately 5 to 10 ft below the constriction for the centered, normal openings.
5. The effects of the constriction on depth extended upstream the entire length of the flume (60-foot reach).

6. The wide scatter evidenced in the backwater coefficient data, K^* , makes impossible any direct contribution to modifying the calculation procedure in regard to K^* for the FHWA backwater method. This scatter may be attributable to the small h^* values obtained in the experiment.
7. The parameter λ^*/b is statistically related to the opening ratio, Froude number, abutment shape and/or spur dike and roughness pattern. Approximately 77 percent of the total variance is accounted for by these variables.
8. A graphical analysis of the parameter h^*/y_0 showed a similar relationship as demonstrated above for the dimensionless parameter λ^*/b .
9. A strong relationship exists between roughness pattern and Froude number. When Froude number is included in a predictive equation for the parameter λ^*/b the relative additional prediction capability provided by the addition of the variable for roughness pattern is marginal. This was noted in the analysis of the two roughness patterns B and C (Flood Plain 75 percent, Main Channel 75 percent and Flood Plain 75 percent and Main Channel 25 percent), respectively. This may be partly attributable to the relative insensitivity of the parameter λ^*/b .
10. A similar comparison between roughness patterns B and D (Flood Plain 75 percent, Main Channel 75 percent and Flood Plain 50 percent and Main Channel 50 percent) using the parameter λ^*/b indicated that differences noted in the parameter solely attributable to the roughness pattern were negligible.
11. The data collected in this experiment do not provide a sufficient basis, when taken alone without additional experimentation, to justify major changes in Hydraulics Design Bulletin No. 1 - Hydraulics of Bridge Waterways.

VIII. RECOMMENDATIONS

A backwater method which is useable to the highway design engineer must have two characteristics:

1. Easily understood and implemented and
2. Reasonably accurate results.

The methods currently in general use adequately satisfy the first criterion but in many instances not the second. Future research must be directed to improving the accuracy of the various methodologies without seriously affecting their level of difficulty by a careful blend of physical model and prototype information coupled with computer simulation using advanced numerical techniques such as the Finite Element Model.

To this end, the recommendations listed below deal principally with two areas of interest: improvement of the data collection effort, and further analysis and interpretation of the data, particularly where research efforts could most rapidly advance the state of the art.

DATA COLLECTION

1. *The Soundness of the Large Scale Roughness Elements Must be Scrupulously Maintained.*

A major and important distinction between this and previous experiments was the use of large scale roughness. The simulation of prototype conditions proved sensitive to the movement of fairly small portions of the elements.

This sensitivity was further documented by including varying numbers of roughness elements in the constriction. In order to maintain reproducibility of results, a program of constant repair and attention must be run simultaneously with experimentation.

2. *The Roughness Elements Must Be Spaced to Facilitate Varying the Length of the Opening and Installing Spur Dikes.*

Due to the sensitivity of backwater to the roughness elements the experimental matrix should be scoped to avoid, to the extent possible, movement of the roughness elements. This is particularly the case in regard to the testing of spur dikes.

3. *Automated Velocity and Depth Measurement Equipment Should be Used to Gather Information.*

The use of automated sensing equipment requires a large initial investment which can often appear prohibitive. However, this investment decreases operating costs, shortens data collection time and guarantees a known uniformity of measurement error. Automated sensing equipment particularly lessens human measurement and recording bias and is highly recommended as a worthwhile additional initial expense.

4. *The Data Base Should Be Further Expanded to Include Other Slopes.*

The present configuration of the flume allowed only one slope to be used in the experiment. The simulation of other slopes would allow the expansion of the data base to cover a larger set of prototype conditions.

5. *Undistorted Models Are More Suitable for Study of Point Effects of Flood Plain Roughness and Bridge Contraction on Backwater.*

DATA ANALYSIS AND INTERPRETATION

1. *The Data Base Should Be Used to Calibrate the Two-Dimensional Finite Element Model, Developed as Part of this Study.*

In many instances, useful comparisons between particular independent variables were not possible due to missing runs caused by time and money constraints. Often this severely limited the data analysis possible and the strength of the conclusions drawn. This is particularly evident when comparing the effects of varying roughness element patterns. An effort directed along such a plan of study would allow "handbook" information to be developed describing turbulence exchange coefficients, ranges of coefficients for varying situations, and roughness estimates for field conditions.

2. *The Federal Highway Administration Design Bulletin No. 1 on Hydraulics of Bridge Waterways Should Be Updated.*

The information developed in Recommendation 1 immediately above could be used to update Bulletin No. 1 to reflect the additional findings. The emphasis in this task is on the needs of the design engineer, which are distinctly different from those of field data collectors or theoretical hydraulicians.

3. *Other Data Analyses Beyond the Scope of this Effort Should Be Performed.*

Other recommended data analyses include:

- a. Investigate the shape of the maximum backwater as a function of the various main channel and flood plain roughness element densities. Since a large portion of the data collected includes difficult-to-obtain flood plain information, this provides a logical extension of the current study.
- b. Compare selected portions of the collected data with field behavior.

- c. Evaluate the revised Geological Survey method for computing average approach flow line length and exit losses using the flume data.

LIST OF REFERENCES

1. Federal Highway Administration, Department of Transportation, *Hydraulics of Bridge Waterways*, Hydraulics Design Series No. 1 (1973).
2. H. K. Liu, J. N. Bradley and E. J. Plate, "Backwater Effects of Piers and Abutments," Civil Engineering Section, Colorado State University (1957).
3. C. E. Kindsvater and R. W. Carter, "Tranquil Flow Through Open-Channel Constrictions," ASCE Transactions, Paper No. 2771 (1954).
4. V. R. Schneider *et al.*, "Computation of Backwater and Discharge at Width Constriction of Heavily-Vegetated Flood Plains," U.S. Geological Survey.
5. Hydrologic Engineering Center, U.S. Army Corps of Engineers, "HEC-2 Water Surface Profiles," 723-02A (Davis, California: 1973).
6. F. A. Nagler, "Obstruction of Bridge Piers to the Flow of Water," ASCE Transactions, Paper No. 1409 (1917).
7. T. Rehbock, "A Method for Determining the Backwater Due to Bridge Piers in Streaming Flow" (Technical University of Karlsruhe: 1921). Trans. E. F. Wisely.
8. E. L. Yarnell, Bridge Piers and Channel Obstructions," U.S. Department of Agriculture Technical Bulletin No. 442 (1934).
9. E. W. Lane, "Experiments on the Flow of Water Through Contractions in an Open Channel," ASCE Transactions, Vol. 83, pp. 1910-20.
10. H. J. Tracy and R. W. Carter, "Backwater Effects of Open-Channel Constrictions," ASCE Transactions, Paper No. 2771 (1954).
11. F. M. Henderson, *Open Channel Flow* (The Macmillan Co., 1966).
12. C. F. Izzard, Discussion of "Backwater Effects of Open-Channel Constrictions," ASCE Transactions, Paper No. 2771 (1954).

13. C. F. Izzard, Discussion of "Tranquil Flow Through Open-Channel Constrictions," ASCE Transactions, Paper No. 2770 (1954).
14. J. N. Bradley, "Hydraulics of Bridge Waterways," Bureau of Public Roads Office of Engineering and Operations, U.S. Department of Transportation (1970).
15. E. M. Laursen, "Bridge Backwater in Wide Valleys," Proc. ASCE, HY4 (April 1970).
16. C. L. Yen and D. R. Overton, "A Method for Flow Computation in Flood Plain Channels," *International Symposium on Stochastic Hydraulics*, Pittsburgh, May 31 to June 2, 1971.
17. J. L. Myers, *Fundamentals of Experimental Design*, 2nd ed. (Boston: Allyn and Bacon, Inc., 1972).
18. A. J. Duncan, *Quality Control and Industrial Statistics*, 3rd ed. (Homewood, Ill.: Richard D. Irwin, Inc., 1965).
19. Fred N. Kerlinger and Elazar J. Pedhazur, *Multiple Regression in Behavioral Research* (Holt, Rinehart and Winston, Inc., 1973).
20. W. J. Dixon (ed.), *BMD: Biomedical Computer Programs*, Health Sciences Computing Facility, Department of Biomathematics, School of Medicine, University of California at Los Angeles (Los Angeles: University of California Press, 1974).
21. M. T. Tseng, *Evaluation of Flood Risk Factors in the Design of Highway Stream Crossings, Vol. III: Finite Element Model for Bridge Backwater Computation*, FHWA-RD-75-53, FHWA, Department of Transportation, April 1975.

TE
662

. A3 no. FHQA-

RD- 75-580RROWER

Form DOT F 1720
FORMERLY FORM DOT



DOT LIBRARY



00054898

